Function of triterpenes in *Arabidopsis thaliana* and their anti-inflammatory activities in mammalian hepatoma cells

Inaugural-Dissertation

zur

Erlangung des Doktorgrades

der Mathematisch-Naturwissenschaftlichen Fakultät

der Universität zu Köln

vorgelegt von

Dorian Alexander Baumann

aus Köln

Köln 2018

Die dieser Dissertation zugrundeliegenden experimentellen Arbeiten wurden in der Zeit von Januar 2015 bis Januar 2018 am Botanischen Institut der Universität zu Köln im Rahmen der Internation Max Planck Research School angefertigt.

Berichterstatter:	Prof. Dr. Stanislav Kopriva
	PD Dr. Tamara Gigolashvili
Tag der Disputation:	15.05.2018

Kurzzusammenfassung

Pflanzliche Triterpene zählen zu der Gruppe der Sekundärmetabolite. Sie umfassen eine Vielzahl von cyclischen Verbindungen aus dreißig Kohlenstoffatomen, die zum Teil enzymatisch modifiziert sind. Bemerkenswert ist die Bildung von Gen-Clustern aus Genen zur Triterpensynthese, welche epigenetisch reguliert werden können. Darüber hinaus ist wenig über ihre physiologische Funktionsweise in der Pflanze bekannt, aber sie scheinen sehr spezialisierte Funktionen in der pflanzlichen Immunantwort und dem Wachstum einzunehmen. Zwei Beispiele für pflanzliche Triterpene sind Marneral und Thalianol. Diese werden hauptsächlich in Wurzeln junger Keimlinge synthetisiert. Die Akkumulation von Marneral oder Thalianol führt in *Arabidopsis thaliana* zum Zwergwuchs, allerdings ist ihre exakte Funktion bisher unbekannt. Des Weitern weisen andere Triterpene, wie Betulin, entzündungshemmende Eigenschaften in tierischer Zellkultur auf. Dennoch ist das pharmakologische Potential der meisten Triterpene nicht vollständig entschlüsselt. Diese Arbeit beschäftigt sich daher mit der Untersuchung der physiologischen Funktion von Triterpenen in Pflanzen, sowie der Suche nach neuen Triterpenen mit entzündungshemmenden Eigenschaften im Nrf2-EpRE-Signalweg in tierischer Zellkultur. Der Nrf2-EpRE-Signalweg ist ein relevantes Wirkstoffziel in vielen pharmakologischen Studien.

Um die entzündungshemmenden Eigenschaften von Triterpenen zu untersuchen, wurden Reporter-Gen-Studien in Mausleber-Tumorzellen durchgeführt, welche mit triterpen-enthaltenen *Rhodobacter capsulatus* Extrakte behandelt wurden. Untersuchungen an bakteriellen Extrakten die heterolog synthetisierte Triterpene enthalten bieten gegenüber aufgereinigten Wirkstoffen eine Zeitersparnis durch den Verzicht von komplexen Aufreinigungsschritten. Im Ausgang der Experimente wurden keine neuen Triterpene mit entzündungshemmenden Eigenschaften in bakteriellen Extrakten identifiziert. Dieses Resultat ist wahrscheinlich auf eine zu geringe Wirkstoffkonzentration oder auf inaktive Substanzen zurückzuführen. Dennoch konnten entzündungshemmende Eigenschaften in einem anderen Sekundärmetabolit namens Prodigiosin, welches kein Triterpen ist, in bakteriellen Extrakten nachgewiesen werden. Zukünftig ermöglicht diese Anwendung eine neue Möglichkeit für ausgedehnte Untersuchungen weiterer Metaboliten im Hintergrund bakterieller Expressionssysteme.

Die physiologischen Funktionen pflanzlicher Triterpene in *Arabidopsis thaliana* wurde am Beispiel von Marneral und Thalianol untersucht. Arabidopsis *marneral synthase 1* (*mrn1*) und *thalianol synthase* (*thas*) Gen-Knockout-Mutanten wurden gekreuzt und ihr

Wachstumsphänotyp, sowie ihre Reaktion auf abiotischen und biotischen Stress wurden erforscht. Zudem wurde eine mögliche Vernetzung von marneral und thalianol zu pflanzlichen Hormonsignalwegen studiert. Ein kombinierter Verlust von Marneral und Thalianol in Arabidopsis führte nicht zu einem veränderten Wachstumsphänotyp. Jedoch geben die erzielten Resultate Hinweise auf eine positive Korrelation zum phytosulfokin-α-abhängigen Wurzelwachstum. Des Weiteren führte der Verlust der beiden Gene zu einer leicht erhöhten Abwehr gegenüber wurzel-assoziierten mikrobiellen Pathogenen. Ob diese leicht erhöhte Abwehr in der Wurzel von *mrn1*thas* im Zusammenhang mit dem gestörten Phytosulfokin-α-Signalweg steht, sollte in zukünftigen Untersuchungen geklärt werden. Obwohl dies getestet wurde, konnte keine Funktion von Marneral und Thalianol im Zusammenhang mit dem Jasmonat-Signalweg und der abiotischen Stressantwort beobachtet werden.

Zusammengefasst bietet diese Arbeit einen neuen Ansatz in der tierischen Zellkultur zur Untersuchung entzündungshemmender Moleküle in bakteriellen Extrakten. Außerdem liefert sie neue Erkenntnisse für eine physiologische Funktion von Marneral und Thalianol in der pflanzlichen Immunantwort und dem Phytosulfokin-α-Signalweg.

Abstract

Plant triterpenes belong to the class of secondary metabolites. They encompass a highly diverse range of ring structures consisting of thirty carbon atoms which can be enzymatically modified. Importantly, genes for their biosynthesis are arranged in epigenetically regulated gene clusters. However, very little is known about the physiological function of triterpenes in plants, but some triterpenes fulfill specialized roles in plant defense and growth. Two examples for triterpenes are marneral and thalianol. Marneral and thalianol are mainly synthesized in the roots of young seedlings. Accumulation of marneral or thalianol leads to a dwarfed phenotype in *Arabidopsis thaliana*, but their cellular function is unknown. Furthermore, other triterpenes like betulin exhibit anti-inflammatory properties in mammalian cells. However, the pharmacological potential of most triterpenes has not yet been fully investigated. Therefore, the aim of this thesis was to shed a light on the physiological function of triterpenes in plants and to elucidate their potential in triggering the anti-inflammatory Nrf2-EpRE pathway in animal cells. The Nrf2-EpRE pathway has become an important drug target in pharmacological research topics.

For elucidating anti-inflammatory activities of triterpenes, a reporter-gene-assay was performed, in which murine hepatoma cells were treated with triterpene containing *Rhodobacter capsulatus* extracts. Using bacterial extracts containing recombinant synthesized triterpenes instead of fully purified compounds had a time-saving advantage by skipping purification protocols. As a result, no new anti-inflammatory triterpenes in bacterial extracts were identified, probably due to low triterpene concentrations or due to non-bioactive compounds. However, an anti-inflammatory activity of a non-triterpene metabolite, prodigiosin, in bacterial extracts was demonstrated. This proof of concept opens new opportunities for future studies on large-scale compound screenings of recombinant synthesized metabolites in bacterial extracts.

The physiological functions of triterpenes in *Arabidopsis thaliana* were investigated using the example of marneral and thalianol. Arabidopsis *marneral synthase 1* (*mrn1*) and *thalianol synthase* (*thas*) knock-out lines were crossed and their growth phenotype and their response to abiotic and biotic stress were analyzed. Furthermore, a putative linkage of marneral/thalianol and growth hormones was investigated. Combinatorial loss of marneral and thalianol in Arabidopsis did not lead to an altered plant growth. Nevertheless, the results provide evidence for a positive correlation between marneral and thalianol and the phytosulfokine-α mediated root growth. Furthermore, lacking marneral and thalianol led to a slightly increased defense against pathogenic root-associated microbiota. Whether slightly increased root defense in

*mrn1*thas* is connected to impaired phytosulfokine-α signaling has to be investigated in future studies. Although it was tested, a function for marneral and thalianol in jasmonate signaling and abiotic stress response could not be proven.

This thesis provides a new approach for screenings of anti-inflammatory compounds in the context of complex bacterial extracts. It also delivers first evidence for a function of marneral and thalianol in phytosulfokine-α signaling and a slightly negative influence on plant defense for both triterpenes.

Table of Contents

Chapter 1

Introduction into plant triterpenes

1.1 What are plant triterpenes?

Triterpenes encompass a highly diverse range of structures, containing thirty carbon atoms. They belong to the class of secondary metabolites which not only present in plants, but also in animals and fungi. In contrast to primary metabolites, secondary metabolites are not crucial for growth and development, but their absence lead to a reduced fitness. Often secondary metabolites have a highly specialized function, for example in pathogen defense, as hormones, or as pigments (Wink, 2010).

Plant triterpenes, but also structurally related sterols, are built from isoprenoid units (IPPs) and often form ring structures, consisting of monocycles (6), bicycles (6/6), tricycles (6/6/5), tetracycles (6/6/6/5 and 6/6/6/6), or pentacycles (6/6/6/6/5 and 6/6/6/6/6) that are carbon rings with five to six carbon atoms per ring (Figure 1-1). Sterols and triterpenes are distinguished based on ring conformation. The linear precursor molecule of sterol 2,3-oxidosqualene is cyclized into a chair-boat-chair (CBC) ring conformation, while in triterpene synthesis 2,3-oxidosqualene is cyclized into the chair-chair-chair conformation (CCC) (Thimmappa et al., 2014). These scaffolds can be decorated with additional chemical groups and polysaccharides that lead to high structure complexity and great number of different scaffolds (Chapter 1.2).

The physiological function, regulation, and importance of triterpenes in plants are not fully understood yet (Chapter 1.4). However, triterpene research is becoming increasingly important, also for commercial applications (Król et al., 2015; Ci et al., 2017; Miettinen et al., 2017a).

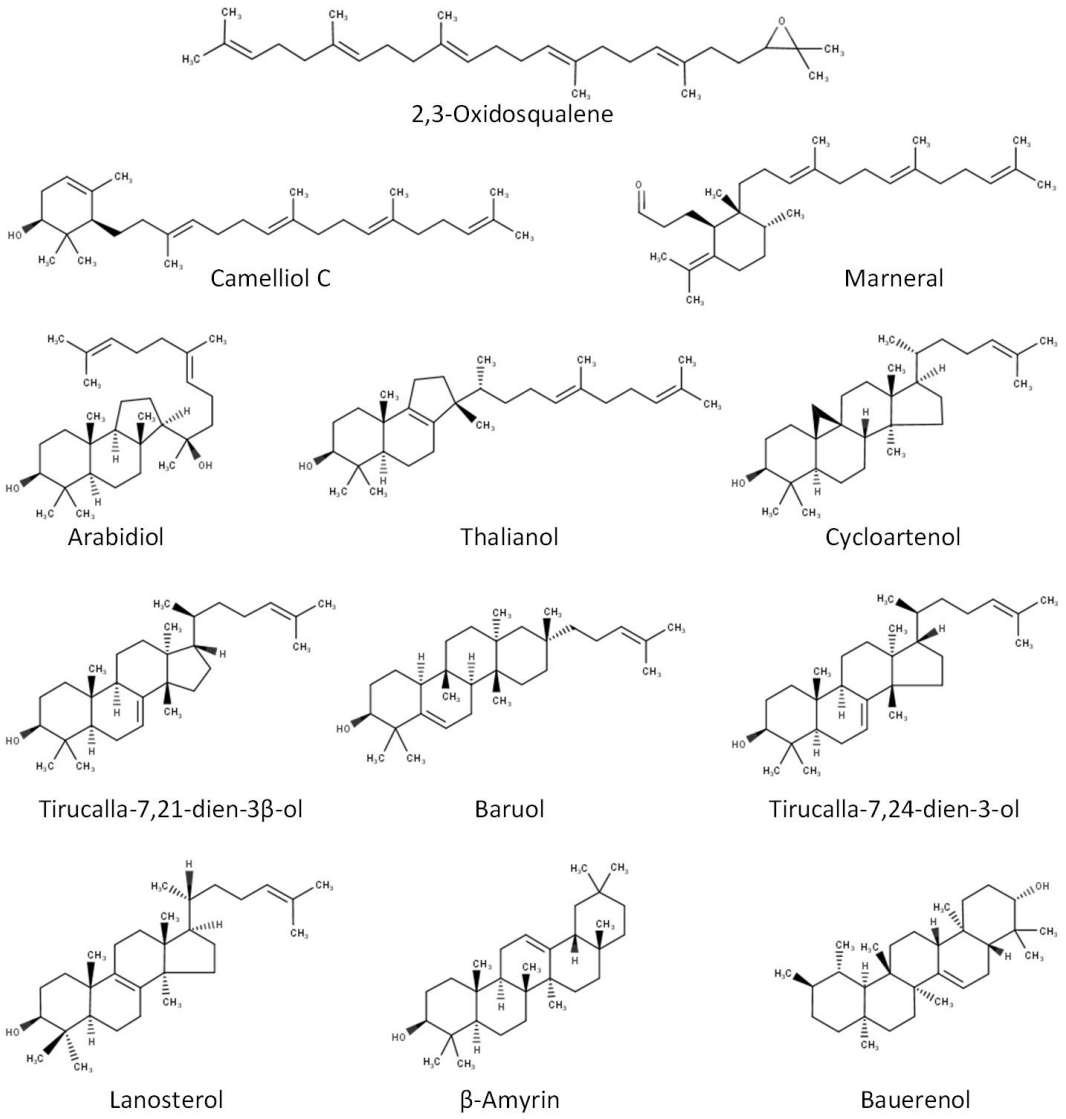

Figure 1-1: Major triterpene and sterol scaffolds in *Arabidopsis thaliana* (addapted fromThimmappa et al., 2014)

1.2 Biosynthesis of plant triterpenes

Triterpenes belong to the most diverse group of secondary metabolites in the plant kingdom. Hundreds of different triterpene structures are known and due to their diversity their total amount of structures seem to be almost endless (Thimmappa et al., 2014; Hill and Connolly, 2015).

One feature all triterpenes have in common is that they are all formed from IPPs (Chappell, 2002). IPPs are synthesized via two distinct pathways in plants, the plastidic mevalonate (MVA) and the peroxisomal 2-C-methyl-D-erythritiol 4-phosphate (MEP) pathway (McGarvey and Croteau, 1995; Lichtenthaler, 1999). The IPP ISOMERASE converts IPP to

dimethylallyl pyrophosphate (DMAPP) (Lützow and Beyer, 1988). Next, in the cytosol two IPP and one DMAPP molecule are condensed by FARNESYL DIPHOSPHATE SYNTHASE (FPPS) to C_{15} carbon farnesyl diphosphate (FPP) that is the natural precursor of sesquiterpenes (McGarvey and Croteau, 1995; Phillips et al., 2008). The SQUALENE SYNTHASE (SQS) is then connecting two FPP molecules to a C_{30} squalene molecule (Jarstfer et al., 2002). In *Arabidopsis thaliana* the *SQS* gene is widely expressed in all tissues throughout plant development and the enzyme is located in the endoplasmic reticulum (ER) (Busquets et al., 2008). Next, squalene is converted to 2,3-oxidosqualene, the precursor molecule for all known angiosperm cyclic triterpenes and sterols (Rasbery et al., 2007). The cyclization of linear 2,3-oxidoosqualene by oxidosqualene cyclases (OSCs) is the first enzymatic reaction resulting in a triterpene or sterol product. To synthesize a diverse array of triterpene scaffolds, plants express multiple OSCs. For example, the *Arabidopsis thaliana* genome encodes 13 OSCs (summarized in Table 1-1). Some OSCs exhibit a strong product specificity, while other OSCs like the Arabidopsis BARUOL SYNTHASE 1 (BARS1) synthesize in addition to baruol 13 other triterpene scaffolds ranging from mono- to pentacycle triterpenes (Lodeiro et al., 2007). Triterpene scaffolds can then be oxygenized through cytochrome P450 oxygenases, including hydroxylation reactions, cyclization, epoxidation, ring-opening and dealkylation (Seki et al., 2015; Miettinen et al., 2017a). Furthermore, triterpene scaffolds can be decorated with oligosaccharide chains by uridine diphosphate (UDP) dependent glycosyltransferases. Glycosylated triterpenes have a higher water solubility and are often referred as saponins (Vincken et al., 2007; Thimmappa et al., 2014).

Table 1-1: *Arabidopsis thaliana* OSCs and their reaction products (adapted from Thimmappa et al., 2014)

OSC	Gene number	Products	Reference
BARUOL SYNTHASE 1 (BARS1)	AT4G15370	Mixed products[1+2]	Lodeiro et al., 2007
CAMELLIOL C SYNTHASE 1 (CAMS1)	AT1G78955	Mixed products [3,4,5]	Kolesnikova et al., 2007b
CYCLOARTENOL SYNTHASE 1 (CAS1)	AT2G07050	Cycloartenol	Corey et al., 1993
LANOSTEROL SYNTHASE 1 (LSS1)	AT3G45130	Lanosterol	Kolesnikova et al., 2006
LUPEOL SYNTHASE 1 (LUP1)	AT1G78970	Mixed products [6,5,7,8,9]	Herrera et al., 1998
LUPEOL SYNTHASE 2 (LUP2)	AT1G78960	Mixed products [5,8,10,11,12,13,14,9,]	Kushiro et al., 2000
LUPEOL SYNTHASE 4 (LUP4)	AT1G78950	β-Amyrin	Shibuya et al., 2009
LUPEOL SYNTHASE 5 (LUP5)	AT1G66960	Mixed products[10,UC]	(Ebizuka et al., 2003)
MARNERAL SYNTHASE 1 (MRN1)	AT5G42600	Marneral	Xiong et al., 2006
PENTACYCLIC TRITERPENE SYNTHASE 1 (PEN1)	AT4G15340	Mixed products[16,17]	Xiang et al., 2006; Kolesnikova et al., 2007a
PENTACYCLIC TRITERPENE SYNTHASE 3 (PEN3)	At5G36150	Mixed products [18,13,19,20,21,22]	Morlacchi et al., 2009
PENTACYCLIC TRITERPENE SYNTHASE 6 (PEN6)	AT1G78500	Mixed products [12,11,15,UC]	Ebizuka et al., 2003
THALIANOL SYNTHASE (THAS)	AT5G48010	Thalianol	Fazio et al., 2004

[1]baruol; [2] achilleol B; [3]camelliol C; [4]achilleol A; [5]β-amyrin, [6]3β,20-dihydroxylupane, [7]germanicol, [8]taraxasterol; [9]Ψ-taraxasterol, [10]tirucalla-7,21-dien-3β-ol; [11]lupeol; [12]bauerenol; [13]butyrospermol; [14]multiflorenol; [15]α-amyrin; [16](3S,13R)-malabarica-17,21-dien-3,14-diol (arabidiol); [17](3S,13R,21S)-malabarica-17-en-20,21-epoxy-3,14-diol (arabidiol 20,21-epoxide); [18]tirucalla-7,24-dien-3-ol; [19]tirucallol; [20]isotirucallol; [21]13H-malabarica-14(27),17,21-trien-3-ol; [22]dammara-20,24-dien-3-ol; [UC]additional uncharacterized products.

1.3 Triterpene synthesis genes are organized in gene clusters

Grouping of genes on the chromosome into gene clusters for coordinated metabolite syntheses is a common feature in bacteria (Stahl and Murray, 1966). The evolutionary context for gene cluster formation is unknown. One hypothesis is that horizontal gene transfer may drive the evolution of gene clusters and increase fitness (Lawrence and Roth, 1996). However, in nearly all eukaryotes no “operon like” gene clusters were identified and it was presumed that genes are distributed randomly across the chromosome (Blumenthal, 1998; Lee and Sonnhammer, 2003). In 2003, gene clustering in *Saccharomyces cerevisiae*, *Homo sapiens*, *Caenorhabditis elegans*, *Arabidopsis thaliana*, and *Drosophila melanogaster* were demonstrated for the first time (Lee and Sonnhammer, 2003). Eukaryotic gene clusters were not only identified for co-regulated genes, but were shown for genes that are involved in the same metabolic pathway or that are associated in protein–protein complexes (Hurst et al., 2004). In contrast to bacterial operons, genes within gene clusters are driven by independent or bidirectional promoters (Dávila López et al., 2010).

The first plant gene cluster was reported for maize 30 years after identification of microbial gene clusters (Frey et al., 1997). Probably plant gene clusters did not develop by horizontal

gene transfer from microbes but from gene duplication events (Field et al., 2011). Each cluster could span a range between 35 kilo base pairs (kb) to several hundred kb on the chromosome (Boycheva et al., 2014; Nützmann and Osbourn, 2014). Their regulation is tightly controlled and their expression depends on cell type, developmental stages, and environmental triggers (Nützmann and Osbourn, 2014). Most likely, gene clusters are mainly regulated by repressive chromatin signatures (Yu et al., 2016). Transcription factors are unknown, except for the cucurbitacin cluster in cucumber and the momilactone or phytocassane/oryzalide diterpene clusters in rice (Okada et al., 2009; Shang et al., 2014; Yu et al., 2016). Until now, many plant gene clusters have been reported and triterpene biosynthesis is also organized by gene clusters. However, it remains unknown why some metabolic pathways are not clustered (Kliebenstein and Osbourn, 2012; Yu et al., 2016). Prominent examples for triterpene gene clusters are the marneral and thalianol gene clusters in *Arabidopsis thaliana* that are described in Chapter 4.1.1.1 in more detail (Field et al., 2011). Based on screenings of genomic histone 3 lysine trimethylation (H3K27me3) chromatin signatures, more triterpene gene clusters could be identified in different plant species (Yu et al., 2016). The avenacin cluster in oat contains five genes spanning a genomic region over 100 kb, providing that gene clusters are also present in monocots (Yu et al., 2016). Avenacin is a saponin and involved in plant defense (Chapter 1.4). Furthermore, also other monocots like maize containing a gene cluster, e.g. for 2,4-dihydroxy-7-methoxy-1,4-benzoxazin-3-one biosynthesis (Yu et al., 2016). In addition, gene number could be relatively high in gene clusters. The arabidiol-baruol gene cluster in Arabidopsis harbors 16 genes in total (Zhang et al., 2007; Yu et al., 2016).

Besides existence of gene clusters, little is known about their exact regulation and the physiological function of their intermediate- and end products. However, the avenacin cluster provides evidence for the importance of correct cluster regulation in plant growth and defense as described in Chapter 1.4 (Papadopoulou et al., 1999; Kemen et al., 2014).

1.4 Physiological function of plant triterpenes

Very little is known about the physiological function of plant triterpenes. Nevertheless, it is known that some triterpenes are incorporated in plant defense response whereas others are involved in plant development.

Plants facing pathogens and pests synthesize *de novo* a wide array of secondary metabolites with antimicrobial properties. These defense compounds are named phytoalexins (Ahuja et al., 2012). The first direct evidence for triterpenes that function as phytoalexins was found in

the late 1990's. *Saponin-deficient* (*sad*) mutants of diploid oat species *Avena strigose* revealed a compromised resistance against root-infecting fungi *Gaeumannomyces graminis var. tritici*, *Fusarium culmorum* and *Fusarium avenaceum* (Papadopoulou et al., 1999). *Sad1* encodes a β-amyrin synthase in oat that is involved in saponin avenacin A-1 biosynthesis pathway in root tips (Qi et al., 2006). Mutations in *Sad3* and *Sad4* which act downstream of *Sad1*, lead to stunted root growth, membrane trafficking defects in the root epidermis, and root hair deficiency that is caused by accumulation of monodeglucosyl avenacin A-1. In oat *sad1*sad3* and *sad1*sad4* double mutants, a strong growth retardation was not observed, leading to the conclusion that dysregulation and uncontrolled avenacin accumulation could lead to cytotoxicity (Mylona et al., 2008). Besides antimicrobial properties of triterpenes, betulinic acid, and betulinic acid derivatives from *Zizyphus xylopyrus* provided evidence for antifeedant properties against the pest tobacco caterpillar *Spodoptera litura* F (Jagadeesh et al., 1998). In addition, an antifeedant function of betulinic acid and ursolic acid from the chinese chastetree *Vitex negundo* against the agricultural pest *Achoea janata* was demonstrated (Chandramu et al., 2003).

Moreover, triterpenes are involved in plant development. Accumulation of β-amyrin in *sad2* oat mutant leads to a greater proportion of epidermal cells becoming trichoblasts in roots which results in a super hairy root phenotype (Kemen et al., 2014). *Sad2* expression is proposed to be under control of a highly conserved root development process that is present in both monocots and eudicots, including *Arabidopsis thaliana* (Kemen et al., 2014). Earlier, a role for *A. thaliana* MARNERAL SYNTHASE (MRN1) and THALIANOL SYNTHASE (THAS) in plant growth were reported which is studied in Chapter 4 (Field and Osbourn, 2008; Go et al., 2012). In addition to the functions of triterpenes in plant defense and development, ursolic acid triterpene derivatives from the apple variety Annurca function as antioxidant in apple fruits (D'Abrosca et al., 2005).

Furthermore, plant triterpenes possess a high potential as drugs in human medicine. Oleanolic acid, ursolic acid, and betulin are three plant triterpenoids with anti-inflammatory activities that could function as treatments against chronic diseases (Gupta et al., 1969; Liby and Sporn, 2012; Król et al., 2015). Specifically, betulin and betulinic acid have antifungal, antiviral, and anti-carcinogenic properties (Gong et al., 2004; Shai et al., 2008; Machado et al., 2009; Alakurtti, 2013; Król et al., 2015). Both are able to induce the nuclear factor erythroid-2-related factor-2 (Nrf2)-electrophile response element (EpRE) pathway in mammalian cells that is involved in cell detoxification and reduction of reactive oxygen species (ROS) (Surh et al., 2008; Król et al., 2015; Ci et al., 2017). Oleanolic acid and ursolic acid could be easily

harvested from rosemary leaves, olive pulps, and olive leaves (Jaeger et al., 2009). This is a great advantage for the pharma industries, but isolation of other triterpene compounds from plant material could face some difficulties. For example, in betulin production the birch or plane bark of trees have to be harvested (Laszczyk et al., 2006; Jaeger et al., 2009). Furthermore, some triterpenes are only present in small amounts within plant tissues. For an increased pharmacological activity often molecule scaffold modifications have to be conducted (Liby et al., 2007; Field and Osbourn, 2008). Heterologous plant triterpene synthesis in microbial expression host could present a solution for up-scaling production yields and generating a vast structure variety (Fukushima et al., 2013; Arendt et al., 2017; Loeschcke et al., 2017). For identification of novel heterologous synthesized triterpenes with anti-inflammatory activities, an easy and cost efficient approach without complicated triterpene purification steps from expression cultures would be favorable. One approach for identification of inflammation preventive triterpenes is presented in Chapter 3.

1.5 Aim

The vast range of plant triterpenes is mostly unexplored and their physiological functions are for the greater part unknown. However, the examples of avenacin, β-amyrin or ursolic acid provide evidence for triterpenes importance in plant fitness (D'Abrosca et al., 2005; Mylona et al., 2008; Kemen et al., 2014). In addition, plant triterpenes like betulin have a profound pharmacological potential (Gong et al., 2004; Shai et al., 2008; Machado et al., 2009; Alakurtti, 2013; Król et al., 2015). Unfortunately, industrial triterpene isolation from some plant material, including trees, strongly depends on environmental factors and climate (Jäger et al., 2009). Furthermore, triterpene scaffolds often have to be chemical modified to unfold their full potential (Liby et al., 2007). Heterologous synthesis of plant triterpenes in microbial expression hosts could offer a solution for an independent production and establishment of large triterpene structure libraries (Loeschcke et al., 2017).

The aim of this thesis is to shed a light on the physiological function of triterpenes in plants and elucidate their potential in triggering Nrf2-EpRE related anti-inflammatory pathway in animal cells. The thesis addresses triterpene anti-inflammatory activities in mammalian cells by using a luciferase based reporter-gene-assay with triterpene containing bacterial extracts. This approach is described in Chapter 3 in more detail. To validate relevance of triterpenes besides the examples of avenacin, β-amyrin, and ursolic acid, the physiological function of marneral and thalianol in *Arabidopsis thaliana* will be unraveled in a reverse genetic approach, using *Arabidopsis thaliana* knock-out lines, as explained in Chapter 4.

Chapter 2

Material and Methods

2.1 Material

2.1.1 Disposable material

Disposable material	Company
20 µl/ 200 µl/ 1000 µl pipette tips	VWR International; Radnor, PA, USA
1.5 ml/ 2.0 ml reaction tube	Axygen™, Corning; Corning, NY, USA Sarstedt; Hildesheim, Germany
2.5 ml/ 5 ml/ 10 ml/ 25 ml pipettes	Brand; Wertheim, Germany
15 ml/ 50 ml reaction tube	Falcon™, Corning; Corning, NY, USA
Beaker, measuring cylinder	VWR International; Radnor, PA, USA
Cuvettes	Carl Roth; Karlsruhe, Germany
Comb tips	Eppendorf; Hamburg, Germany
Cover glass	Carl Roth; Karlsruhe, Germany
Glass bottles	Fisherbrand™, Thermo Fisher Scientific; Waltham, MA, USA
Glass pearls (2.7 mm)	Carl Roth; Karlsruhe, Germany
Inoculation loops	VWR International; Radnor, PA, USA
Kryo freezing tube	Sarstedt; Nümbrecht, Germany
Object slide	Carl Roth; Karlsruhe, Germany
PCR reaction tube	Sarstedt; Nümbrecht, Germany
PCR plate, white	Nunc™, Thermo Fisher Scientific; Waltham, MA, USA
PCR plate, transparent	Sarstedt; Nümbrecht, Germany
Petri dish	Sarstedt; Nümbrecht, Germany
Pots (9 cm)	Pöppelmann; Lohne, Germany
Square plates (12 x 12 cm)	Corning; Corning, NY, USA

2.1.2 Equipment

Equipment	Company
Autoclave system	Systec; Bergheim, Germany
Balance XP205	Mettler Toledo; Zürich, Switzerland
Balance XB220A/ BJ2200C	Precisa; Dietikon, Switzerland
Binocular microscope	Zeiss; Oberkochen, Germany
Centrifuge, 5424; 5430R; 5810R	Eppendorf; Hamburg, Germany
Centrifuge, PCV-2400	Grant; Cambridge, GB
Bead ruptor 24	Omni international; Kennesaw, GA, USA
Centrifuge Heraeus™ Megafuge™	Heraeus™ Megafuge™; Thermo Fisher Scientific; Waltham, MA, USA
CFX96 Real-Time System	Bio-Rad; Hercules, CA, USA
Gel documentation, GelDoku XR+	Bio-Rad; Hercules, CA, USA
Heat block, Thermomixer C	Eppendorf; Hamburg, Germany
Incubator, ecotron	Infors HT; Switzerland
Incubator for cell culture, InCu safe MCO-20 AIC	Sanyo; Moriguchi, Japan
Laminar floor hood	Kojair; Vilppula, Finland
Magnet stirrer MGS-1001	LMS; Tokyo, Japan
Microwave	Samsung; Seoul, South Korea
Microscope, AE31	Motic; Hong Kong, China
Nanodrop, ND-10000	Thermo Fisher Scientific; Waltham, MA, USA
Neubauer chamber	Celeromics Technologies; Valencia, Spain
pH meter	Eutech instruments™, Thermo Fisher Scientific; Waltham, MA, USA
Pipette set	Eppendorf; Hamburg, Germany
Plant growth chamber, MLR-352	Panasonic; Kadoma, Japan
Plate reader, Infinite M200 Pro	Tecan; Männedorf, Switzerland

Equipment	Company
Thermocylcer C10000 Touch	Bio-Rad; Hercules, CA, USA
Tissue lyser, II	Quiagen, Hilden, Germany
Transformer	Bio-Rad; Hercules, CA, USA
Ultra-sonic bath, Elmasonic	Elma; Singen, Germany
Vacuum pump	Vacuubrand; Wertheim, Germany
Vortex, VTX-3000	LMS; Tokyo, Japan
Water Arium® pro UV ultrapure water system	Sartorius; Göttingen, Germany
Water bath	GFL; Burgwedel, Germany

2.1.3 Chemicals and enzymes

Chemicals and enzymes	Company
2,3-Oxidosqualene	Sigma-Aldrich; Munich, Germany
α-Mem	Gibco™, Thermo Fisher Scientific; Waltham, MA, USA
α-Amyrin	Sigma-Aldrich; Munich, Germany
Accutase, stem pro cell dissociation reagent	Thermo Fisher Scientific; Waltham, MA, USA
Agarose	Sigma-Aldrich; Munich, Germany
ATP disodium salt	Sigma-Aldrich; Munich, Germany
β-Amyrin	Sigma-Aldrich; Munich, Germany
Betulin	Sigma-Aldrich; Munich, Germany
Betulinic acid	Sigma-Aldrich; Munich, Germany
Fetal bovine serum (FBS)	Biochrom, Berlin, Germany
Cycloartenol	Sigma-Aldrich; Munich, Germany
DMSO	Carl Roth; Karlsruhe, Germany
DTT	Duchefa; Haarlem, Netherlands
EDTA	Sigma-Aldrich; Munich, Germany
Ethanol	VWR International; Radnor, PA, USA
Geneticin G418	Sigma-Aldrich; Munich, Germany
H_2O_2	Sigma-Aldrich; Munich, Germany
HCl	Sigma-Aldrich; Munich, Germany
Isopropanol	Sigma-Aldrich; Munich, Germany
KOH	Sigma-Aldrich; Munich, Germany
Lanosterol	Sigma-Aldrich; Munich, Germany
L-Glutamine	Sigma-Aldrich; Munich, Germany
Lithium chloride	Sigma-Aldrich; Munich, Germany
Luciferin	Sigma-Aldrich; Munich, Germany
Lupeol	Sigma-Aldrich; Munich, Germany
Mannitol	Sigma-Aldrich; Munich, Germany
Methyl jasmonate	Sigma-Aldrich; Munich, Germany
$MgCl_2$	Sigma-Aldrich; Munich, Germany
MTT	Sigma-Aldrich; Munich, Germany
M0245 murashige & skoog media (MS), including modified vitamins	Duchefa; Haarlem, Netherlands
Phenol - chloroform - isoamyl alcohol mixture	Sigma-Aldrich; Munich, Germany
Phytosulfokine-α	PolyPeptide Group; Malmö, Sweden
Perligran	Knauf; Iphofen, Germany
Sodium dodecyl sulfate (SDS)	Sigma-Aldrich; Munich, Germany
Sodium hypochlorite	Sigma-Aldrich; Munich, Germany
Sorbitol	Sigma-Aldrich; Munich, Germany
Squalene	Sigma-Aldrich; Munich, Germany
Sucrose	Sigma-Aldrich; Munich, Germany
tBHQ	Sigma-Aldrich; Munich, Germany
tris(hydroxymethyl)-aminomethane (TRIS)	Sigma-Aldrich; Munich, Germany

2.1.4 Kits

Kits	Company
GoTaq® G2 Flexi DNA Polymerase	Promega; Madison, WI, USA
GoTaq® qPCR Master Mix	Promega; Madison, WI, USA
Pierce BCA Protein Assay Kit	Thermo Fisher Scientific; Waltham, MA, USA

2.1.5 Buffers and solutions

Chemicals and Kits	Composition/ Company
DNA extraction buffer	50 mM Tris-HCl (pH 7.5); 300 mM NaCl; 10% sucrose
Luciferase buffer (2x stock)	100 mM Tris-HCl (pH 7.8); 20 mM $MgCl_2$; 2 mM EDTA; distilled water
Luciferase buffer	7.5 ml Luciferase buffer stock (2x); 150 mM DTT; 150 mM ATP; 50 mM luciferin; filled up to 15 ml with distilled water
MTT stock solution	5 mg/ ml MTT in PBS
Passive lysis buffer (PLB)	Promega; Madison, WI, USA
PBS buffer	Gibco™, Thermo Fisher Scientific; Waltham, USA
TAE buffer (50x stock)	2 M Tris/HAc (pH 7.5); 50 mM EDTA
RNA extraction buffer	80 mM Tris-HCl (pH 9.0); 10% SDS; 150 mM LiCl; 50 mM EDTA

2.1.6 Media

Medium	Composition
½ MS medium	2.2 g/l MS M0245; H_2O (pH 5.7, KOH); 0.8% agarose for solid media
α-Mem medium	α-Mem; 15% FBS; 1 mM L-glutamine; 100 U/ ml Penicillin and streptomycin mix; 417 µg/ ml geneticin G418
Lysogeny broth medium (LB-medium)	5 g/l yeast extract; 10 g/l peptone; 10 g/l NaCl; 12 g/l agarose for solid media
Freezing medium	Gibco™, Thermo Fisher Scientific; Waltham, USA
Soil, type VM	Einheitserde; Sinntal-Altengronau, Germany pH 5.8; 1 g/l KCl; 100 mg/l N; 180 mg/l P_2O_5; 180 mg/l K_2O; 200 mg/L S; 500 mg/l Mg

2.1.7 Oligonucleotides

2.1.7.1 Oligonucleotides for T-DNA insertion analysis

Primer	Sequence (5‘ → 3‘)	Target
LBb1.3	ATTTTGCCGATTTCGGAAC	SALK
MRN1.1_LP	CTATTACGCGGCATGTCAGG	SALK_152492
MRN1.1_RP	AGTTGAGGACCGTGCAAAAC	SALK_152492
MRN1.2_LP	AACAAGTTCCATTGTGGTTCG	WiscDsLoxHS206_12C
MRN1.2_RP	TTGTCTCGTGTTAAGGGGATG	WiscDsLoxHS206_12C
THAS1.1_LP	ATGTGGGGGATGAAGATATTG	SALK_064244
THAS1.1_RP	GCTAAAGAAACATGCAGACACC	SALK_064244
WiscDsLoxHs_LB4	TGATCCATGTAGATTTCCCGGACATGAAG	WiscDsLoxHS

2.1.7.2 Oligonucleotides for RT-PCR and qPCR

Primer	Sequence (5‘ → 3‘)	Target
qPCR_CYP71A12_LP	TGTGGTGTTTGGTCCCTATG	AT2G30750
qPCR_CYP71A12_RP	TTGTTCGTGAGCAGATTGAGA	AT2G30750
qPCR_JAZ10_LP	GGTCGCTAATGAAGCAGCATC	AT5G13220
qPCR_JAZ10_RP	TCTGTCTCCATCGACGACTCG	AT5G13220
qPCR_MRN1_LP	TATAGAGTGCTGCATACACTTCCAC	AT5G42580
qPCR_MRN1_RP	CCCAAACTGGCATACCTCCATTAT	AT5G42580
qPCR_MRO_LP	CTATTAGTTCCGCGACTATTAAGCG	AT5G42590
qPCR_MRO_RP	TGATCACCTGTGTGCCCG	AT5G42590
qPCR_MYB51_LP	GGCCAATTATCTTAGACCTGACA	AT1G18570
qPCR_MYB51_RP	CCACGAGCTATAGCAGACCATT	AT1G18570
qPCR_PP2A_LP	CAAGAGGTTCCACACGAAGGA	AT1G69960
qPCR_PP2A_RP	TGTAACCAGCACCACGAGGA	AT1G69960
qPCR_THAH_LP	GTAGAAGAGGGGGAGAAAGAAGAC	AT5G48000
qPCR_THAH_RP	CCAAGCTAGTAACGGAAGAGGTAG	AT5G48000
qPCR_THAS_LP	CAGCATGGCAACCAGTTGAA	AT5G48010
qPCR_THAS_RP	GCTGACCCCGTACATTCTACA	AT5G48010
qPCR_VSP2_LP	TCAGTGACCGTTGGAAGTTGTG	AT5G24770
qPCR_VSP2_RP	GTTCGAACCATTAGGCTTCAATATG	AT5G24770
RT_Actin_long_LP	TAACTCTCCCGCTATGTATGTCGC	AT3G18780
RT_Actin_long_RP	CCACTGAGCACAATGTTACCGTAC	AT3G18780
RT_MRN1_LP	GAGCATGTCAAAGAGTTACTCCG	AT5G42580
RT_MRN1_RP	AGAAGGGAGCATCCAAATCTC	AT5G42580
RT_MRN1_LP2	GTTAGACAAAGAGCACTACGAACC	AT5G42580 (Go et al., 2012)
RT_MRN1_RP2	ACACTCAAGGTACTCTTGCTCC	AT5G42580 (Go et al., 2012)
RT_THAS_LP	TCATGACGAATCCACCAGAT	AT5G48010
RT_THAS_RP	GCTGACCCCGTACATTCTACA	AT5G48010

2.1.8 Organisms

2.1.8.1 *Arabidopsis thaliana* genotypes

In this thesis, homozygous mutant lines were obtained in the background of ecotype Columbia-0 (Col-0, NASC-Nr. N1093). Homozygosity of T-DNA insertions were verified in T-DNA insertion analysis with polymerase chain reaction (Chapter 2.2.3.3.2).

ID	AT number	Source
coi1-34	AT2G39940	Acosta et al., 2013
Col-0		Kopriva workgroup, University of Cologne, Germany
ninja-1	AT4G28910	Acosta et al., 2013
mrn1	AT5G42580	SALK_152492
mrn1_2	AT5G42580	WiscDsLoxHS206_12C
*mrn1*thas*	AT5G48010/ AT5G42580	Cross between SALK_064244 and SALK_152492
*pskr1/2*psy1r*	AT2G02220/ AT5G53890/ AT1G72300	Mosher et al., 2013
thas	AT5G48010	SALK_064244

2.1.8.2 Root associated bacteria

Strain	Class	Source
Burkholderia glumae	Betaproteobacteria	Kopriva workgroup, University of Cologne, Germany
Massilia sp. Root133	Betaproteobacteria	Bai et al., 2015
Pseudomonas sp. Root401	Gammaproteobacteria	Bai et al., 2015
Pseudomonas sp. Root68	Gammaproteobacteria	Bai et al., 2015
Pseudoxanthomonas sp. Root65	Gammaproteobacteria	Bai et al., 2015
Rhodanobacter sp. Root480	Gammaproteobacteria	Bai et al., 2015

2.1.8.3 *Rhodobacter capsulatus* and *Pseudomonas putida* strains

Bacteria expressing different plant triterpene synthases were received as dried n-hexane extracts from Dr. Thomas Drepper and Dr. Anita Loeschcke workgroup from the institute of molecular enzyme technology (University Düsseldorf, Germany) and suspended in dimethyl sulfoxide (DMSO) (personal communication with Dr. Thomas Drepper and Dr. Anita Loeschcke, 2015, Institute of Molecular Enzyme Technology, University Düsseldorf, Germany; Domröse et al., 2015).

Strain	Construct
Pseudomonas putida KT2440	pTREX
Pseudomonas putida KT2440	pTREX-pig
Rhodobacter capsulatus 37b4	
Rhodobacter capsulatus 37b4	pRhon5Hi-2
Rhodobacter capsulatus 37b4	pRhon5Hi-2-*SQS*
Rhodobacter capsulatus 37b4	pRhon5Hi-2-*SQS-SQE*
Rhodobacter capsulatus 37b4	pRhon5Hi-2-$BARS1_{His\text{-}tag}$-*SQS-SQE*
Rhodobacter capsulatus 37b4	pRhon5Hi-2-$CAMS1_{His\text{-}tag}$-*SQS-SQE*

Strain	**Construct**
Rhodobacter capsulatus 37b4	pRhon5Hi-2-*CAS1*$_{His\text{-}tag}$-*SQS-SQE*
Rhodobacter capsulatus 37b4	pRhon5Hi-2-*LUP11*$_{His\text{-}tag}$-*SQS-SQE*
Rhodobacter capsulatus 37b4	pRhon5Hi-2-*MRN1*$_{His\text{-}tag}$-*SQS-SQE*
Rhodobacter capsulatus 37b4	pRhon5Hi-2-*PEN1*$_{His\text{-}tag}$-*SQS-SQE*
Rhodobacter capsulatus 37b4	pRhon5Hi-2-*THAS*$_{His\text{-}tag}$-*SQS-SQE*
Rhodobacter capsulatus B10SΔE	
Rhodobacter capsulatus B10SΔE	pRhon5Hi-2
Rhodobacter capsulatus B10SΔE	pRhon5Hi-2-*SQS*
Rhodobacter capsulatus B10SΔE	pRhon5Hi-2-*SQS-SQE*
Rhodobacter capsulatus B10SΔE	pRhon5Hi-2-*BARS1*$_{His\text{-}tag}$-*SQS-SQE*
Rhodobacter capsulatus B10SΔE	pRhon5Hi-2-*CAMS1*$_{His\text{-}tag}$-*SQS-SQE*
Rhodobacter capsulatus B10SΔE	pRhon5Hi-2-*LSS1*$_{His\text{-}tag}$-*SQS-SQE*
Rhodobacter capsulatus B10SΔE	pRhon5Hi-2-*LUP11*$_{His\text{-}tag}$-*SQS-SQE*
Rhodobacter capsulatus B10SΔE	pRhon5Hi-2-LUP2$_{His\text{-}tag}$-*SQS-SQE*
Rhodobacter capsulatus SB1003	
Rhodobacter capsulatus SB1003	pRhon5Hi-2
Rhodobacter capsulatus SB1003	pRhon5Hi-2-*SQS*
Rhodobacter capsulatus SB1003	pRhon5Hi-2-*SQS-SQE*
Rhodobacter capsulatus SB1003	pRhon5Hi-2-*BARS1*$_{His\text{-}tag}$-*SQS-SQE*
Rhodobacter capsulatus SB1003	pRhon5Hi-2-*CAMS1*$_{His\text{-}tag}$-*SQS-SQE*
Rhodobacter capsulatus SB1003	pRhon5Hi-2-*CAS1*$_{His\text{-}tag}$-*SQS-SQE*
Rhodobacter capsulatus SB1003	pRhon5Hi-2-*LUP11*$_{His\text{-}tag}$-*SQS-SQE*
Rhodobacter capsulatus SB1003	pRhon5Hi-2-*LUP2*$_{His\text{-}tag}$-*SQS-SQE*
Rhodobacter capsulatus SB1003	pRhon5Hi-2-LUP5$_{His\text{-}tag}$-*SQS-SQE*
Rhodobacter capsulatus SB1003	pRhon5Hi-2-*MRN1*$_{His\text{-}tag}$-*SQS-SQE*
Rhodobacter capsulatus SB1003	pRhon5Hi-2-*PEN1*$_{His\text{-}tag}$-*SQS-SQE*
Rhodobacter capsulatus SB1003	pRhon5Hi-2-*PEN3*$_{His\text{-}tag}$-*SQS-SQE*
Rhodobacter capsulatus SB1003	pRhon5Hi-2-*PEN6*$_{His\text{-}tag}$-*SQS-SQE*

2.1.8.4 Murine hepatoma cell line

Stable murine hepatoma cell line Hepa-1C1C7, containing a firefly luciferase (LUX) fused to an EpRE-(mouse glutathione-S-transferase Ya (mGST-Ya)) promoter element, was provided by division of toxicology at the Wageningen University, Netherlands (Boerboom et al., 2006).

2.1.9 Computer software

Software	**Company/ Developers**
CFX-manager	Bio-Rad; Hercules, CA, USA
i-control	Tecan; Männedorf, Switzerland
Office	Microsoft; Redmond, WA, USA
Prism	Graphpad; La Jolla, CA, USA
Snapgene	GSL Biotech LLC, Chicago, IL, USA
ImageJ	Wayne Rasband; Bethesda, MD, USA
Rosette tracker	De Vylder et al., 2012

2.2 Methods

2.2.1 Cultivation of murine hepatoma cell culture Hepa-1C1C7 EpRe-LUX

For long time storage, hepatoma cells were frozen in liquid nitrogen. For cultivating, frozen cell aliquots were evenly transferred on a cell culture petri dish, containing 13 ml α-Mem media (37 °C). Cells were incubated at 37 °C, 5% CO_2 and 95% air humidity. After 48 to 72 h, cells were grown confluent on petri dish surface and passaged to a new petri dish. For passaging, cells were washed two times with 10 ml PBS buffer (37 °C). Subsequently, 2 ml accutase were spread over petri dish to detach cells from petri dish surface. Reaction was stopped by 10 ml α-Mem media (37 °C). Next, solution was transferred on new petri dish, diluted $^1/_4$, $^1/_8$, and $^1/_{16}$ in 13 ml α-Mem media (37 °C). In this way cell culture was kept up to 20 passages, before thawing a new glycerol stock.

2.2.2 Cell based assays

2.2.2.1 Preparation of standard solutions

For preparation of stock solution, α-Amyrin, β-Amyrin, betulin, betulinic acid, cycloartenol, lanosterol, lupeol, squalene, 2,3-oxidosqualene, and tert-butylhydroquinone (tBHQ) were diluted in DMSO, ranging from 0.1 mM to 20.0 mM. All solutions were stored at -20 °C.

2.2.2.2 Preparation of bacterial extracts

Hydrophobic phase of transformed *Rhodobacter capsulatus* strains B10SΔE, 37b4, and SB1003 were extracted twice with acetone in addition to n hexane and dried (Loeschcke et al., 2017). These strains are described in more detail in Chapter 3.1.4.1. Extracts were diluted in 9 µl DMSO/1 OD_{600} cells in culture media. For better solubility, solutions were heated up for 10 min at 38 °C, while shaking. Afterwards, extracts were treated with ultrasonic for 4 min and heated for 10 min 60 °C, while shaking.

Within dried ethanol phase extracts of 1 ml *Pseudomonas putida* cultures, 30 µg prodigiosin was measured with LC-MS (personal communication with Dr. Thomas Drepper and Dr. Anita Loeschcke, 2015, Institute of Molecular Enzyme Technology, University Düsseldorf, Germany). Pellets were solved in DMSO to a final concentration of 300 µM prodigiosin. All extracts were stored at -80 °C.

2.2.2.3 Preparation of 96 well plates

For cell based assays, cells grown up to 80% confluency. They were detached from plastic as described above (Chapter 2.2.1). To ensure similar conditions in each experiment, cells were counted using a Neubauer chamber. 20,000 cells were distributed into each well of a clear 96 well plate to a final volume of 200 µl per well by adding α-Mem media (37 °C). The plate was incubated at 37 °C, 5% CO_2 and 95% air humidity for 24 h. Next, wells were washed with 200 µl PBS (at 37 °C), and 200 µl media, supplemented with standard solutions, bacterial extract (0.5 to 1.5% (v/v)), or DMSO (negative control) was applied per well. After additional 24 h incubation, medium was removed with a vacuum pump. Wells were washed with 200 µl PBS and 40 µl passive lysis buffer (PLB) were added into each well. Cell lysis took place at room temperature (RT) on a shaker for 15 min at 600 rpm. Subsequently, the insoluble cell compartments were pelleted at 2900x g for 15 min at 4 °C. The supernatant were used for colorimetric detection and quantification of total protein and luciferase assay, as described below.

2.2.2.4 Colorimetric detection and quantitation of total protein

For quantification of protein content in cell lysate *Pierce BCA Protein Assay Kit* was used. This method is based on the reduction of Cu^{+2} to Cu^{+1} by protein in an alkaline medium with colorimetric detection of Cu^{+1} using a reagent containing bicinchoninic acid (BCA). 15 µl of 2 mM EDTA was applied into each well of a clear 96 well micro titer plate. 10 µl cell lysate supernatant was added (Chapter 2.2.2.3). Kit solutions, named A and B, were mixed in a 50:1 ratio. 200 µl AB solution was pipetted into each well. The reactions were incubated for 30 min at 37 °C. The reaction resulted in a purple-colored product. Sample absorbance was measured at λ = 562 nm using a microplate reader and software I-control. Typically, 6 to 8 technical replicates were conducted. The protein content per well was calculated using a linear regression line that was based on absorbance at different bovine serum albumin (BSA) concentrations (Figure 2-1).

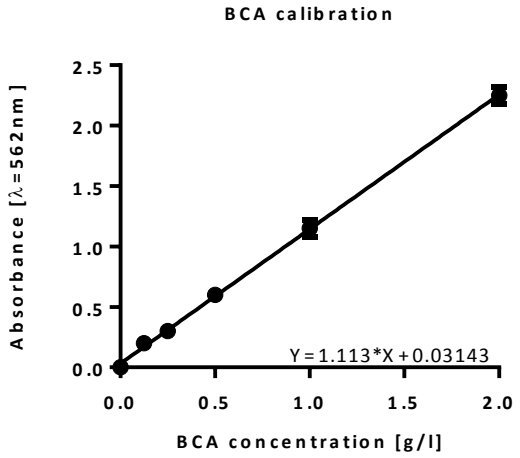

Figure 2-1: BCA protein content calibration
The BCA calibration was conducted as described in *Pierce BCA Protein Assay Kit* users protocol for each experiment. Linear regression was calculated with MS EXCEL.

2.2.2.5 Luciferase reporter-gene-assay

Firefly luciferases are commonly used in reporter-gene-assays and originally derive from beetle *Photinus pyralis*. In presence of oxygen and ATP, this enzyme converts luciferin to oxyluciferin that emits a greenish yellow light between λ = 550 to 570 nm. An EpRE-(mGST-Ya)-LUX construct in murine hepatoma cells was used as reporter for anti-inflammatory properties of tested molecules and extracts (Boerboom et al., 2006).

15 µl of 2 mM EDTA was applied into each well of a white 96 well micro titer plate. 10 µl cell lysate supernatant was added into each well (Chapter 2.2.2.3). For each experiment, 1x luciferase buffer was prepared freshly from a 2x luciferase buffer stock. This buffer was kept dark and on ice. 100 µl buffer was then applied by a microplate reader. After adding buffer to a well, the microplate reader determined luminescence [relative light units (RLU)]. The microplate reader was programmed with software I-control: Plate; part of plate; well; injector A; 100 µl, speed 200 µl/ s; wait 2 s; luminescence, interrogation 10.000 ms; attenuation none. Typically, 6 to 8 technical replicates were conducted.

2.2.2.6 Calculation of luciferase activity

Luciferase activity was normalized against protein content and subtracted from background luminescence for each well as follows. RLUs of background control $\bar{x}_{background}$ were subtracted from RLUs of each well x and divided by the mean protein concentration $\bar{y}$ of the respective treatment, to obtain z. Next, z was divided with $\bar{z}_{DMSO}$ of respective DMSO control

to obtain fold change data of luciferase activity. The fold change data is logarithmized with $\log_2$ for better comparison between experiments.

$$\text{Log}_2 \text{ luciferase activity} = \text{Log}_2 \left(\frac{\text{x} - \bar{\text{x}}_{\text{background}}}{\bar{\text{y}}} \Big/ \bar{\text{z}}_{\text{DMSO}} \right)$$

2.2.2.7 Cell viability assay

For estimation of cell viability that includes cell survival and proliferation after treatment, quantitative colorimetric assays were conducted using tetrazolium salts. Applying 3-(4,5-dimethylthiazol-2-yl)-2,5-diphenyltetrazolium bromide (MTT) to living cells, MTT is proposed to be converted in mitochondria by NAD(P)H-dependent cellular oxidoreductase enzymes to formazan that forms insoluble crystals. These crystals are dissolved in HCl and absorb light at λ = 570 nm. Due to intact mitochondria being required for this enzymatic reaction, this assay is used to measure cytotoxic and cytostatic compound activity (Mosmann, 1983).

MTT working solution was prepared from 1:10 dilution of stock solution in PBS. 96 well plates were prepared as described above, except that they were not lysed (Chapter 2.2.2.3). After washing with 100 µl PBS (37 °C), cells were treated with 10 µl MTT working solution (37 °C) and incubated at 37 °C, 5% CO_2 and 95% air humidity for 2 h. After incubation, crystals were dissolved in 100 µl of 40 mM HCl in isopropanol at 37 °C for 30 min. The plate was mixed gently and incubated for further 30 min. The reaction resulted in a purple-colored product. Sample absorbance was measured at λ = 570 nm using a microplate reader and software I-control. Typically, 6 to 8 technical replicates were conducted. The cell viability was calculated using a linear regression line that represents absorbance, or oxidoreductase enzyme activity for different cell counts (Figure 2-2). Absorbance of background control $\bar{x}_{background}$ were subtracted from absorbance of each well x and divided by the slope of regression line $\bar{y}$ of the respective treatment, to obtain z. Next, z was divided with $\bar{z}_{DMSO}$ of respective DMSO control to obtain fold change data cell viability. The fold change data is logarithmized with $\log_2$ for better comparison between experiments.

$$\text{Log}_2 \text{ cell viability} = \text{Log}_2 \left(\frac{x - \bar{x}_{background}}{\bar{y}} \Big/ \bar{z}_{DMSO} \right)$$

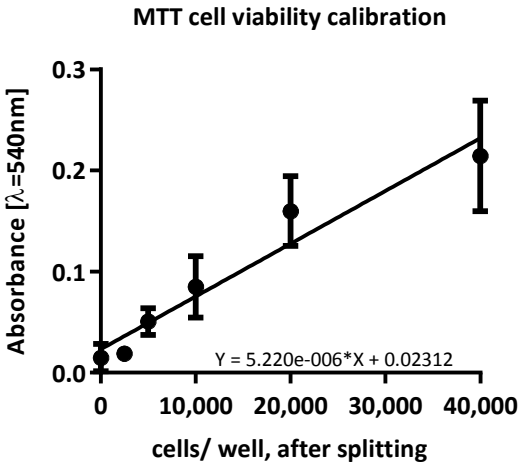

Figure 2-2: MTT cell density calibration
Different cell numbers were transferred into a 96 well plate: 0; 2,500; 5,000, 10,000; 20,000; 40,000. Absorbance after MTT treatment was conducted after 2 days, as described in material and methods 2.2.2.7. Standard deviation is presented as error bar.

2.2.3 *Arabidopsis thaliana* cultivation and plant growth experiments

2.2.3.1 Plant material

Arabidopsis thaliana T-DNA knock-out lines SALK_152492 (AT5G42600, referred as *mrn1*), WiscDsLoxHS206_12C (AT5G42600, referred as *mrn1_2*) and SALK_064244 (AT5G48010, referred as *thas*) were ordered at The European Arabidopsis Stock Centre (Berardini et al., 2015). T-DNA lines were generated in the background of *Arabidopsis thaliana* Columbia-0 ecotype and containing genomic T-DNA insertions that disrupt correct gene expression (Alonso et al., 2003; Woody et al., 2007). SALK_152492 and SALK_064244 were crossed by transferring pollen from one plant to flower stamp of another under binocular microscope and was named *mrn1*thas*.

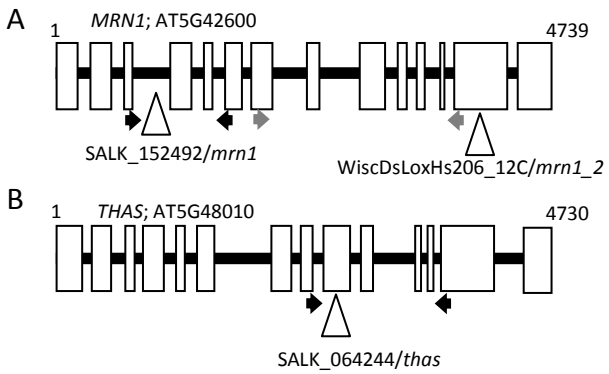

Figure 2-3: T-DNA insertion lines
A: SALK152492 has a T-DNA insertion in 3rd intron of *MRN1*. WiscDsLoxHS206_12C has a T-DNA insertion in 13th exon of *MRN*1. Black and gray arrows indicate RT-PCR primer pairs RT_MRN1_LP + RT_MRN1_RP and RT_MRN1_LP2 + RT_MRN1_RP2, respectively. B: SALK_064244 has a T-DNA insertion in 8th exon of THAS. Black arrows indicate RT-PCR primer pairs RT_THAS_LP + RT_THAS_RP (Chapter 2.2.3.3.6).

2.2.3.2 Plant growth conditions

Plants were either cultivated on soil media or ½ MS media. For cultivation on soil, seeds were put onto soil in 9 cm pots and were stratified at 4 °C in the dark for 4 days. The soil was a mixture of *Einheitserde type VM* and *Perligran* (100~150 g/70 L). Next, seedlings were transferred into a growth chamber at 20 °C, 60% air humidity, and 150 µE light under long-day conditions (16h light/8 h dark). After further 7 days, seedlings were separated onto new soil. For cultivation on ½ MS media, seeds were first sterilized with chlorine gas (125 ml sodium hypochlorite and 5 ml concentrated HCl) for 3.5 h. Thereafter, seeds were transferred onto 45 ml ½ MS media (0.5% sucrose) in 12 cm square plates. Next, seeds were stratified at 4 °C in the dark for 4 days and incubated under long-day conditions in an environmental test chamber (22 °C, 150 µE).

2.2.3.3 Molecular biologic methods

2.2.3.3.1 Extraction of genomic DNA

Genomic DNA (gDNA) was extracted out of ~20 mm² leaf material in a one-step approach (Berendzen et al., 2005). This method is suited for large scale gDNA isolation. Plant material was transferred into a 1.5 ml reaction tube containing 4 glass beads and 300 µl DNA extraction buffer supplemented with 10% sucrose. Leaf material was ground in a bead disruptor at RT. Afterwards solid cell compartments were sediment at 12000x g for 5 min. gDNA was used for polymerase chain reaction in T-DNA insertion analysis.

2.2.3.3.2 T-DNA insertion analysis with polymerase chain reaction (PCR)

The homozygosity of T-DNA insertions in Arabidopsis genome was verified with polymerase chain reaction (PCR) (Saiki et al., 1988). PCR is used for specific DNA fragment amplification on a template DNA.

In the first step, template DNA is denatured at 95 °C. After denaturation, DNA is cooled down to 54 - 60 °C. At this temperature, short oligonucleotides/ primers with free 3' hydroxy-termini specifically annealed to DNA template. For T-DNA insertion analysis gene specific primer pairs were designed to amplify wild-type alleles: left primer (LP) and right primer (RP) (Figure 2-4 A). T-DNA specific left border primer (LBP) with LP or RP primers were used to verify T-DNA insertions. Thermostable GoTaq® DNA polymerase then extended DNA strain at 72 °C. Denaturation, annealing, and extension are repeated 35 to 40 times. DNA amplification products were separated by size on an agarose gel with gel electrophoresis (Figure 2-4; Chapter 2.2.3.3.3). The standard PCR for T-DNA insertion analysis in extracted gDNA was set up as follows:

4.0 µl	5x green GoTaq® reaction buffer
2.0 µl	25 mM $MgCl_2$
0.4 µl	10 mM dNTPs
0.4 µl	10 µM primer 1
0.4 µl	10 µM primer 2
1.0 µl	template DNA
0.1 µl	5 U/µl DNA GoTaq® polymerase
ad 20 µl	H_2O

PCR was realized in a thermo cycler for tight control of temperatures and timing:

1. denaturation	95 °C	180 s	
2. denaturation	95 °C	45 s	x 35
3. annealing	54 °C	45 s	
4. extension	72 °C	90 s	
5. extension	72 °C	180 s	
6. chill	12 °C	∞	

Afterwards, amplified DNA was separated by size in an agarose gel.

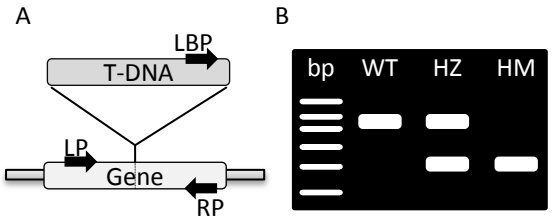

Figure 2-4: T-DNA insertion analysis
A: Genomic T-DNA insertion can be amplified by T-DNA specific left border primer (LBP) and gene specific right primer (RP). Wild-type allele is amplified by using left primer (LP) and RP. B: Gel electrophoresis of amplification products. Fragments that are corresponding to homozygous wild-type allele, heterozygous T-DNA insertion (HZ), and homozygous T-DNA insertion (HM). bp is the DNA ladder marker.

2.2.3.3.3 Agarose gel electrophoresis

Agarose gel electrophoresis is used for DNA separation by size. The agarose gel matrix was made out of 1x TAE buffer containing 1 - 2% agarose. The agarose was dissolved by heating and 0.5 µg/mL ethidium bromide (EtBr) is added. EtBr is a dye intercalates into DNA molecules and later DNA was visualized under UV light. Next, gel is poured in a self-made plastic framework with pockets for DNA samples. Hardened gel is transferred into a gel chamber filled with 1x TAE buffer. Amplified DNA fragments from PCR already contained a green loading dye and 20 µl were transferred into gel pockets. After sample transfer, an electrical field was applied on the agarose gel (150 V, 300 mA, 30 min). Since the DNA backbone is negatively charged, DNA moved to the anode in electrical field and molecules were separated by size through the gel matrix. 1 kB DNA ladder was used as size reference Figure 2-5. After gel electrophoreses DNA molecules were visualized and documented under UV light (example in Figure 2-4 B).

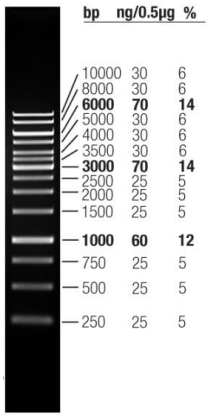

Figure 2-5: GeneRuler™ 1 kb DNA Ladder
Separation of GeneRuler™ 1 kb DNA Ladder on a 1% agarose gel (Thermo Fisher Scientific; Waltham, MA, USA).

2.2.3.3.4 RNA isolation

For transcription analysis, RNA was extracted from plant tissues. Around 50 - 100 mg frozen plant material in 1.5 ml reaction tubes were homogenized with 3 to 4 glass beads in a cooled tissue lyser at 25 kHz for 30 s. Next, 500 µl RNA extraction buffer was added and mixed for 15 s. Afterwards, 500 µl phenol-chloroform-isoamylalcohol mix was pipetted into the solution and mixed for 15 s. Samples were consecutively placed on a shaker at 200 rpm, till all samples were ready for centrifugation at 21000x g for 25 min. Each sample formed a phenolic and an aqueous phase. The aqueous phase contained the RNA and was transferred into new 1.5 ml reaction tube. 500 µl phenol-chloroform-isoamylalcohol mix were added and centrifuged again. This step was repeated one more time. Aqueous supernatant was then transferred into 130 µl 8 M LiCl to precipitate RNA. This solution was mixed properly and stored at -20 °C for 1 d. On the following day, samples were thaw on ice and RNA was pelleted at 21000x g for 20 min at 4 °C. Supernatant was discarded and RNA pellet was dissolved in 300 µl H_2O by placing sample for 10 min at 65 °C while shaking at 200 rpm. RNA was precipitated with 100 µl 8 M LiCl, mixed and stored at -20 °C for 1 d. On third day, samples were thawed on ice and RNA was pelleted at 21000x g for 20 min at 4 °C. RNA pellet was washed with 400 µl 79% EtOH at 21000x g for 5 min at 4 °C. EtOH was discarded carefully and RNA was dried for 5 min under the fume hood. Dry RNA pellets were resolved in 30 µl H_2O at 65 °C for 10 min, while shaking at 200 rpm. Final RNA concentration was measured in triplicates with a nanodrop at λ=260 nm.

2.2.3.3.5 Reverse transcription

Reverse transcription was used to synthesize complementary DNA (cDNA) from messenger RNA (mRNA). Generally reverse transcriptase enzymes derived from RNA-containing retroviruses. Here, a novel QuantiTect Reverse transcriptase was used (QIAGEN, Germany). First, 200 – 800 ng RNA was transferred into a PCR reaction tube and was diluted to 6 µl with H_2O on ice. For gDNA degradation, 1 µl gDNA wipeout buffer were added and incubated at 42 °C for 3 min. For cDNA synthesis 2 µl RT buffer, 0.5 µl RT primer mix, and 0.5 µl reverse transcriptase were supplemented. Samples were mixed and heated at 42 °C for 30 min. Enzymes were then deactivated at 90 °C for 3 min. Synthesized cDNA was stored at -20 °C and used for reverse transcription polymerase chain reaction and Real-time polymerase chain reaction (Chapter 2.2.3.3.6 and 2.2.3.3.7).

2.2.3.3.6 Reverse transcription polymerase chain reaction (RT-PCR)

Reverse transcription polymerase chain reaction (RT-PCR) is a semi-quantitative method to determine gene transcript levels. The protocol is based on general PCR protocol, but with minor changes (Chapter 2.2.3.3.2). First, 0.5 µl cDNA (corresponding to 20 ng RNA) was used. Second, primer pairs were designed to amplify ~500 bp gene fragments that span different exons (Figure 2-3). Third, *ACTIN* transcription level was used as reference gene in each sample. In thermos cycler, 30 PCR cycles for *ACTIN* and up to 41 PCR cycles for *MRN1* and *THAS* amplification were used.

2.2.3.3.7 Real-time polymerase chain reaction (qPCR)

Real-time polymerase chain reaction (qPCR) is a highly sensitive method for gene transcript detection. In qPCR the fluorescent dye SYBR Green was used for DNA detection. It is only fluorescent when it intercalates into double-stranded DNA. Therefore, fluorescence intensity is proportional to the amount of amplified DNA and was recorded during PCR process. qPCR primer pairs were designed to amplify 70 - 150 bp of target gene, spanning different exons. SERINE/THREONINE PROTEIN PHOSPHATASE 2A (PP2A, AT1G69960) was used as reference gene. For procedure, GoTaq® qPCR Master Mix was used for qPCR:

5 µl	GoTaq® qPCR Master Mix
4 µl	1 µM primer-mix (primer 1 and 2)
2 - 8 ng	cDNA
ad 10 µl	H_2O

The temperature protocol was established as follows:

1. denaturation	95 °C	120 s	
2. denaturation	95 °C	15 s	
3. annealing	59 °C	30 s	x 40
4. extension	60 °C	30 s	
5. denaturation	95 °C	30 s	
6. annealing	59 °C	30 s	melting
7. extension	60 °C	30 s	curve
9. denaturation	95 °C		

Relative transcript level was calculated by ddC_T method (Livak and Schmittgen, 2001). Melting curve analysis was performed to confirm primer specificity. The C_T value of a sample is the cycle number when a global fluorescence threshold is exceeded. For calculation C_T

values of target and reference genes are subtracted in the first step. In the second step C_T values are normalized to a control (e.g. Col-0, untreated). In this thesis, expression level is given on a logarithmic scale (relative expression).

First step: $\Delta C_T = C_{T\,(\text{target gene})} - C_{T\,(\text{reference gene})}$

Second step: $\Delta\Delta C_T = \Delta C_T - \Delta C_{T\,(\text{standardization})}$

Relative expression: $\text{RE} = -\Delta\Delta C_T$

Calculating fold-change: $\text{relative quantification (RQ)} = 2^{-\Delta\Delta C_T}$

2.2.3.4 Plant growth assays

2.2.3.4.1 Phytosulfokine-α and methyl jasmonate treatment

To investigate the link between triterpene synthesis and phytosulfokine-α (PSK-α) or jasmonic acid signaling, *Arabidopsis thaliana* seedlings were treated with hormones and root growth was measured. First, seeds were sterilized with chlorine gas and 1 mM PSK-α solution as well as 10 µM methyl jasmonate (MeJa) solution were prepared. Second, seeds were placed onto ½ MS media (0.5% sucrose) in square plates and stratified at 4 °C in the dark for 4 days. Next, seeds were grown in plant growth chamber for 7 days. New ½ MS media supplemented with 0.1 µM PSK-α, 10 µM MeJa, or H_2O (Mock) were prepared. Seedlings were carefully transferred onto new media in a row out of 8 plants horizontally and incubated in plant growth chamber for further 7 days. For growth measurement, plants were photographically documented and gain in root length was quantified in ImageJ software.
For transcription studies, plants were grown on ½ media (0.5% sucrose) for 14 days and sprayed with 1 µM PSK-α, 10 µM MeJa, or H_2O (Mock) solution. After 4 h, plant roots were frozen in liquid nitrogen and stored at -80 °C, till RNA was isolated (Chapter 2.2.3.3.4).

2.2.3.4.2 Abiotic stress treatment

Abiotic stress was simulated by chemical treatments and rosette size was chosen as output as described in literature (Claeys et al., 2014). Seeds were sterilized with chlorine gas. Next, 12 seeds were spread across a 4 x 3 raster on ½ MS media (0.5% sucrose) per square plate supplemented with 1 mM H_2O_2, 50 mM NaCl, 25 mM mannitol, 75 mm sorbitol; or H_2O (Mock). Seeds were stratified for 4 days at 4 °C in the dark and then were incubated under long day conditions for 21 days. Seedlings were photographically documented and rosette anatomy was analyzed with rosette tracker software (De Vylder et al., 2012). This software

automatically calculates rosette leaf area, diameter, compactness and stockiness (Figure 2-6). The compactness describes the ratio between the area of the rosette and the area enclosed by a convex hull around the rosette (Arvidsson et al., 2011). The stockiness describes the circularity of a plant. It is defined as $4x\pi x\text{rosette area}/(\text{perimeter})^2$ and ranging from 0 to 1 (perfect circle) (Jansen et al., 2009; De Vylder et al., 2012).

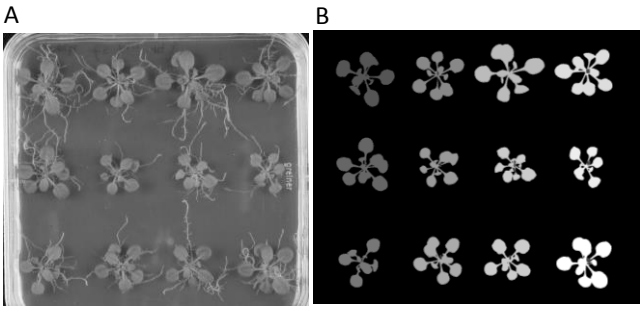

Figure 2-6: Rosette tracking in rosette tracker software
A: Image of 21 days old seedlings. B: Recognition of single rosettes in rosette tracker software (De Vylder et al., 2012).

2.2.3.4.3 Plant bacteria co-cultivation assay

To investigate plant microbe interactions in triterpene deficient plants, plant bacteria co-cultivation assays were conducted. Bacterial strains were received from Anna Koprivova (Kopriva workgroup, University of Cologne, Germany) and the Max Planck Institute for Plant Breeding Research (Cologne, Germany) (Chapter 0). Bacteria were stored in LB media (50% glycerol) at -80 °C. For experiment, seeds were sterilized with chlorine gas and were placed onto ½ MS media (0.5% sucrose) in square plates. After stratification at 4 °C in the dark for 4 days, seeds were germinated under long-day conditions for 7 days (Figure 2-7). On day 6, 5 ml LB media was inoculated with bacteria and incubated at 28 °C. Alternatively, *Burkholderia glumae* pre-culture was prepared at day 5 and incubated at 30 °C. For co-cultivation, 3 ml bacteria pre-culture were pelleted at 1200x g for 3 min. Next, cell pellet was washed two times with 3 ml 10 mM $MgCl_2$ and suspended in 3 ml 10 mM $MgCl_2$. Optical density of bacteria solution was measured at λ=600 nm and diluted to OD_{600}=0.01 in 10 mM $MgCl_2$. Warm ½ MS media (43 °C) was supplemented with bacteria solution to final $OD_{600}=5x10^{-6}$ or $5x10^{-5}$. $MgCl_2$ was used as Mock control. 7 day old seedlings were carefully transferred onto inoculated ½ MS media, 8 seedlings per plate. After further incubation under long-day conditions for 11 or 14 days, seedling fresh weights were measured and plant root material was frozen in liquid nitrogen and stored at -80 °C.

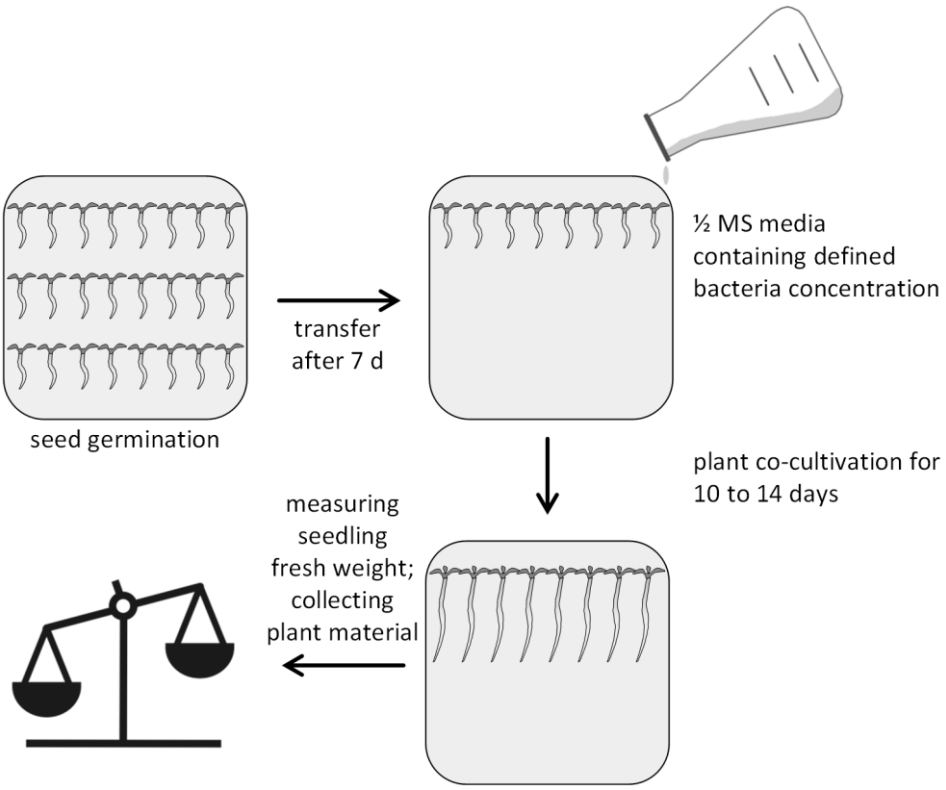

Figure 2-7: Plant bacteria co-cultivation assay
Arabidopsis seeds were germinated on 45 ml ½ MS media (0.5% sucrose) for 7 days. Next, seedlings were transferred onto new ½ MS media supplemented with bacteria solution (OD_{600}=5x10^{-6} or 5x10^{-5}). Plants and bacteria were co-cultivated for additional 11 or 14 days. Seedlings fresh weight were measured and plant material were frozen in liquid nitrogen and stored at -80 °C.

Chapter 3

Anti-inflammatory activity of plant triterpenes on nuclear factor erythroid-2-related factor-2 (Nrf2) - electrophile response element (EpRE) pathway in murine hepatoma cells Hepa-1C1C7

3.1 Introduction

Cancer is one of the most widespread diseases in our civilization. In Germany, over 450,000 new cases were reported in 2013. Since 1970s, the rate of new cases has doubled, but at the same time the mortality rate has decreased. This phenomenon could be explained by the demographic aging of population within this time span (Barnes et al., 2016). Nevertheless, huge efforts in science are accountable for success in cancer treatments. And one paragon for developing new drugs for cancer treatments are secondary metabolites produced by living organisms. One point of application is chemoprevention of cancer development that is related to induction of genetic instability by inflammatory mediators (Colotta et al., 2009).

3.1.1 Cancer chemoprevention by Nrf2-EpRE anti-inflammatory pathway

Cancer development is described in three distinct phases: (1) initiation; (2) promotion; (3) progression. (1) The cancer initiation is an irreversible process induced by genotoxic DNA upon exposure to endogenous or exogenous carcinogens. (2) Cancer promotion is a long-lasting but reversible growth process of the initiated cell by clonal expansion that results in tumor formation. And (3), the tumor develops invasive and metastatic potentials that leads to neoplastic transformation (Moolgavkar, 1978). One key aspect in cancer development is inflammatory process. In healthy tissue, inflammation is a protective immune response for stabilizing homeostasis after internal and external harmful stimuli (Serhan, 2014). Nevertheless, prolonged inflammation or infections could lead to chronic inflammation that causes DNA damage, aberrant tissue repair, hampered regulation of transcription- and growth factors, and suppression of T cell immune response (Elinav et al., 2013; Zhang et al., 2017). For example, inflammatory tissue could be simulated by chronic ultraviolet (UV) B radiation treatment that damages healthy tissues. This stimulation leads to reactive oxygen species (ROS) production and is inactivating p53 tumor suppressor gene that contributes to skin carcinogenesis (Hattori et al., 1996; Halliday, 2005). ROS could directly alter genomic DNA and modulates cellular signaling pathways that change epigenetic mechanisms (Mikhed et al., 2015).

Upon harmful inflammation responses that cause oxidative stress and push carcinogenesis, cells synthesize antioxidant- and cytoprotective (phase-2) enzymes (Dinkova-Kostova and Talalay, 2008; Eggler et al., 2008). Phase-2 enzymes could be superoxide dismutase, NAD(P)H:quinone oxidoreductase 1 (NQO-1), and glutathione S-transferases that lead to detoxification and elimination of carcinogens, or antioxidant enzymes such as heme oxygenase-1 (HO-1), and enzymes that regulate the reducing environment of the cell (Eggler

et al., 2008). Gene expression of phase-2 enzymes is regulated by 5'-upstream cis-acting regulatory sequences, named electrophile response elements (EpREs) or antioxidant response elements (ARE) (Itoh et al., 1997). Nuclear factor erythroid-2-related factor-2 (Nrf2) was shown to induce expression of EpRE regulated genes *in vivo* and *in vitro* (Jeyapaul and Jaiswal, 2000; McMahon et al., 2001). More than 230 genes are regulated by Nrf2-EpRE pathway (Kwak et al., 2003). Nrf2 can activate EpREs via two mechanisms (Figure 3-1). In non-active state, Nrf2 is bound to Kelch-like ECH-associated protein 1 (Keap1) (Figure 3-1 A). Keap1 functions as substrate adaptor protein for Cullin 3-dependent E3 ubiquitin ligase (Cul3) complex that maintains a constant Nrf2 level by ubiquitin-proteasome degradation (Zhang et al., 2004; Zhang et al., 2005). After conformational changes of Keap1 by oxidation or electrophile modification, Nrf2 is released, Nrf2 escapes degradation processes and enters the nucleus (Tong et al., 2006). More recently, a second Keap1 independent mechanism for Nrf2 release through Wnt signaling pathway was proposed for hepatocytes (Rada et al., 2015) (Figure 3-1 B). Wnt signaling pathway has a distinct function in cell proliferation, migration, differentiation, and often is dysregulated in cancer cells (Morris and Huang, 2016). In this second model, Nrf2 is phosphorylated by glycogen synthase kinase-3 (GSK-3) Axin1 complex that leads to ubiquitin-proteasome dependent Nrf2 degradation. Upon WNT activation by WNT-3A, Axin1-GSK-3 complex is recruited by lipoprotein receptor related protein 5/6 (LRP5/6)-and Frizzled receptor that results in Nrf2 release (Rada et al., 2015). Released Nrf2 enters the nucleus, binds EpREs and activates anti-oxidant and detoxifying enzyme expression (Figure 3-1 C) (Surh et al., 2008).

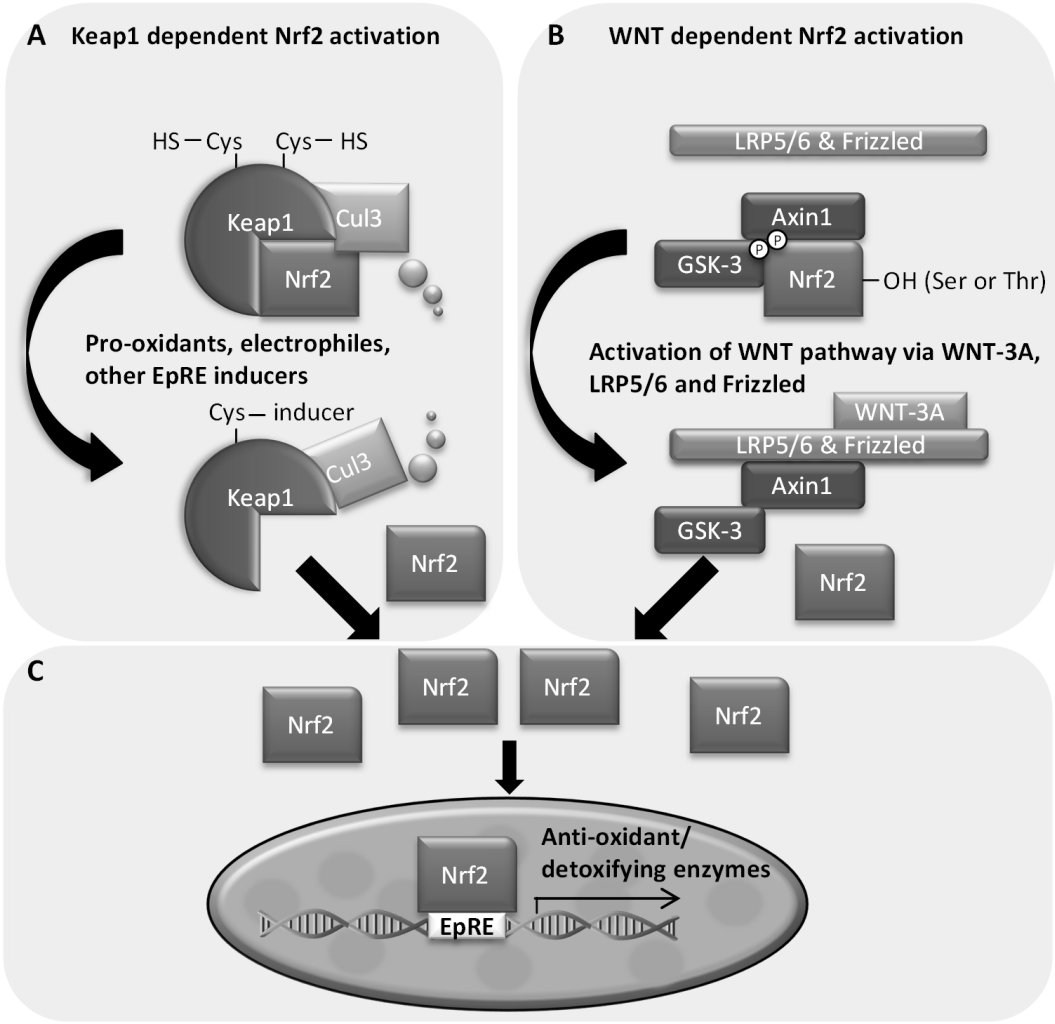

Figure 3-1: Two proposed mechanisms for Nrf2 release and EpRE mediated induction of phase-2 enzyme expression

(A) Nrf2 is stabilized by Keap1 cysteine thiol modifications. Keap1 is an adaptor protein for Cul3 dependent ubiquitin ligase complex that induces degradation of Nrf2 under basal conditions. Oxidants can cause conformational changes of Keap1 and release of Nrf2 (Surh et al., 2008). (B) Nrf2 is degraded by phosphorylation via GSK-3 Axin1 complex. Upon WNT-3 signaling, GSK-3 Axin1 complex binds to LRP5/6 and Frizzled receptor complex and releases Nrf2 (Rada et al., 2015). (C) Free Nrf2 binds to EpREs inside the cell core and activate anti-oxidant and detoxifying enzyme expression (Surh et al., 2008).

The Nrf2-EpRE pathway provides a broad resistance mechanism against exposure of toxicants and their resulting ROS and inflammation reactions. However, it should be mentioned that pushing Nrf2 release in some cancers could result in increased cancer fitness. Mutations in Keap1 interaction motif of Nrf2 were reported for human esophageal, skin, lung, head, and neck tumors which led to prevention of Keap1 mediated Nrf2 degradation (Kim et al., 2010). Nevertheless, due to great potential of Nrf2 to take part of suppressing inflammation associated carcinogenesis, it is commonly used as marker for screenings in pharmacology, as described below.

3.1.2 Nrf2-EpRE pathway as marker for anti-inflammatory compound screenings

Phytochemicals are present in many medical plants and in our vegetables. They possess a great potential for cancer chemoprevention (Park and Pezzuto, 2002). One target for chemoprevention is the Nrf2-EpRE pathway. For example, it was shown that curcumin, a diferuloylmethane derived from turmeric rhizomes, terminates the Nrf2-Keap1 complex. This leads to an increased Nrf2 EpREs binding and an raised phase-2 enzyme expression (Balogun et al., 2003). Nevertheless, there is still a need for novel chemopreventive phytochemicals that could be used in pharmacological cancer treatments and chemo therapy. Therefore, reporter cell lines containing EpRE driven firefly luciferase enzymes are one approach for identification of bioactive compounds.

For mechanistic studies on EpRE-mediated gene expression by phytochemicals, a stable luciferase reporter cell line was established (Boerboom et al., 2006). As genetic background they have chosen the murine hepatoma cell line Hepa-1c1c7. This cell line was shown to be a suitable *in vitro* system for chemoprotective enzyme induction, providing a relative insensitivity to any cytotoxic effects in comparison to different rodent cell lines (El-Sayed et al., 2007). The transformed hepatoma cell line contains an EpRE enhancer element from the regulatory region of the mouse glutathione-S-transferase Ya (mGST-Ya) gene fused to a firefly luciferase (LUX) (Boerboom et al., 2006). Luciferase expression in Hepa-1c1c7 EpRE(mGST-Ya)-LUX cells could be induced by 50 µM tert-butylhydroquinone (tBHQ) which is a known EpRE inducer (Yoshioka et al., 1995; Boerboom et al., 2006).

In this thesis, the murine Hepa-1c1c7 EpRE(mGST-Ya)-LUX strain was utilized for chemopreventive or anti-inflammatory bioactivity research on plant derived triterpenes.

3.1.3 Chemopreventive potential of plant triterpenes

Many phytochemicals, derived from edible plants, have been demonstrated to kill cancerous cells or to inhibit carcinogenesis (Park and Pezzuto, 2002). Few triterpenes were reported to present chemopreventive properties. In addition, there are some plant derived or artificially modified plant triterpenes that activate Nrf2-EpRE pathway, for example betulin (lup-20(29)-ene-3*β*, 28-diol) and oleanolic acid (3β-hydroxyolean-12-en-28-oic acid) (OA) derivatives (Loboda et al., 2012).

Betulin is contained in many species of birch trees and can be isolated from dried outer bark that contains up to 30% betulin (Šiman et al., 2016). For betulin and the betulin derived

betulinic acid, many biological effects on human and animal health like antifungal, antiviral, and anti-carcinogenic properties were reported (Gong et al., 2004; Shai et al., 2008; Machado et al., 2009; Alakurtti, 2013; Król et al., 2015). In addition, betulin is able to hamper inflammatory responses in lipopolysaccharide (LPS)-triggered macrophages and endotoxin-shocked mice (Ci et al., 2017). Bacterial LPS are known to activate toll-like receptor-4 (TLR4) complex on host cells that triggers ROS production accompanied by systemic inflammatory responses and sepsis (de Souza et al., 2007). The inflammatory suppression process initiated by betulin is linked to Nrf2 activation that results in phase-2 enzyme expression. Notably, Nrf2-EpRE induction is not only concentration dependent, but it also seem to be a matter of cell type. Human keratinocytes fosters a greater response to betulin than human microvascular endothelial cells when the effect of betulin on the Nrf2-EpRE pathway was investigated (Ci et al., 2017).

OA is one of the best characterized triterpenes with a known anti-inflammatory function, first described in the 1960´s of the last century (Gupta et al., 1969). Later, anti-carcinogenic properties for OA were demonstrated in different studies (Tokuda et al., 1986; Yoshimi et al., 1992; Fujiwara et al., 2011). Synthetic oleanolic acid molecules (SO) with increased anti-cancerous efficiency over OA in many *in vivo* models were synthesized (Liby et al., 2007). Prominent SOs are the cyano-3,12-dioxooleana-1,9(11)-dien-28-oic acid (CDDO) and its methyl ester (CDDO-Me) and its imidazolide (CDDO-Im) (Loboda et al., 2012). CDDO like molecules activates phase-2 enzyme expression in a dose dependent manner, but phase-2 enzyme expression was strongly repressed in Nrf2 knock-out mice and cells (Liby et al., 2005). CDDO derivatives passed clinical phase I and II trials, but failed phase III trials owing to unspecified safety concerns (Pergola et al., 2011; Hong et al., 2012; de Zeeuw et al., 2013). Furthermore, lupeol slightly induces EpRE driven gene expression and thus is a further candidate (Wu et al., 2014).

Triterpenes were reported in many studies for anti-carcinogenic properties, *in vivo* and *in vitro*. Betulin and CDDO derivatives demonstrated their relevance in chemoprevention of inflammation associated diseases (Liby et al., 2007; Ci et al., 2017). Despite throwbacks in clinical trials, executed studies preserve important knowledge for drug discovery and usage of Nrf2-EpRE pathway for medical treatments: Firstly, higher Nrf2 specificity may result in lower toxicity and therefore more triterpenoid structures should be studied on Nrf2 specificity; Secondly, Nrf2 could protects against progressive tissue damage rather than reversing pre-existing pathologies (Zhang, 2013).

3.1.4 Heterologous plant derived triterpene synthesis

Industry is challenging difficulties when producing plant metabolites. Plant growth in the field depends on many biotic and abiotic factors that cannot be predicted. Yields could be too low to feed the needs of the people. Therefore, heterologous synthesis of plant metabolites in microorganisms could be useful, because growth environment can be controlled, genetic engineering increases yields and liquid cultures could be increased to industrial scales. On the other side, market access of new synthetic or semi-synthetic drugs could have consequences into economic issues when other suppliers are undercut, or production costs overweight previous production methods (Peplow, 2013). Nonetheless, heterologous metabolite synthesis is forming future industry and will likely become increasingly important.

For heterologous plant terpene synthesis *Saccharomyces cerevisiae* were often used as expression host. For example, the anti-malarial sesquiterpene drug artemisinin was synthesized in a semi-synthetic yeast platform (Ro et al., 2006; Paddon et al., 2013). General strategies for terpene engineering involve enhancement of the MVA pathway activity by mutating 3-hydroxy-3-methyl-glutaryl-coenzyme A (HMG-CoA) reductases (Ro et al., 2006; Shiba et al., 2007), replacement of endogenous with repressive promoters of competitive pathway branches (Kirby et al., 2008), and screenings of yeast deletion collections to identify gene deletions that improves isoprenoid production (Özaydin et al., 2013; Arendt et al., 2017). *Saccharomyces cerevisiae* was used to express triterpene decorating CYP716 enzymes from diverse medical plants to characterize their reaction products and to discover new potential triterpene structures (Miettinen et al., 2017b).

Besides yeast as expression host for terpenes, further microbial but also photosynthetic hosts could be possible production platforms. Each platform brings benefits, but also disadvantages in heterologous synthesis, as summarized in Table 3-1. Proteobacteria *Rhodobacter capsulatus* as expression host for triterpenes is highlighted in Chapter 3.1.4.1.

Table 3-1: Comparison of different photosynthetic and microbial expression hosts for (heterologous) triterpene production
Taken from Arendt et al., 2016.

Host	Advantages	Disadvantages
Escherichia coli	Scalable in bioreactors Fast growth Simple genetic makeup Easy transformation	Requires sugar source Prokaryote, absence of ER may impair P450 activity Incorrect posttranslational modifications and protein folding
Yeast	Scalable in bioreactors Fast growth Simple genetic makeup Easy transformation	Requires sugar source Incorrect posttranslational modifications and protein folding
Cyanobacteria	Scalable in bioreactors Fast growth Simple genetic makeup Photoautotrophic No need for arable land	Lack of engineering tools Prokaryote, absence of ER may impair P450 activity
Algae	Scalable in bioreactors Fast growth Simple genetic makeup Photoautotrophic No need for arable land	Lack of engineering tools
Mosses	Scalable in bioreactors Fast growth Simple genetic makeup Photoautotrophic Stress tolerant Homologous recombination	Lack of engineering tools
Transient plant expression	Rapid analysis of multiple genes Photoautotrophic	Requires large volumes of expensive Agrobacterium cultures
Plant cell cultures	Scalable in bioreactors	Requires sugar source Expensive cultivation media Complex genetic makeup and genetic instability
Transgenic plants	Photoautotrophic Modern agricultural tool available	Complex genetic makeup and metabolic background Slow growth Possible competition with food production

3.1.4.1 Triterpene synthesis in *Rhodobacter capsulatus*

Rhodobacter capsulatus is a further expression host for heterologous triterpene biosynthesis. This bacterium is a photosynthetic α-proteobacterium that grows under aerobic an anaerobic conditions (Strnad et al., 2010). It is a metabolically versatile host which can be transformed for high-level protein production and squalene synthesis (Katzke et al., 2010; Khan et al., 2015).

Recently, lupeol, and cycloartenol were synthesized in transformed *Rhodobacter capsulatus* strain SB1003 (Loeschcke et al., 2017). The basic principle is to exploit endogenous FPP synthesis and expressing exogenous *SQS*, *SQE*, and *OSC* enzymes under control of endogenous P_{nif} promoter of the nitrogenase-encoding nifHDK operon (Loeschcke et al.,

2017). In this thesis, dried n-hexane extracts from three transformed *Rhodobacter capsulatus* strains were received for functional triterpene analysis (Chapter 2.1.8.3): (1) wild-type strain SB1003; (2) a transformed wild-type strain B10S with non-functional geranylgeranyl diphosphate synthase (c*rtE*) that results in FPP accumulation (referred as B10SΔE) ; (3) wild-type strain 37b4 that lacks exopolysaccharide coating which could lead to increased production yields (Marrs, 1974; Omar et al., 1983; Klipp et al., 1988; Loeschcke et al., 2017; Troost, 2017). All strains were transformed with expression vectors for triterpene synthesis (Figure 3-2). The OSC enzymes had a C-terminal histidine tag. In liquid chromatography - mass spectrometry (LC-MS) studies, squalene and 2,3-oxidosqualene were detected. In addition, cycloartenol and lupeol were discovered in *CAS1* and *LUP1* expressing bacteria. However, further triterpene compounds could not be detected in bacterial extracts by LC-MS, but might be present (personal communication with Dr. Thomas Drepper and Dr. Anita Loeschcke, 2016, Institute of Molecular Enzyme Technology, University Düsseldorf, Germany).

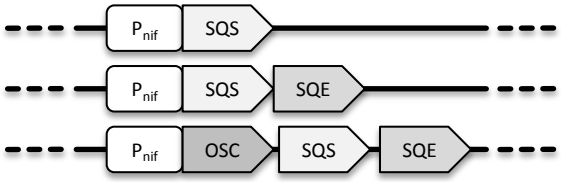

Figure 3-2: Schematic representation of expression constructs used for triterpenoid biosynthesis in *Rhodobacter capsulatus* strains

The respective genes were arranged as synthetic operons, using Pnif promoter for transcription activation: *SQS*; *SQS+SQE*; *OSC* (histidine tag)+*SQS+SQE* (modified, Loeschcke et al., 2017). Detailed list of used *OSCs* are presented in Chapter 2.1.8.3.

3.1.5 Aim

Phytochemicals offer great opportunities for cancer prevention and medical treatments. The plant triterpenes OA and betulin provide beneficial effects on mammalian health (Liby et al., 2007; Ci et al., 2017). However, only few plant triterpenes were characterized for their biological activity and triterpene enrichment from plant tissue could be linked to ecological and economical drawbacks which are unfavorable for new drug discoveries (Yadav et al., 2010; Peplow, 2013; Šiman et al., 2016). Heterologous expression in microbial hosts could offer a solution for plant triterpene synthesis in higher yields and establishment of a vast compound library. Besides yeast, one promising candidate for heterologous triterpene synthesis is *Rhodobacter capsulatus* (Loeschcke et al., 2017).

In this chapter, anti-inflammatory activities of secondary metabolites, especially of plant triterpenes, in murine liver cancer cells Hepa-1C1C7 will be investigated. A luciferase based reporter-gene-assay using the Nrf2-EpRE pathway will serve as a quick screening tool for anti-inflammatory compound screenings. First, bioactivity of betulin will be demonstrated during assay establishment. Afterwards, anti-inflammatory activity of heterologous synthesized triterpenes in *Rhodobacter capsulatus* extracts and prodigiosin (2-methyl-3-pentyl-6-methoxyprodiginine), a non-triterpene non-plant compound, in *Pseudomonas putida* extracts will be analyzed (Boerboom et al., 2006; Domröse et al., 2015; Loeschcke et al., 2017). Using bacterial extracts instead of purified compounds have the advantage that no complex, time-consuming, and expensive purification steps have to be performed for molecular analysis.

3.2 Results

3.2.1 tBHQ and betulin induced luciferase expression in EpRE-LUX cells

Prior to bioactivity studies of plant triterpenes contained in *Rhodobacter capsulatus* extracts on Nrf2-EpRE pathway in murine liver cancer cells Hepa-1C1C7, a functional luciferase in EpRE-LUX cells had to be confirmed. For verification of a functional EpRE-LUX construct, cells were treated with tBHQ or betulin in a dilution series ranging from 0.3 to 50.0 µM followed by luciferase activity measurement which was utilized as marker for EpRE induction (Figure 3-3).

tBHQ significantly induced luciferase activity in EpRE-LUX cells already at 5 µM (Figure 3-3 A). The maximal luciferase activity was obtained after 30 µM tBHQ treatment. While 30 µM tBHQ raised the luciferase activity 6-fold, 50 µM tBHQ led to a slightly reduced signal. Additionally, betulin activated luciferase activity at 30 µM (Figure 3-3 B). Lower betulin concentrations only induced luciferase activity slightly in comparison to untreated cells. No drastic changes in protein concentration of EpRE-LUX cell lysate were observed (Figure 6-1 A+B). Betulin concentrations above 100 µM did not lead to a stronger luciferase induction than the 2.6-fold increase by 30 µM betulin (Figure 6-1 C+D).

The strong luciferase activation by tBHQ and betulin is in line with other studies and demonstrate that the cultivated murine liver cancer cells Hepa-1C1C7 contain a functional EpRE-LUX. Bioactivity of additional triterpenes, sterols and triterpene precursor molecules squalene and 2,3-oxidosqualene were investigated next.

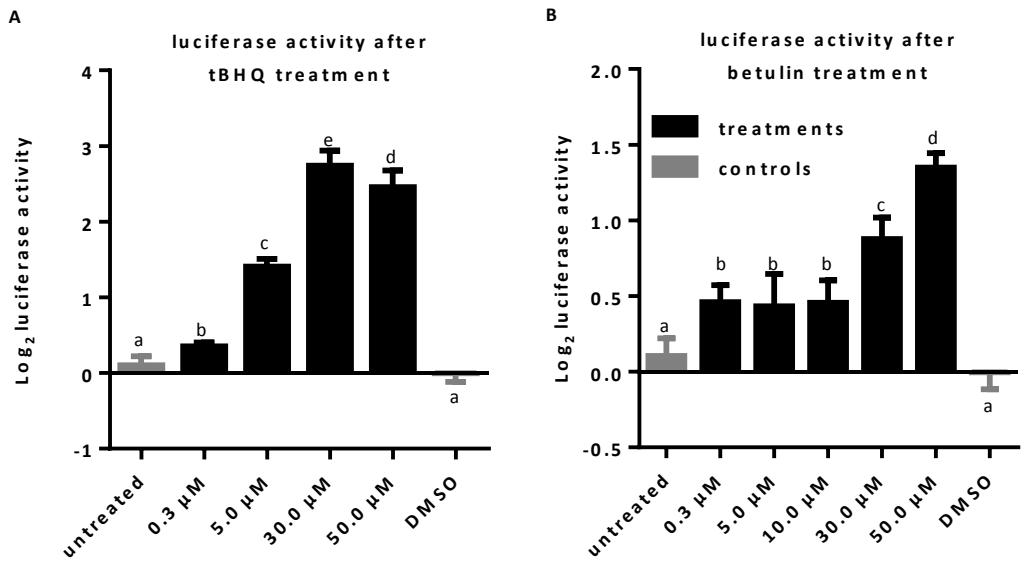

Figure 3-3: Luciferase activity of EpRE-LUX cells treated with tBHQ and betulin at different concentrations

EpRE-LUX cells were seeded onto a 96-well plate with 20.000 cells/ well and incubated for 1 day. tBHQ (A) and betulin (B) were diluted in DMSO and applied in dilutions between 0.3 to 50.0 µM with a max. amount of 1% DMSO per well (n=6); e.g. cells treated with 50.0 µM tBHQ grew in presence of 1% DMSO, while cells treated with 0.3 tBHQ grew in presence of 0.006% DMSO. After 1 day incubation protein content and relative light units (RLU) at λ=550 nm were measured in cell lysate. RLUs were normalized to protein level and set in ratio to 1% DMSO control. The y-axes represent luciferase activity on a Log_2 scale. Statistical analysis was performed by one-way ANOVA with Tukey's test and significance levels were set at $P \leq 0.05$ and indicated by small letters. Controls are visualized in gray and samples are presented in black. Standard deviation is presented as error bar.

3.2.2 Low concentrated triterpenes did not induced luciferase expression in EpRE-LUX cells

The previous experiment demonstrated functional luciferase activation by tBHQ and betulin in EpRE-LUX cells. We asked whether further triterpenes, sterols and triterpene precursor molecules are able to activate EpREs. To answer this question, we treated EpRE-LUX cells with 2 µM α-Amyrin, β-Amyrin, betulin, betulinic acid, cycloartenol, lanosterol, lupeol, squalene and 2,3-oxidosqualene and emitted RLU were referred as indication for EpRE activation (Figure 3-4). Mentioned chemicals and used concentration were selected based on their commercial availability.

No luciferase induction in EpRE-LUX cells in neither treatment was observed, except in 2 µM tBHQ control treatment (Figure 3-4 A). After lanosterol and squalene treatment, the basal luciferase activity was slightly reduced, but no differences in concentration of used proteins were observed between treatments (Figure 4-2 A). To exclude bioactivity of lanosterol and squalene at lower concentrations, 0.001, 0.01, 0.1 and 3.0 µM lanosterol or squalene were applied to EpRE-LUX cells (Figure 3-4 B). No activation of luciferase activity

was observed at these lanosterol and squalene concentrations, but negative effect of squalene on luciferase activity was diminished at 0.1 µM and lower. After 3 µM lanosterol treatment, no negative effect on luciferase activity could be reproduced. In addition, no alteration in protein content of cell lysate was measured (Figure 4-2 A+B). Notably, triterpene and sterol concentrations at 2 µM or lower did not activate luciferase activity in EpRE-LUX cells. Higher triterpene concentrations could still lead to a luciferase induction as described for betulin in Chapter 3.2.1.

For studying bioactivity of triterpenes contained in bacteria extracts, the question on how the bacteria extract composition affects luciferase expression in presence or absence of bioactive compounds in EpRE-LUX cells had to be solved.

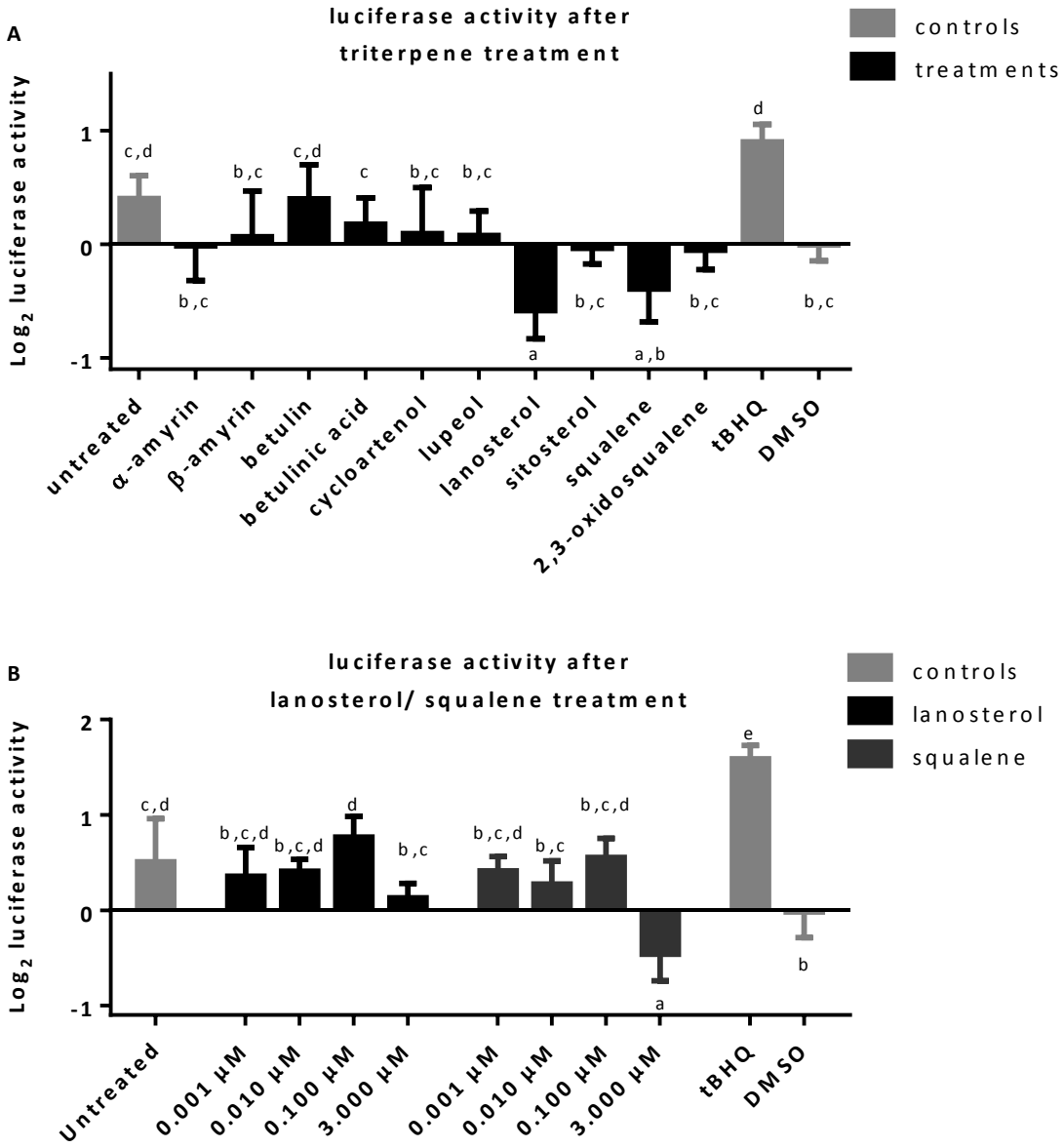

Figure 3-4: Luciferase activity of EpRE-LUX cells treated with 2 µM triterpenes, sterols or precursor molecules

EpRE-LUX cells were seeded onto a 96-well plate with 20.000 cells/ well and incubated for 1 day. A: α-Amyrin, β-Amyrin, betulin, betulinic acid, cycloartenol, lanosterol, lupeol, squalene, 2,3-oxidosqualene and tBHQ were diluted in DMSO and applied in 2 µM to cells, containing 1% DMSO (n=6). B: Cells were treated with 0.001, 0.01, 0.1 and 3.0 µM lanosterol or squalene (n=6). After 1 day incubation protein content and RLUs at λ=550 nm were measured in cell lysate. RLUs were normalized to protein level and set in ratio to 1% (A) or 1.5% (B) DMSO control. The y-axes represent luciferase activity on a Log_2 scale. Statistical data analysis was performed by one-way ANOVA with Tukey's test and significance levels were set at $P \leq 0.05$ and indicated by small letters. Untreated and 50 µM tBHQ control is visualized in gray. Samples are shown in black. Standard deviation is represented as error bar.

3.2.3 *Rhodobacter capsulatus* extracts spiked with betulin induced luciferase expression

We addressed the hypothesis whether hydrophobic phase extracts from *Rhodobacter capsulatus* contain substances that induce luciferase activity in EpRE-LUX cells or hamper bioactivity of EpRE activating compounds like betulin and tBHQ, further experiments were conducted. Dried extract from *Rhodobacter capsulatus* strain 37b4, transformed with pRhon5Hi2 empty vector, was diluted in DMSO. Next, the solution was applied in two concentrations (0.5% and 1%, corresponding to OD_{600}=0.056 or 0.112 of original bacteria culture) to EpRE-LUX cells in presence or absence of 50 µM betulin. In addition to previous experiments, cell viability was estimated after treatments with MTT assay (Figure 3-5).

Hydrophobic phase extracts of *Rhodobacter capsulatus* diluted in DMSO did not induce luciferase activity in EpRE-LUX cells at 0.5 and 1% (vol/ vol) (Figure 3-5 A). 50 µM betulin induced luciferase activity in EpRE-LUX cells (Figure 3-3). Cell treatment with bacterial extracts spiked with 50 µM tBHQ led to a 2-fold increase in luciferase activity, while 0.5% bacterial extract spiked with betulin was slightly more efficient than spiked 1.0% extract. No drastic changes in cell lysate protein concentration were observed (Figure 6-3 A). The cell viability, a term for the amount of cells that are alive and biological active, was significantly hampered after any treatment containing betulin in comparison to DMSO control (Figure 3-5 B). Only small influence on cell viability by bacterial extract treatment was observed. Despite the decrease in cell viability through betulin, no altered ratios in luciferase activity was calculated when normalizing RLU to cell viability instead of protein content; but betulin treatments resulted in a 4-fold luciferase increase, instead of 2-fold (Figure 6-3 B).

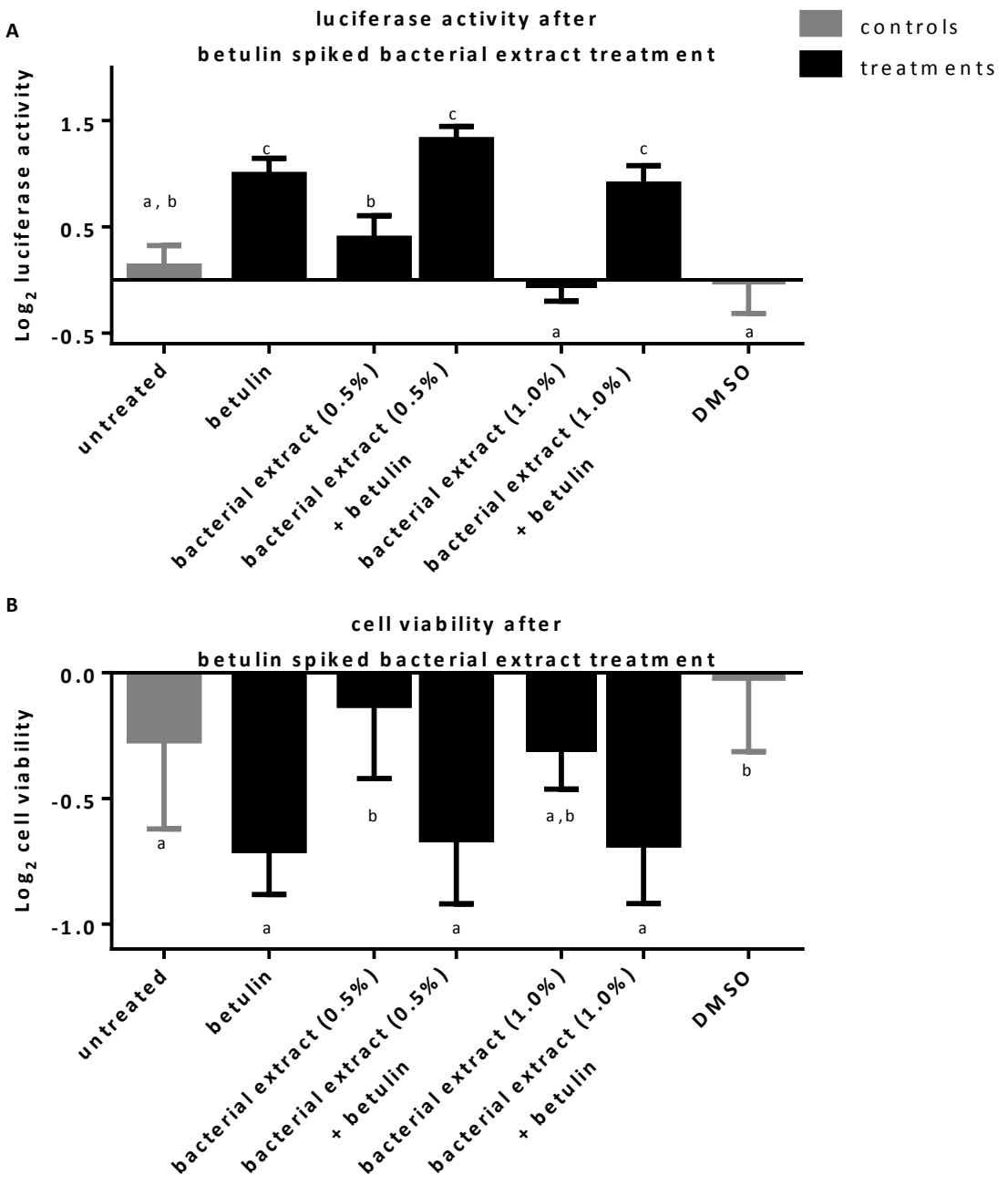

Figure 3-5: Luciferase activity of EpRE-LUX cells treated with bacterial extract spiked with 50 µM betulin

EpRE-LUX cells were seeded onto a 96-well plate with 20.000 cells/ well and incubated for 1 day. Dried hydrophobic phase extracts from *Rhodobacter capsulatus* 37b4 pRhon5Hi2 were diluted in 9 µl DMSO/ 1 OD_{600} bacteria. Next, cells were treated with 0.5% or 1.0% bacterial extract in presence or absence of 50 µM betulin (n=6). After 1 day incubation protein content and RLUs at λ=550 nm were measured in cell lysate. A: The y-axis represents luciferase activity on a Log_2 scale by normalizing RLUs to protein level and set them in ratio to 1.5% DMSO control. B: Biologically active cells were estimated by MTT assay at λ=550 nm, set in ratio to DMSO control and plotted on a Log_2 y-axis. Statistical data analysis was performed by one-way ANOVA with Tukey's test and significance levels were set at $P \leq 0.05$ and indicated by small letters. Untreated control is visualized in gray and samples in black, while standard deviation is represented as error bar.

This experiment revealed that betulin's bioactivity on EpRE-LUX cells that is not inhibited in presence of hydrophobic phase extracts of *Rhodobacter capsulatus*. Therefore this murine

hepatoma cell line is suitable for general chemopreventive compound screenings of triterpene molecules within complex bacterial matrix, or *Rhodobacter capsulatus* extracts at least. We received further dried hydrophobic phase extracts from Rhodobacter *capsulatus* strains 37b4, SB1003 and B10SΔE, expressing *SQS*, *SQE* and/ or one *Arabidopsis thaliana OSC* by Dr. Dreppers workgroup (Düsseldorf, Germany). These extracts were analyzed in a similar manner on their ability to induce luciferase expression in EpRE-LUX cells as marker biological active compounds.

3.2.4 Extracts from *Rhodobacter capsulatus* OSC expressing strains did not induce luciferase expression

In this thesis, chemical bioactivity of triterpenes contained in bacterial hydrophobic phase extracts should be studied. Murine liver cancer cells Hepa-1C1C7, containing a luciferase fused to an EpRE, were used as model for chemoprevention of cancer, or bioactivity. We received dried hydrophobic phase extracts from *Rhodobacter capsulatus* strains 37b4, SB1003 and B10SΔE, expressing *SQS*, *SQE* and/ or one *Arabidopsis thaliana OSC*, by Dr. Dreppers workgroup (Düsseldorf, Germany). The bacterial expression system is described in Chapter 3.1.4.1. Unfortunately, only precursor molecules squalene and 2,3-oxidosqualene, as well as lupeol and cycloartenol were detected by LC-MS analysis (CEPLAS metabolite platform, Cologne, Germany), but signals corresponding to further triterpenoids were not identified. Nevertheless, these extracts were analyzed on their bioactivity, presuming that corresponding triterpenoid compounds were present in sufficient amounts but not detected.
In this thesis, dried extracts equivalent to OD_{600}=1 bacteria culture were suspended in 9 µl DMSO. In assay, total extract in cell media was 0.5% to 1.0% which corresponds to OD_{600}=0.056 to OD_{600}=0.112 of original bacteria culture.

3.2.4.1 *Rhodobacter capsulatus* B10SΔE extracts did not induce luciferase expression

Dried hydrophobic phase *Rhodobacter capsulatus* B10SΔE extracts were suspended in 9 µl DMSO/ 1 OD_{600} bacteria. Extracts origins from bacteria transformed with pRhon5Hi2 plasmid containing *SQS*, *SQS+SQE* or *SQS+SQE+OSC* (*BARS1*, *CAMS1*, *CAS1*, *LSS1*, *LUP1*, *LUP2*). EpRE-LUX cells were treated with 0.5% of these extracts and luciferase activity was calculated (Figure 3-6). 0.5% extract corresponds to OD_{600}=0.056 of original bacteria culture. No significant differences in luciferase activity were detected between the extract treatments

and the DMSO or untreated control. In addition, no remarkable significant in cell lysate protein content between different treatments were observed (Figure 6-4 A).

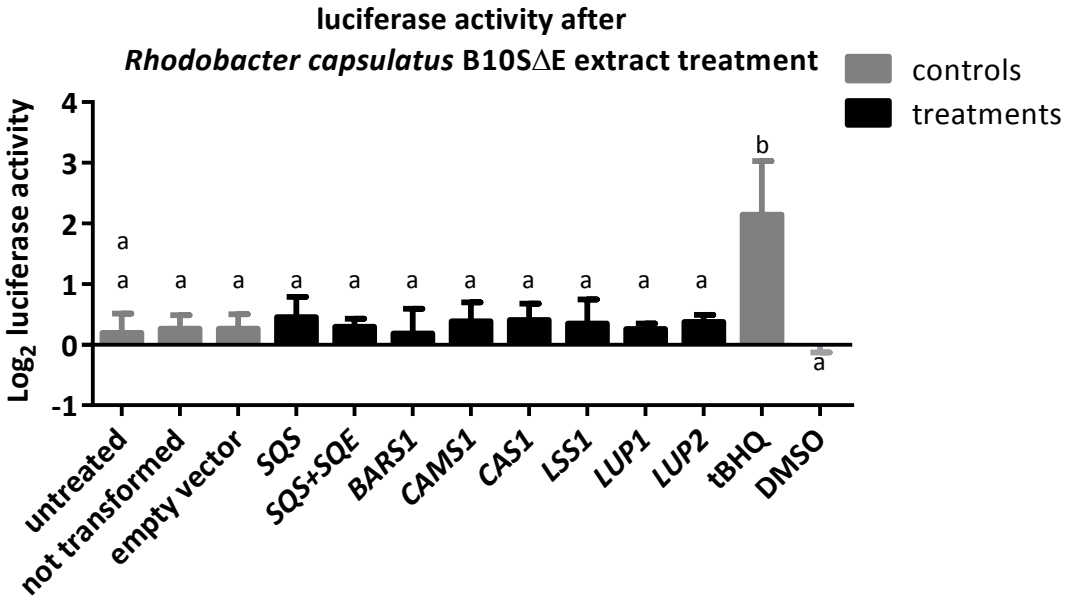

Figure 3-6: Luciferase activity of EpRE-LUX cells treated with *Rhodobacter capsulatus* B10SΔE extract
EpRE-LUX cells were seeded onto a 96-well plate with 20.000 cells/ well and incubated for 1 day. Dried hydrophobic phase *Rhodobacter capsulatus* B10SΔE extracts expressing *SQS*, *SQS+SQE* or *SQS+SQE+OSC* (*BARS1*, *CAMS1*, *CAS1*, *LSS1*, *LUP1*, *LUP2*) were suspended in 9 µl DMSO/ 1 OD600 bacteria and 0.5% extract were applied to cells (n=6). After 1 day incubation protein content and RLUs at λ=550 nm were measured in cell lysate. RLUs were normalized to protein level and set in ratio to 0.5% DMSO control. The y-axis represents luciferase activity on a Log2 scale. Statistical data analysis was performed by one-way ANOVA with Tukey's test and significance levels were set at $P \leq 0.05$ and indicated by small letters. Controls are visualized in gray: untreated cells, not transformed bacteria control, empty vector control, 50 µM tBHQ control. Samples are shown in black. Standard deviation is represented as error bar.

3.2.4.2 *Rhodobacter capsulatus* 37b4 extracts did not induce luciferase expression

Extracts from another *Rhodobacter capsulatus* strain, strain 37b4 were studied, because of different traits between these strains and their different conditions for heterologous molecule synthesis, e.g. Strain 37b4 is lacking exopolysaccharides and could use carbon elsewhere. These extracts were diluted in DMSO as previously described and luciferase activity of EpRE-LUX cells were estimated (Chapter 3.2.4.1). Extracts containing *MRN* or *THAS* raised the luciferase activity to a 2.5-fold level, but still not significant to untreated control (Figure 3-7). Further biological replicates did not support an EpRE-LUX activating role for THAS or MRN extracts (Figure 6-4 B+C).

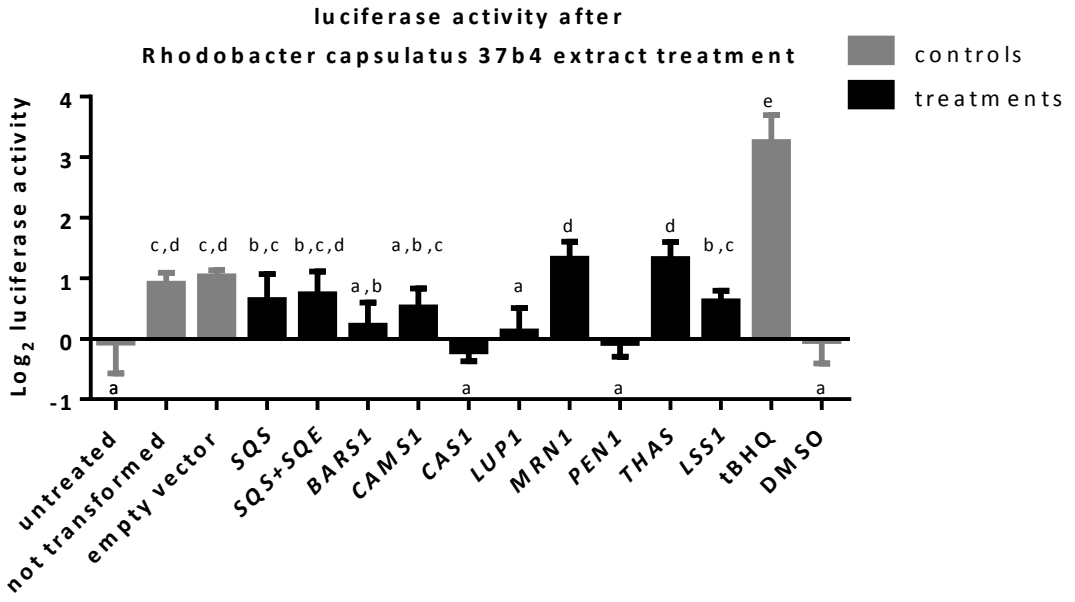

Figure 3-7: Luciferase activity of EpRE-LUX cells treated with *Rhodobacter capsulatus* 37b4 extract
EpRE-LUX cells were seeded onto a 96-well plate with 20.000 cells/ well and incubated for 1 day. Dried hydrophobic phase *Rhodobacter capsulatus* B10SΔE extracts containing *SQS*, *SQS+SQE* or *SQS+SQE+OSC* (*BARS1*, *CAMS1*, *CAS1*, *LUP1*, *MRN*, *PEN1*, *THAS*, *LSS1*) were diluted in 9 µl DMSO/ 1 OD_{600} bacteria and 0.5% extract were applied to cells (n=6). After 1 day incubation protein content and RLUs at λ=550 nm were measured in cell lysate. RLUs were normalized to protein level and set in ratio to 0.5% DMSO control. The y-axis represents luciferase activity on a Log_2 scale. Statistical data analysis was performed by one-way ANOVA with Tukey's test and significance levels were set at $P \leq 0.05$ and indicated by small letters. Controls are visualized in gray: untreated, extract of not transformed bacteria, extracts of bacteria containing empty vector control and 50 µM tBHQ. Samples are shown in black. Standard deviation is represented as error bar.

3.2.4.3 *Rhodobacter capsulatus* SB1003 extracts did not induce luciferase expression, but were toxic to the cells

The third *Rhodobacter capsulatus* strain SB1003 was transformed with *SQS*, *SQS+SQE* or *SQS+SQE+OSC* (*BARS1*, *CAS1*, *CAMS1*, *LUP1*, *LUP2*, *LUP5*, *MRN*, *PEN1*, *PEN3*, *PEN6*, *THAS* or *LSS*) by Drepper workgroup. Dried hydrophobic phase extracts were diluted in DMSO and applied to EpRE-LUX cells. No emitted light by luciferase was detected, except in untreated control, DMSO control, *LUP2* and *THAS* extract treatments. The emitted light of cell lysate on other treatments matched with blank values (Figure 6-4 D). Furthermore, protein level was strongly reduced in lysate of EpRE-LUX cells treated with bacterial extracts in comparison to untreated and DMSO control (Figure 3-8). Reduced protein level hints to a toxicity of extract treatment to the cells. But this toxic effects were absent when using a different lot of dried hydrophobic *Rhodobacter capsulatus* extracts (Figure 6-4 E+F).

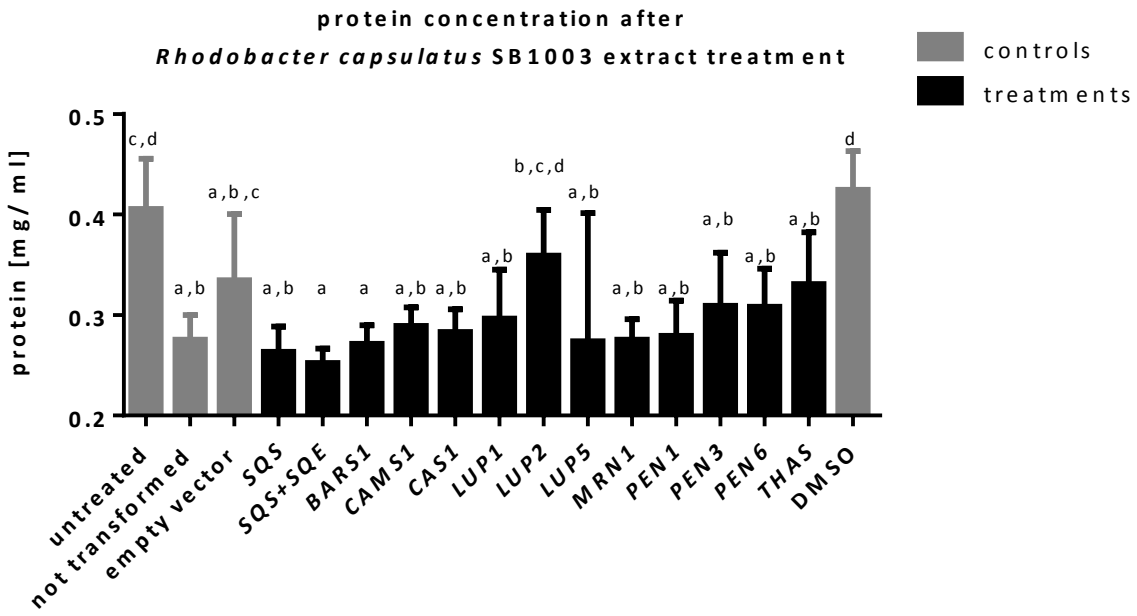

Figure 3-8: Protein concentration of EpRE-LUX cell lysates treated with *Rhodobacter capsulatus* SB1003 extracts

EpRE-LUX cells were seeded onto a 96-well plate with 20.000 cells/ well and incubated for 1 day. Dried hydrophobic phase *Rhodobacter capsulatus* SB1003 extracts containing *SQS*, *SQS+SQE* or *SQS+SQE+OSC* (*BARS1*, *CAMS1*, *CAS1*, *LUP1*, *LUP2*, *LUP5*, *MRN*, *PEN1*, *PEN2*, *THAS*) were diluted in 9 µl DMSO/ 1 OD_{600} bacteria and 1.0% extract were applied to cells (n=8). After 1 day, protein concentrations within cell lysate were calculated. The y-axis represents protein concentration on a linear scale starting at 0.2 mg protein/ ml cell lysate. Statistical data analysis was performed by one-way ANOVA with Tukey's test and significance levels were set at $P \leq 0.05$ and indicated by small letters. Controls are visualized in gray: untreated cells, not transformed bacteria, bacteria extract containing empty vector pRHon5Hi control and 1.0% DMSO control. Samples are shown in black. Standard deviation is presented as error bar.

Our data suggest that extracts from *Rhodobacter capsulatus* B10sΔE and 37b4, expressing plant triterpene cyclases *BARS1*, *CAMS1*, *LUP1*, *LUP2*, *MRN1*, *PEN1*, *THAS* or *LSS1*, have no impact on EpREs in murine liver cancer cells Hepa-1C1C7 containing EpRE-LUX. This observation is set under the premise that all plant triterpene cyclases are functional and are synthesizing their corresponding molecule, which failed to be proven. Therefore different expression systems and/ or expression of further triterpene cyclases could be conducted to receive additional insights into bioactivity of plant triterpenes.

Furthermore bacterial extracts from a different expression system for heterologous metabolite synthesis were supplied by Dr. Dreppers workgroup – bacteria *Pseudomonas putida* synthesizing prodigiosin, a bacterial metabolite with anti-cancerous and antibiotic properties (Loeschcke et al., 2017).

3.2.5 Anti-inflammatory activity of prodigiosin synthesized in *Pseudomonas putida* on EpRE-LUX cells

In previous studies observations demonstrated that in EpRE-LUX cells luciferase was induced by betulin in combination with *Rhodobacter capsulatus* extract (Figure 3-5). No bioactive extracts from *Rhodobacter capsulatus* expressing OSCs were identified (Chapter 3.2.4). Nevertheless, we investigated extracts from a different expression host, gram-negative *Pseudomonas putiada*, synthesizing prodigiosin. Prodigiosin was extracted from bacteria with ethanol by Dr. Dreppers workgroup and prodigiosin concentration was estimated at 93 µM, using LC-MS. Concurrently extract of *Pseudomonas putida* containing empty vector was spiked with tBHQ and induced luciferase activity in EpRE-LUX cells (Figure 6-5 A+B).

3.2.5.1 Prodigiosin containing bacterial extracts induced luciferase expression

To address a biological function for prodigiosin in EpRE regulation dried ethanol extracts of *Pseudomonas putida* containing prodigiosin were diluted with DMSO to gather 300 µM prodigiosin. EpRE-LUX cells were treated with different concentrations of bacterial extracts and luciferase activity and protein content were analyzed.

Already lowest tested prodigiosin concentration, 0.15 µM, activated luciferase expression (Figure 3-9 A). The maximal 5.7fold induction was observed after 0.3 µM prodigiosin treatment. Higher prodigiosin concentrations led to a reduction in luciferase activity. Measured RLUs in cells treated with 3.0 µM prodigiosin were strongly reduced and below basal level. According to this, protein concentration in cell lysate was stepwise reduced after 0.15 µM prodigiosin treatment and higher (Figure 3-9 B).

This data suggest a role for prodigiosin to activate EpRE-Nrf2 pathway. Furthermore a decrease in cell lysate protein concentration hints to cell toxicity by prodigiosin and then cell viability was studied.

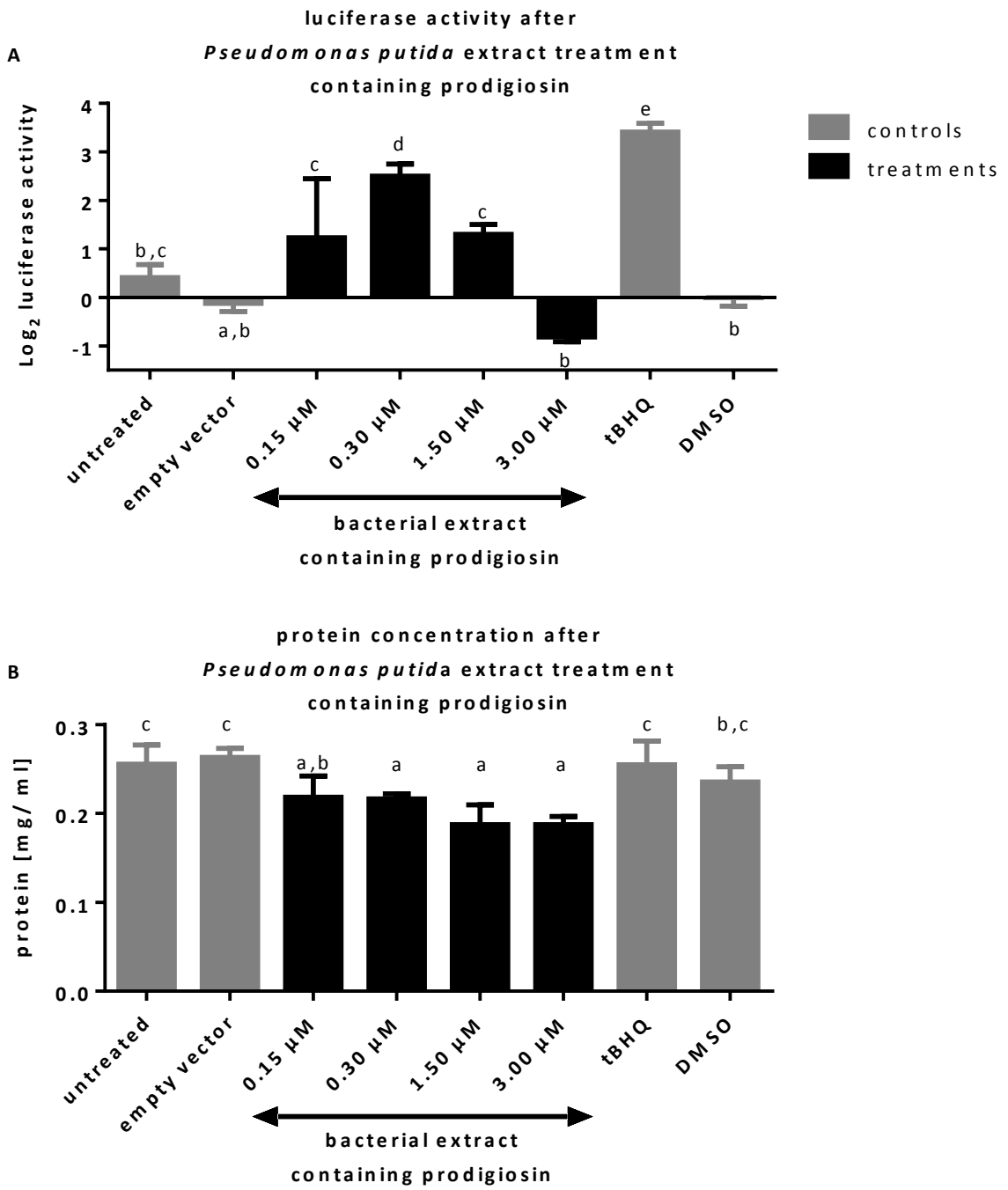

Figure 3-9: Luciferase activity and protein concentration of EpRE-LUX cells treated with *Pseudomonas putida* extracts containing prodigiosin

EpRE-LUX cells were seeded onto a 96-well plate with 20.000 cells/ well and incubated for 1 day. Dried ethanol extract from *Pseudomonas putida* containing prodigiosin was diluted in DMSO to 300 µM prodigiosin. Next, cells were treated with bacterial extracts containing 0.15, 0.30, 1.50 or 3.00 µM prodigiosin (n=6). After 1 day incubation protein content and RLU at λ=550 nm were measured in cell lysate. A: The y-axis represents luciferase activity on a Log2 scale by normalizing RLUs to protein level and set them in ratio to 1.0% DMSO control. B: Protein concentration of cell lysate after treatment is plotted on a linear y-axis. Statistical data analysis was performed by one-way ANOVA with Tukey's test and significance levels were set at $P \leq 0.05$ and indicated by small letters. Controls are visualized in gray: untreated cells, empty vector control, tBHQ positive control and DMSO solvent control. Samples are presented as black bars. Standard deviation is presented as error bar.

3.2.5.2 Cell viability was decreased by prodigiosin containing bacterial extracts

Prodigiosin is reported as anti-cancerous drug with tumor specific cell toxicity. For verification of cell toxicity in *Pseudomonas putida* extracts containing prodigiosin, cell viability measurement after prodigiosin treatment was carried out and influence of cell viability on luciferase activity was estimated. Cell viability measurement was performed with MTT assay.

Cell viability was strongly reduced in EpRE-LUX cells after *Pseudomonas putida* extracts treatment containing prodigiosin (Figure 3-10 A). Already 0.15 µM prodigiosin resulted in decreased cell viability. 3 µM prodigiosin led to a 2.5fold reduction in cell viability. Cell viability was unaffected by *Pseudomonas putida* extracts containing empty vector. Additionally, luciferase activation pattern was similar to previous experiment when normalizing emitted RLU of luciferase to cell viability (Figure 3-10 B). Maximal luciferase induction was measured after 0.3 µM prodigiosin (5.7-fold).

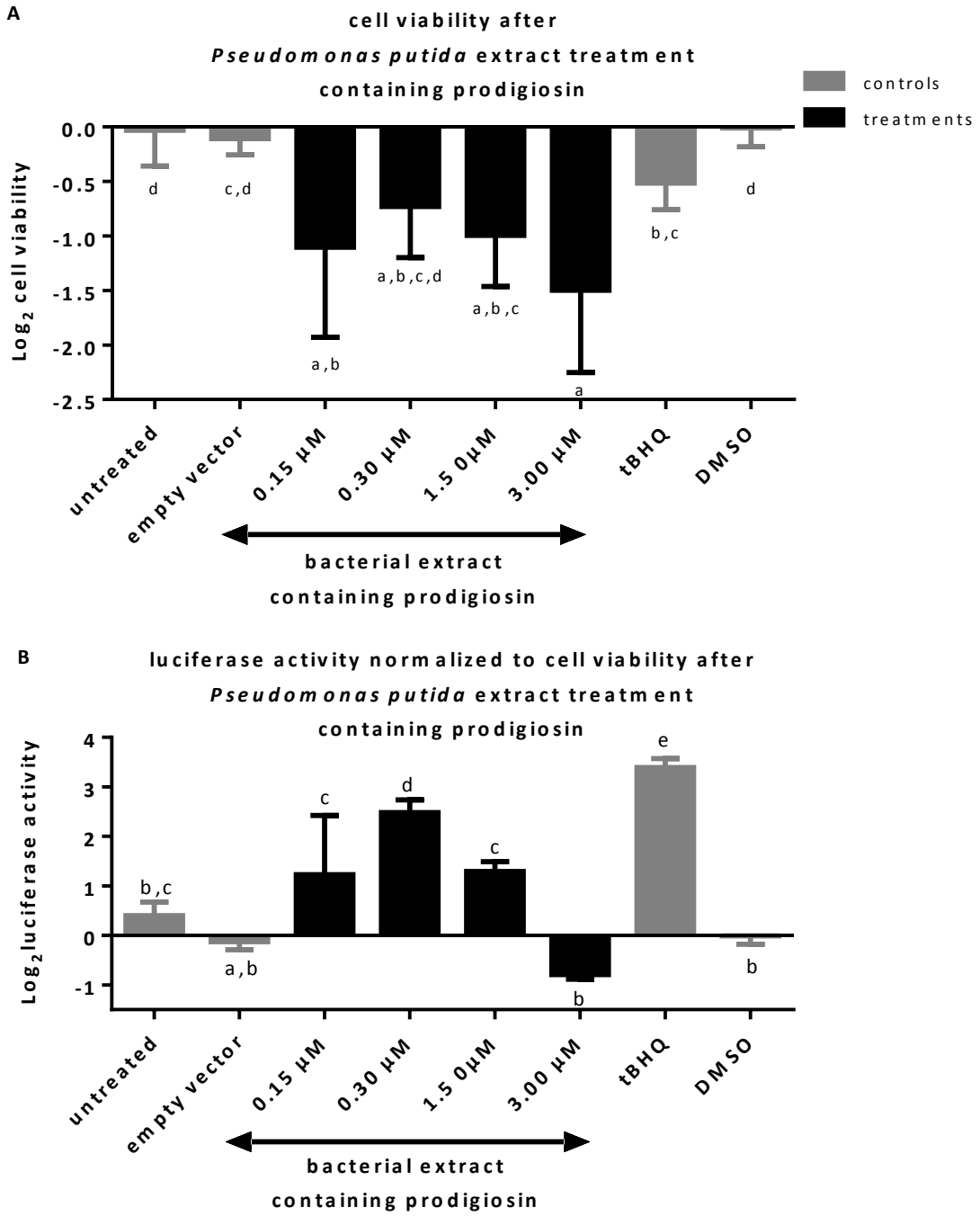

Figure 3-10: Cell viability and luciferase activity of EpRE-LUX cells treated with *Pseudomonas putida* extracts containing prodigiosin

EpRE-LUX cells were seeded onto a 96-well plate with 20.000 cells/ well and incubated for 1 day. Dried ethanol extract from *Pseudomonas putida* containing prodigiosin was diluted with DMSO to a 300 µM prodigiosin concentrations. Next, cells were treated bacterial extracts containing 0.15, 0.30, 1.50 or 3.00 µM prodigiosin (n=6; same experiment as Figure 3-9). After 1 day incubation cell viability and RLU at λ= were measured. A: Biologic active cells were estimated by MTT assay at λ=550 nm, set in ratio to DMSO control and was plotted on a Log_2 y-axis. B: The y-axis represents luciferase activity on a Log2 scale by normalizing RLUs to cell viability and set them in ratio to 1.0% DMSO control. Statistical data analysis was performed by one-way ANOVA with Tukey's test and significance levels were set at $P \leq 0.05$ and indicated by small letters. Controls are visualized in gray: untreated cells, empty vector control and tBHQ positive control. Samples are presented as black bars. Standard deviation is presented as error bar.

To our knowledge, these results provide first evidence for prodigiosin activating EpRE in mammalian cells. We have combined novel biotechnological with cell cultural approaches to identify chemopreventive compounds activating EpRE-LUX in highly complex bacterial extracts.

3.3 Discussion

3.3.1 Murine liver cancer cell line Hepa-1C1C7 EpRE-LUX is a suitable screening platform for anti-inflammatory compounds in bacterial extracts

To elucidate anti-inflammatory activity of plant triterpenes in animal cells, an efficient assay system should be established. This system should be capable of detecting active triterpene compounds in molecular diverse background of bacterial extracts. The mammalian Nrf2-EpRE pathway was selected as model for bioactivity screenings, because of its relevance in inflammation associated carcinogenesis and regulation by certain dietary phytochemicals (Eggler et al., 2008; Surh et al., 2008). Boerboom et al. constructed a stable murine hepatoma EpRE-LUX reporter cell line for studies on EpRE-mediated gene expression (Boerboom et al., 2006). In this study, this reporter line was used to unravel biological activity of heterologous synthesized triterpenes in *Rhodobacter capsulatus* extracts.

To verify a functional EpRE-LUX reporter construct, cells were treated with tBHQ, a known inducer of Nrf2-EpRE pathway (Yoshioka et al., 1995). Already 30 µM tBHQ induced luciferase activity ~5.6-fold (Figure 3-3 A). In addition, triterpene betulin induced EpRE-mediated gene expression >2-fold and demonstrate that this reporter system is suitable for triterpene bioactivity studies (Figure 3-3 B). Betulin was already reported to induce Nrf2 activity in human microvascular endothelial cells (HMEC-1) (Loboda et al., 2012). This could hint to broader organism specificity for betulin bioactivity. However, further anti-cancerous properties for betulin were reported and decreased cell viability in murine cancer cell line were observed in this study (Figure 3-5 B) (Pfarr et al., 2015; Drag-Zalesińska et al., 2017). Betulin did not activate EpRE-mediated gene expression as strong as tBHQ and a higher concentration was necessary for proper induction. For comparison, to double EpRE-LUX activity, ~5 µM tBHQ or ~30 µM betulin was necessary. Furthermore, cell treatments with 2 µM triterpene and sterol solutions (α-amyrin, β-amyrin, betulin, betuinic acid, cycloartenol, lupeol, lanosterol, sitosterol, squalene, and 2,3-oxidosqualene) did not activate reporter construct which could be explained by lack of anti-inflammatory properties or low

concentration range (Figure 3-4). In the next step, effect of *Rhodobacter capsulatus* extracts on EpRE-LUX reporter cell line was analyzed. Hydrophobic molecules were extracted with n-hexane from *Rhodobacter capsulatus* cultures (Loeschcke et al., 2017). Therefore, they contain many different compounds like ornithine lipids, phospholipids, and ubiquinone (Figure 6-6) (personal communication with Dr. Vera Wewer, 2016, MS Platform, University of Cologne, Germany). Bacterial matrices alone neither induce pRE-LUX reporter activity nor cell viability (Figure 3-5). In addition, combinatorial cell treatments with 50 µM betulin and extracts neither hamper betulin bioactivity nor decrease the cell viability.

These data provide evidence that the EpRE-LUX reporter cell line can be used to measure anti-inflammatory activity of triterpenes and other molecules contained in hydrophobic bacterial extracts. Hydrophilic compounds contained in aqueous phase of bacterial extracts, which were not analyzed in this study, could also be potentially tested in future. The presented approach has the major advantage that compounds are not required to be isolated from *Rhodobacter capsulatus* in complex purification steps, but could be directly used followed by simple molecular phase exactions. This allows the use of different expression strains in parallel in a high-throughput manner.

3.3.2 No anti-inflammatory triterpenes were identified in *Rhodobacter capsulatus* extracts

For research on triterpene function in mammalian Nrf2-EpRE pathway, dried *Rhodobacter capsulatus* extracts of OSC expression strains from Dr. Dreppers workgroup (Düsseldorf, Germany) were used for treatments of a murine hepatoma EpRE-LUX reporter cell line. In detail, *Rhodobacter capsulatus* expression strains (SB1003, 37b4, and B10SΔE) were transformed with pRhon5Hi-2 expression vector containing SQS and SQE in addition to an OSC

In this thesis, dried bacterial extracts were suspended in DMSO and used for hepatoma cell culture treatments. However, EpRE-mediated gene expression was not induced after cell treatment with extracts from transformed B10SΔE strains expressing *SQS*, *SQS+SQE*, or *SQS+SQE+OSC* (*BARS1*, *CMAS1*, *CAS1*, *LSS1*, *LUP1*, or *LUP2)* (Figure 3-6). Similar results were obtained for cell treatments with extracts from strain 37b4 expressing *SQS*, *SQS+SQE*, or *SQS+SQE+OSC* (*BARS*1, *CAMS1*, *CAS1*, *LUP1*, *MRN*, *PEN1*, *THAS*, or *LSS1)*. However, extract from untransformed bacteria already induced luciferase reporter activity 2-fold (Figure 3-7). In comparison to strain B10SΔE, strain 37b4 does not lack crtE and synthesize carotenoids and diterpenes naturally. Carotenoids and diterpenes in extract could have activated EpRE-LUX reporter construct, since it was demonstrated that certain carotenoids

and diterpenes activate Nrf2-EpRE pathway (Linnewiel et al., 2009; Wu et al., 2014; Linnewiel-Hermoni et al., 2015). Interestingly, treatment with extract from strain 37b4 *BARS*, *CAS1*, *LUP1*, and *PEN1* did not trigger luciferase activity which might result from direct or indirect effects, for example from lower a carotenoid and diterpene concentration in extract. The third tested strain was wild-type strain SB1003. Cell treatments with extracts from strain SB1003 expressing *SQS*, *SQS+SQE*, *SQS+SQE+OSC* (*BARS1*, *CAMS1*, *CAS1*, *LUP1*, *LUP5*, *MRN*, *PEN1*, or *PEN2*) and untransformed strain resulted in very strong decrease in hepatoma cell protein content and strong luciferase activity reduction (Figure 6-4 D). Noteworthy, cell treatment with extract of SB1003 empty vector construct, did not resulted in strongly impaired protein content and luciferase activity. Treatments with another SB1003 *SQS* and *SQS+SQE* batch did also not reproduce negative effects on hepatoma cells (Figure 6-4 E+F). Therefore, chemical contamination during hydrophobic phase extraction could be a reason for toxic effect of used Rhodobacter extracts. This observation also demonstrates how sensible this assay system is for contaminations and presence of interfering compounds.

Taken together, no anti-inflammatory triterpenes were identified in *Rhodobacter capsulatus* extracts. However, this does not mean that the triterpenes synthesized by *Rhodobacter capsulatus* have no bioactivity. It is possible that the triterpene concentration range in extracts was too low to induce reporter gene expression. An example that supports this hypothesis is lupeol. Lupeol (1 µM) is reported to induce EpRE activity 2.3-fold in human breast carcinoma EpRE reporter cell line named AREc32 (Xiu et al., 2006; Wu et al., 2014). In *Rhodobacter capsulatus* strain SB1003 *SQS+SQE+LUP1* only minor amounts of lupeol and lupeol derivates were detected, but could not be quantified (Loeschcke et al., 2017). Moreover, many compounds in extracts could interfere with target molecules and impaired LUX activity. Another argument represents the signal intensity of an ion (427.4 mass-to-charge ratio (m/z)) corresponding to cycloartenol in Rhodobacter strain B10SΔE *SQS+SQE+CAS1*. This cycloartenol ion was detected below basal intensity level of the base peak chromatogram in LC-MS (Figure 6-6) (personal communication with Dr. Vera Wewer, 2016, MS Platform, University of Cologne, Germany). Only squalene, 2,3-oxidosqualene and no triterpene derivates (, except lupeol and cycloartenol) were detected in Rhodobacter expression strains. It remains unknown whether expression strains did not synthesize corresponding compounds or they were not detectable by LC-MS method.

3.3.3 Heterologous synthesized prodigiosin activated Nrf2-EpRE pathway

Previous data did not unravel anti-inflammatory triterpene compounds in bacteria extracts (Chapter 3.3.2). However, we decided to prove the possibility of bioactive compound detection within bacteria extracts in another approach and picked the bacteria pigment prodigiosin that was synthesized by heterologous expression host *Pseudomonas putida*. Prodigiosin is a red-colored tripyrrolic molecule with antibacterial, antitumor, immunosuppressive, and antimalarial properties (Han et al., 1998; Lapenda et al., 2014; Hassankhani et al., 2015). Recently it was shown that prodigiosin inhibits significant cancer related Wnt/β-catenin signaling pathway in breast cancer cells (Wang et al., 2016). Prodigiosin could be synthesized by gram-negative *Pseudomonas putida* when transformed with 21 kb prodigiosin biosynthesis gene cluster (*pig*) of human pathogen *Serratia marcescens* (Harris et al., 2004; Domröse et al., 2015). In this study, *Pseudomonas putida* extracts containing prodigiosin were analyzed upon anti-inflammatory activities.

Similar to Rhodobacter extracts, basal bioactivity of *Pseudomonas putida* extracts and their interferences to tBHQ bioactivity on EpRE-LUX reporter were investigated (Figure 6-5). 0.5% and 1.0% (vol-%) *Pseudomonas putida* extracts had no impact on EpRE-mediated gene expression. In addition, tBHQ bioactivity was not impaired when diluted in bacteria extracts. Therefore, we studied effects of Pseudomonas extracts containing prodigiosin in a concentration range. Highest luciferase activity was observed after 30 µM prodigiosin extract treatment while higher concentrations led to activity reduction (Figure 3-9). Furthermore, only *Pseudomonas putida* extracts containing prodigiosin and not empty vector strain inhibited cell viability in murine hepatoma cells (Figure 3-10). Observed cell viability reduction by prodigiosin is in consents with reported literature for human breast cancer cell lines MDA-MB-231 and MDA-MB-468 as well as human colorectal cancer cells HT-29 (Hassankhani et al., 2015; Wang et al., 2016).

This thesis reports for the first time Nrf2 activation by prodigiosin. The exact mechanism is unknown, but it is likely that prodigiosin interferes with the Wnt dependent Nrf2 activation, for the following reason: In inactive Wnt signaling, Axin1 scaffolds Nrf2 and phosphorylated GSK-3, facilitating NRF2 phosphorylation that leads to proteasomal Nrf2 degradation (Figure 3-1 B) (Rada et al., 2015). Prodigiosin prevents phosphorylation of GSK-3 at Ser9 position, but does not initiate GSK-3 degradation (Wang et al., 2016). The failed GSK-3 phosphorylation could lead a destabilized Nrf2 repressor complex and accumulation of non-phosphorylated active Nrf2.

Recently, 13 new prodigiosin derivatives were synthesized in *Pseudomonas putida* by mutasynthesis (Klein et al., 2017). Alternate structures could lead to enhanced bioactivity as well as reduced toxicity which is important for drug development. Some prodigiosin derivatives already undergone clinical phase I/II studies and indicate importance for these compounds in pharmacy (Schimmer et al., 2014).

Chapter 4

Functional characterization of *Arabidopsis thaliana marneral synthase 1* and *thalianol synthase* double knock-out mutant

4.1 Introduction

Marneral is a monocyclic (6) triterpene and was first described in lipid extracts of sword lilies by Franz-Josef Marner (Marner and Longerich, 1992). Thalianol is a tricyclic (6/6/5) triterpene discovered during genome mining studies in *Arabidopsis thaliana* (Fazio et al., 2004) (Figure 1-1). Both are structurally different, but have common features in their biosynthesis and function in *Arabidopsis thaliana*. Nevertheless, previous studies mainly focused on their genomic organization in gene clusters and little is known of their physiological function in plants. This sub-chapter should highlight most important findings regarding marneral and thalianol biosynthesis, function, regulation and outline the aim of this study.

4.1.1 Biosynthesis of marneral and thalianol in *Arabidopsis thaliana*

Enzyme expression for marneral and thalianol synthesis in *Arabidopsis thaliana* is tightly restricted to roots and seedlings (Figure 4-1) (Hruz et al., 2008). The first step in marneral biosynthesis in *Arabidopsis thaliana* is the ring formation of 2,3-oxidosqualene to a bicyclic intermediate by MARNERAL SYNTHASE 1 (MRN1, At5g42600) (Xiong et al., 2006). MRN1 is localized in the endoplasmic reticulum (ER) (Go et al., 2012). In the second step, ring A of the intermediate is then cleaved to form the monocyclic aldehyde triterpene marneral (Figure 4-2). Marneral is then converted to marnerol probably non-enzymatically (Xiong et al., 2006). Thereafter marnerol is oxidized by the enzyme CYP71A16, also referred as MARNERAL OXIDASE (MRO, At5G42590). CYP71A16 belongs to the cytochrome P450 family and likely synthesize multiple marnerol derived products. It is postulated that these reaction products are substrates of the CYP705A12 (At5g42580) enzyme, because this enzyme is tightly co-regulated and forms a gene cluster with *MRN1* and *MRO* (Field et al., 2011). Gene clusters offer the opportunity to tightly regulate multiple genes in parallel as explained in Chapter 4.1.1.1).

Thalianol synthesis in *Arabidopsis thaliana* is similar to that of marneral. The THALIANOL SYNTHASE (THAS, At5g48010) is cyclizing 2,3-oxidosqualene to thalianol (Fazio et al., 2004; Field and Osbourn, 2008). THAS protein is also localized in the ER (Go et al., 2012). In the next step, THALIANOL HYDROXYLASE (THAH, At5g48000) is likely to convert thalianol to different thalian-diol isomers. Thereafter the THALIAN-DIOL DESATURASE (THAD, At5g47990) transforms thalian-diol to desaturated thalian-diol by introducing a new double bond (Field and Osbourn, 2008). *THAS*, *THAH*, and *THAD* as well as *MRN*, *MRO* and *CYP705A12* are arranged in gene clusters (Field et al., 2011).

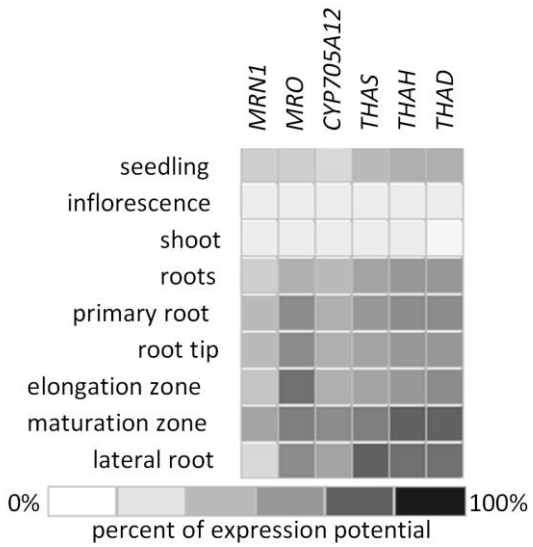

Figure 4-1: Microarray expression profiles of marneral and thalianol gene clusters
MRN1, *MRO*, *CYP705A12*, *THAS*, *THAH* and *THAD* were mainly expressed in roots and seedlings. Data were received from Genevestigator software (Hruz et al., 2008).

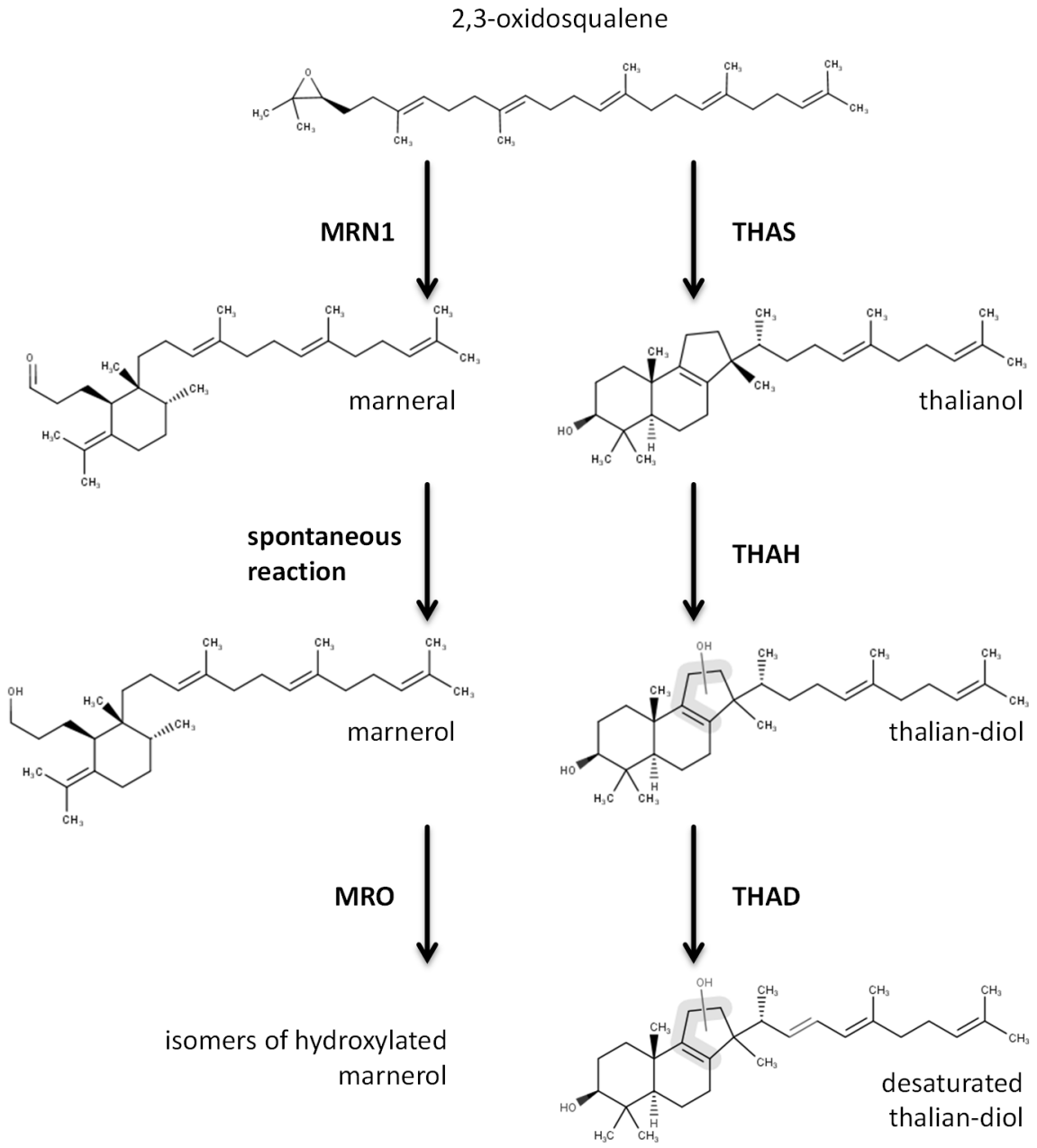

Figure 4-2: Biosynthesis of marneral, thalianol and their elaboration
Marneral and thalianol are synthesized from 2,3-oxidosqualene by THAS and MRN1, respectively. Marneral is spontaneously converted to marnerol that is further progressed by MRO to several isomers of hydroxylated marnerol. Thalianol is hydroxylated to thalian-diol. The hydroxyl group of thalian-diol is located at one of the four available carbon positions in rings B or C. Afterwards, THAD converts thalian-diol to a desaturated thalian-diol (Xiong et al., 2006; Field and Osbourn, 2008; Field et al., 2011).

4.1.1.1 Properties of marneral and thalianol gene clusters

For secondary metabolite synthesis in specialized metabolic plant pathways, genes could be arranged in operon-like gene clusters on the chromosome (Boycheva et al., 2014). Known plant gene clusters spans regions between 35 to 270 kb and incorporate three to ten genes. Genes within these clusters are co-expressed and facilitating a coordinated, tissue-, and time-

specific biosynthesis of a product with low intermediate molecules concentrations (Nützmann and Osbourn, 2014).

MRN1, *MRO* and *CYP705A12* belong to the marneral gene cluster (Field et al., 2011). One remarkable feature is that this cluster is regulated on an epigenetic level by repressing histone 3 lysine trimethylation (H3K27me3) chromatin signatures (Yu et al., 2016). The positive regulator PICKLE (PKL) and its homolog PICKLE RELATED 2 (PKL2) are predicted ATP-dependent chromatin remodeling factors and activates marneral gene cluster expression (Ogas et al., 1999; Aichinger et al., 2009; Yu et al., 2016). Notably, PKL is also a known regulator for meristem activity and cell identity in *Arabidopsis thaliana* roots (Aichinger et al., 2009; Aichinger et al., 2011). On the other side is CURLY LEAF (CLF), a negative regulator for H3K27me3 marked genes (Goodrich et al., 1997; Doyle and Amasino, 2009). CLF represses marneral gene cluster expression (Yu et al., 2016). The thalianol gene cluster is consistent of *THAS*, *THAH*, *THAD* and a *BAHD FAMILY ACYLTRANSFERASE* (Field and Osbourn, 2008). This cluster is also repressed by repressive H3K27me3 modifications (Field and Osbourn, 2008). It is proposed that the marneral and thalianol gene clusters have evolved independently from one common ancestor possibly by tandem gene duplication of an ancestral *OSC/CYP705* (Field et al., 2011).

The plant order of Brassicales has undergone three gene duplication events, the α, β, and γ event (Barker et al., 2010). Phylogenetic analysis of the marneral and thalianol gene clusters support the theory of cluster formation during the α event ~ 23 to 43 million years ago, probably from a common ancestor *OSC*/*CYP705* pair (Figure 4-3) (Barker et al., 2010; Field et al., 2011). This is supported by the finding that in *Arabidopsis lyrata* and *Arabidopsis thaliana*, both species of the Brassicaceae family, the thalianol cluster is present. But *Arabidopsis lyrata* is lacking the marneral cluster which could be explained by deletion events. Furthermore, genomic region of marneral and thalianol gene clusters is pronounced by a significantly high transposable element (TE) density that could have facilitated cluster formation (Field et al., 2011; Field and Osbourn, 2012). After cluster assembly, *THAH*, *MRO* and further enzymes were probably integrated in a multi-step gene recruiting process (Field et al., 2011). In addition, both clusters are located subtelomeric on the chromosome in a high dynamic region. It is unclear how cluster disruption is then prevented, since cluster mutation could lead to toxic intermediate accumulation (Chu et al., 2011; Field and Osbourn, 2012). Probably chromatin modifications protect these clusters from recombinant events (Lichten and De Massy, 2011; Field and Osbourn, 2012).

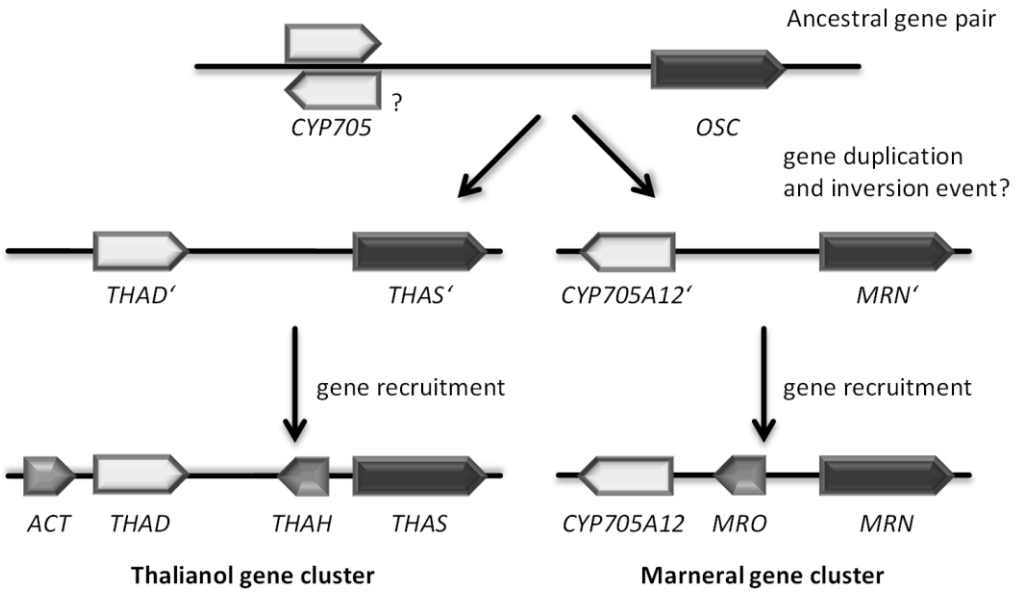

Figure 4-3: Thalianol and marneral gene cluster formation
Both gene clusters probably derived from a common ancestral *CYP705*/*OSC* gene pair and recruited then genes for final cluster formation (modified, Field et al., 2011).

4.1.2 Marneral and thalianol are involved in plant growth and development

The physiological function of marneral and thalianol and their derivatives in *Arabidopsis thaliana* are not deciphered. Nevertheless, based on studies of Arabidopsis mutant lines that are altered in marneral or thalianol biosynthesis, these molecules were implicated in growth and development (Field and Osbourn, 2008; Field et al., 2011; Go et al., 2012).

Arabidopsis loss-of-function T-DNA mutant lines offer a reverse genetic approach for functional gene characterization (Alonso et al., 2003). For a T-DNA inserted activation tagged Arabidopsis *mrn1* mutant, a delayed flowering phenotype with round-shaped rosette leaves were reported. In addition, mutation in *MRN1* results in an aberrant seed morphology, low seed germination rate, and root growth retardation in young seedlings. It is presumed that the aberrant seed morphology is linked to the delayed embryo development (Go et al., 2012). Controversially, no root growth retardation in an independent *mrn1* mutant was observed in a further study (Johnson, 2012). However, lacking marneral derivatives impact the plant development negatively as shown in Arabidopsis *mro* knock-out mutants that accumulate marnerol (Field et al., 2011). Phenotypic analyses of *mro* mutants reveal no striking differences in plant morphology, but rosettes and leaves are slightly smaller than in wild-type. In addition, length of main root in *mro* is reduced about 12 to 16% (Weckopp, 2014). The retarded leaf and root growth in *mrn1* is connected to inhibition of cell expansion or elongation, not by a reduced cell number (Field and Osbourn, 2008). It seems that

accumulation of marnerol and lack of further marneral derivatives has a similar impact as loss of all marneral derivatives.

Another way to gain insights into gene function is to overexpress a gene in a forward genetic approach by using a strong CAULIFLOWER MOSAIC VIRUS 35S (CaMV 35S) promoter fused to the target gene (Kadereit et al., 2014). The downside of using a 35S promoter is that the location of gene expression cannot be controlled and differs from the natural expression patterns. Overexpression of *MRN1* and *MRO* in Arabidopsis results in accumulation of marneral derivatives and lead to a dwarfed plant phenotype. This dwarfed phenotype is even more pronounced when overexpressing *MRN1* and *MRO* together (Field et al., 2011). This finding suggests that tight cluster regulation is important to ensure low intermediate triterpene concentrations which could be harmful for plant growth.

Comparable studies were performed in loss-of-function and gain-of-function mutants of *THAS*. Overexpression of *THAS* in Arabidopsis under the control of CaMV 35S promoter leads to thalianol accumulation in leaves and a dwarfed plant phenotype, similar to overexpression studies of *MRN1* and *MRO* (Field and Osbourn, 2008; Field et al., 2011). In addition, young Arabidopsis seedlings overexpressing *THAS* grow significantly longer roots. The dwarfed phenotype is even stronger when *THAS* and *THAH* are overexpressed together, but is absent in *THAH* overexpression lines itself (Field and Osbourn, 2008). On the other hand, absence of *THAS* gene only has a small impact on rosette size and does not alter root length in Arabidopsis (Field and Osbourn, 2008; Klunder, 2016). Interestingly, roots of *thah* and *thad* loss-of-function mutants are slightly longer than in wild-type (Field and Osbourn, 2008).

Whether these observations in plant growth and development are direct or indirect effects, caused by absence of marneral and thalianol derivatives, remain unsolved. But based on reported observations, marneral and thalianol derivatives might share a similar function in plant growth.

4.1.3 Regulating factors of the marneral and thalianol biosynthesis

As mentioned in Chapter 4.1.1.1, the marneral and thalianol gene clusters are marked with histone modifications that enable gene co-regulation at the level of chromatin. Nevertheless, little is known about transcription factors and environmental conditions that fine tune gene expression for marneral and thalianol biosynthesis when chromatin binding is loose. Fine tuning could be important to control the amount of intermediate products in the synthesis

pathway (Hurst et al., 2004; Yu et al., 2016). Therefore this chapter summarizes the regulation of the marneral and thalianol gene clusters, with the focus on gene transcription.

4.1.3.1 Regulation by plant hormone phytosulfokine-α

Phytosulfokine-α (PSK-α) is a disulfated peptide hormone (Tyr(SO_3H)-Ile-Tyr(SO_3H)-Thr-Gln) (Matsubayashi and Sakagami, 1996). In *Arabidopsis thaliana* the secreted propeptide phytosulfokine is encoded by five genes (Yang et al., 2001; Matsubayashi and Sakagami, 2006). The signal peptide targets the propeptide to the secretory pathway and is sulfated on two positions by the TYROSYLPROTEIN SULFOTRANSFERASE (TPST) in the trans-Golgi (Figure 4-4) (Lorbiecke and Sauter, 2002; Komori et al., 2009). In the apoplast the PSK propeptide is then proteolytically processed to PSK-α (Rautengarten et al., 2005; Srivastava et al., 2008). PSK-α can be perceived by the PSK RECEPTOR 1 (PSKR1) and PSK RECEPTOR 2 (PSKR2). PSKR2 probably plays a minor role in root phytosulfokine signaling pathway (Matsubayashi, 2006; Stührwohldt et al., 2011).

PSKR1 is a plasma membrane-localized leucine-rich repeat (LRR) receptor that contains an auto- and transphosphorylating kinase domain (Matsubayashi et al., 2002; Kwezi et al., 2011; Hartmann et al., 2013). This receptor promotes cell elongation, controls hypocotyl length and root growth in Arabidopsis (Kutschmar et al., 2009; Stührwohldt et al., 2011). In addition, PSK-α is crucial for a functional root stem cell niche (Matsuzaki et al., 2010). *tpst* loss-of-function mutants fail to maintain stem cells and present shorter hypocotyls and roots. By feeding *tpst* seedlings with 0.3 nM PSK-α, root growth is strongly promoted. This promotion is further increased when adding another sulfated peptide, PSY1. Nevertheless, feeding with PSK-α and PSY1 is still not able to rescue stem cell activity (Matsuzaki et al., 2010). This hints to further signaling molecule involved in stem cell maintenance. Furthermore, for PSKR1 activity a calmodulin binding motif within the kinase domain is essential, because Arabidopsis *pskr1(K762E)* mutants lacking this calmodulin binding motif have shorter roots and smaller shoots and demonstrate that this receptor is regulated by calcium/ calmodulin binding (Hartmann et al., 2014). Interestingly, PSK-α signaling is not only involved in cell elongation and stem cell maintenance, but also balancing immune responses of Arabidopsis against biotrophic and necrotrophic pathogens. Loss-of-function mutants *pskr1* and *tpst* are more resistant against biotrophic pathogens like the bacterial pathogen *Pseudomonas syringae pv. tomato* DC3000 while they are more susceptible to necrotrophic fungi like *Alternaria brassicicola* (Mosher et al., 2013). The increased resistance in *pskr1* against biotrophic bacteria is in consensus with increased level of salicylic acid, a plant defense compound, and a reduced amount of jasmonic acid (JA) responsive gene transcripts. JA acts antagonistically

to salicylic acid (SA) and is involved in defense against necrotrophic fungi instead. This resistance effect is directly linked to PSK-α signaling, since exogenous supplemented PSK-α lowers resistance of *tpst* to a wild-type level, but not in *pskr1*/*pskr2*/*psy1receptor* (*psy1r*) triple mutant (Mosher et al., 2013; Mosher and Kemmerling, 2013). It is hypothesized that PSK-α and/ or PSY1 perception results in downregulation of SA depending responses during biotrophic pathogen infection to prevent an over-induction and balancing of this particular signaling pathway that would otherwise leave the plant susceptible to necrotrophic pathogens (Mosher and Kemmerling, 2013).

Unpublished transcriptome data of young Arabidopsis seedlings treated with PSK-α indicate that marneral and thalianol gene cluster expression is induced upon PSK-α treatment (personal communication with Prof. Dr. Margret Sauter, 2013, Institute for Plant Developmental Biology and Physiology, University Kiel, Germany). Indeed, a gene expression study provided evidence for activation of marneral and thalianol gene clusters by PSK-α signaling (Figure 4-5). The same study pointed on an impaired PSK-α root growth induction in loss-of-function *mro* seedlings (Weckopp, 2014). However, similar expression patterns of thalianol and marneral gene clusters substantiate similar functions and more common features.

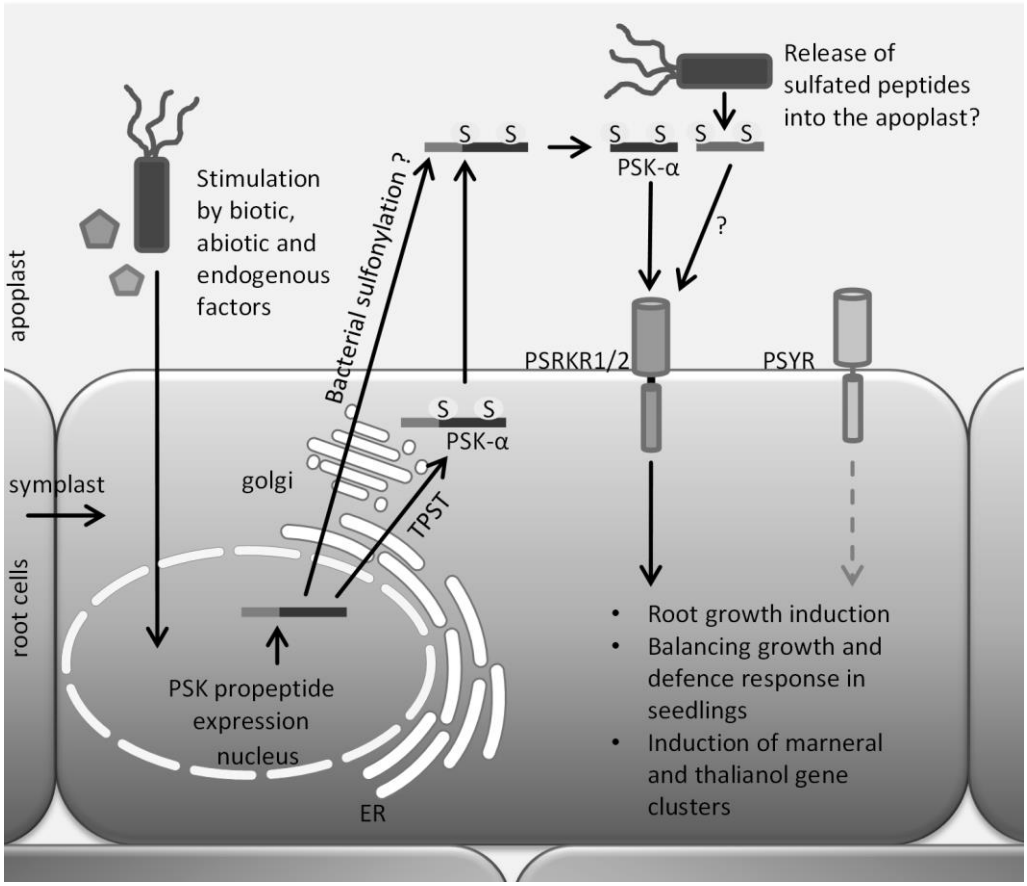

Figure 4-4: Simplified scheme of the phytosulfokine-α pathway
Developmental triggers, abiotic or biotic stimuli could induce expression of PSK propeptides (Yang et al., 2001; Matsubayashi and Sakagami, 2006). In the trans-golgi the propeptide gets disulphated and is secreted into the apoplast (Lorbiecke and Sauter, 2002; Komori et al., 2009). After proteolytic cleavage it is sensed by PSKR1 and PSKR2 that induce Ser/Thr kinase cascade (Rautengarten et al., 2005; Matsubayashi, 2006; Srivastava et al., 2008; Stührwohldt et al., 2011). PSKR activation induces cell elongation in roots, balancing growth and SA/JA level, and induces marneral and thalianol gene cluster expression (Kutschmar et al., 2009; Stührwohldt et al., 2011; Mosher et al., 2013; Mosher and Kemmerling, 2013; Weckopp, 2014). PSY1 receptor activation is proposed to have an additive effect to PSK related processes (Sauter, 2015). Furthermore, bacteria expressing TPST orthologues could disulphate PSK propeptides, or manipulate PSKR1 by secreted sulfated peptides (Pruitt et al., 2015; Park et al., 2016). See Chapter 4.1.3.3 for more information about biotic stress responses.

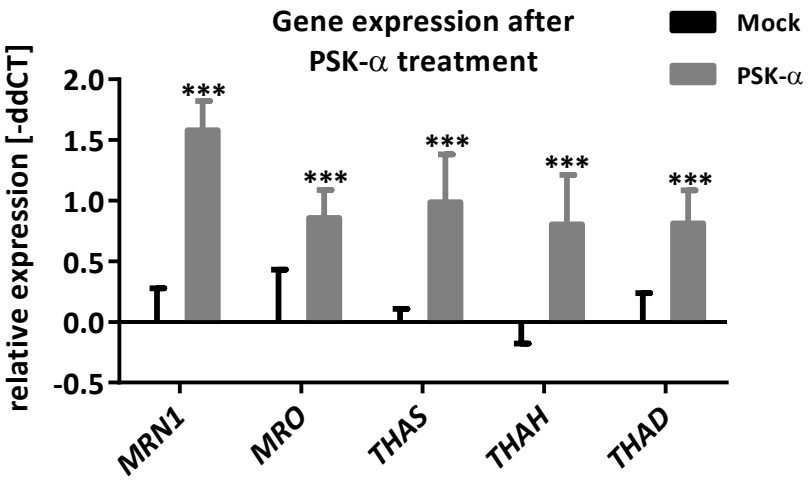

Figure 4-5: Marneral and thalianol gene cluster expression after exogenous PSK-α treatment in Col-0
Gene expression of *MRN1*, *MRO*, *THAS*, *THAH* and *THAD* in 8 days old Arabidopsis seedlings treated with 100 nM PSK-α. The relative expression was calculated with the ddCT method using *PP2A* as reference gene (n=4). Fold changes are shown as Log2 values ± SD. Statistical data analysis was performed by one-way ANOVA with Tukey's test and significance levels were set at * P<0.05, ** P<0.01, ***P<0.001 (Weckopp, 2014).

4.1.3.2 Regulation by jasmonic acid

In nature, plants are facing many different herbivores and necrotrophic fungi. JA was proven to be the main hormone for inducing a massive defense cascade in plants against these threats (Howe and Jander, 2008). The JA signaling pathway is mainly regulated by protein receptor complex containing the F-box protein CORONATINE INSENSITIVE 1 (COI1) which is bound to the JASMONATE ZIM-DOMAIN (JAZ) complex repressor protein, the NOVEL INTERACTOR OF JAZ (NINJA) and transcription factors (TFs). In presence of JA-isoleucine, the COI1 complex is activated, JAZ repressor gets degraded by the 26S proteasome and TFs, like the BASIC HELIX-LOOP-HELIX-PROTEIN-1 (MYC2) TF, are released. The TFs then interact with the MED25 subunit of the Mediator complex, encoded by the *PHYTOCHROME AND FLOWERING TIME1* (*PFT1*) gene, to recruit RNA polymerase II for JA-responsive gene expression (Kidd et al., 2009).

Unfortunately, the downside for JA pathway activation is a reduced growth. Constant JA activation, like in the Arabidopsis mutant lacking a quintet of JAZ repressors (*jazQ*) results in a reduced growth phenotype. However, in loss-of-function *jazQ*photoreceptor phytochrome B (phyB)* mutant the tradeoff between growth retardation and enhanced plant resistance is diminished (Campos et al., 2016). Transcriptome analysis revealed that basal expression level of *MRN*, *THAS*, *THAH* and *THAD* are upregulated in *jazQ* and slightly stronger in *jazQ* phyB* (Campos et al., 2016). That finding indicates that the marneral and thalianol gene clusters are regulated via JA pathway and could also be woven in defense responses besides

plant growth. This hypothesis is supported by further transcription studies in *ninja* and *pft1* (Sundaravelpandian et al., 2013; Gasperini et al., 2015). Furthermore, exogenous applied JA, in form of methyl-JA, induces expression of the marneral and thalianol gene clusters in Arabidopsis seedlings (Winter et al., 2007).

4.1.3.3 Regulation by abiotic and biotic stress

Plants are facing many different challenges during their life cycle: biotic stresses from pathogens, as well as abiotic stresses like droughts, floods, salty/ contaminated soil and more. Pathogens can be distinct in three different classes: (1) biotrophic pathogens feed from the host without killing it; (2) necrotrophic pathogens often have a broader host spectrum and feed from lysing host cells with toxic enzymes which could result in host death; (3) hemibiotrophic pathogens are fed in a biotrophic manner but then change their life style to a necrotrophic diet (Lewis, 1973; Perfect and Green, 2001). The impact of marneral and thalianol derivates on biotic and abiotic stress is little documented.

Since marneral and thalianol gene clusters are mainly expressed in roots, there could be a connection to plant microbe interaction. Challenging of Arabidopsis *thas*, *thah*, and *thad* roots with fungal and bacterial plant pathogens (*Alternaria brassicicola*, *Botrytis cinerea*, and *Pseudomonas syringae pv tomato DC3000*) do not lead to a phenotypic variation in comparison to wild-type (Field and Osbourn, 2008). However, the selected plant pathogens are more common for plant shoots, fruits, and leaf diseases (Windram et al., 2012; Su'udi et al., 2013; Xin and He, 2013). A better model system for plant root microbe interaction could be a soil borne microbe, like the gram-negative pathogenic bacterium *Burkholderia glumae*. This bacterium belongs to the genus Burkholderia within the subphylum of the β-proteobacteria (Hotta et al., 1992). It mainly infects rice and other crop plants, but also harms *Arabidopsis thaliana* (Jeong et al., 2003; personal communication with Prof. Dr. Stanislav Kopriva, 2016, University of Cologne, Germany). Furthermore, plants could also benefit from microbe interactions. In recent years, soil microbiome became an important topic in science, since the microbial ecosystem in soil or microbiome shapes plant performance by improving mineral nutrition. Molecules secreted by plant roots are referred to as root exudates and are proposed for attracting and repelling certain microbes thereby forming microbial community (Walker, 2003; Jacoby et al., 2017). To our knowledge, secreted triterpenoids are only reported in chemical defense against fungal pathogens (Papadopoulou et al., 1999; Osbourn, 2003). However, genome sequencing of the plant microbiome revealed that TPST orthologues in root-associated bacteria exist (Bai et al., 2015; Klunder, 2016). Since PSKR1 is

associated with plant pathogens interaction, this thesis postulated that bacteria containing TPST orthologues could alter PSK-α signaling and influence marneral and thalianol metabolism (Igarashi et al., 2012; Mosher et al., 2013). On the one hand, PSK propeptide contains a signaling peptide that mediates transfer through the secretory pathway into the apoplast (Lorbiecke and Sauter, 2002). In the apoplast, PSK propeptide could be cleaved and sulfated by bacterial TPST orthologues. On the other hand, PSKR1 might be directly activated by sulfated peptides derived from the bacteria.

As sessile organisms, plants need to withstand harsh environmental conditions. Arabidopsis transcriptome data link osmotic and salt stress to *MRN1* gene induction in roots, but not to *MRO* and *CYP71A16* expression (Figure 4-6 A). Interestingly, *THAS* gene expression is induced in roots after leaf wounding and slightly after drought (Figure 4-6 B). In addition, *THAH* and *THAD* expression in roots were induced by wounding and drought exposure in a similar manner (Kilian et al., 2007; Winter et al., 2007).

Taken together, gene clusters for marneral and thalianol biosynthesis share common features regarding their regulatory mechanisms: Both clusters are regulated by H3K27me3 chromatin signatures, are induced by PSK-α and JA signaling and are mainly expressed in roots and young seedlings (Field and Osbourn, 2008; Go et al., 2012; Weckopp, 2014; Campos et al., 2016; Yu et al., 2016). In addition, aberrant marneral or thalianol biosynthesis leads to a retarded plant growth (Field and Osbourn, 2008; Go et al., 2012). These pieces of evidence point to a complementary function of marneral and thalianol in plant growth, development and defense.

Table 4-1: Bacterial strains containing potential TPST orthologues
Protein sequence comparison of functional bacterial TPST like protein RaxST from gram-negative bacterium *Xanthomonas oryzae pv. Oryzae* with sequence information of plant microbiome collection. Experiment was conducted with NCBI protein blast search. Hits are shown with corresponding *Expec*t (E) values and protein query cover (Han et al., 2012; Bai et al., 2015; Klunder, 2016).

E-value	Query cover	Strain	Class
$3x10^{-74}$	94%	Pseudomonas sp. Root68	Gammaproteobacteria
$3x10^{-73}$	94%	Massilia sp. Root133	Betaproteobacteria
$5x10^{-69}$	94%	Pseudoxanthomonas sp. Root65	Gammaproteobacteria
$8x10^{-78}$	90%	Rhodanobacter sp. Root480	Gammaproteobacteria
$8x10^{-70}$	94%	Pseudomonas sp. Root401	Gammaproteobacteria

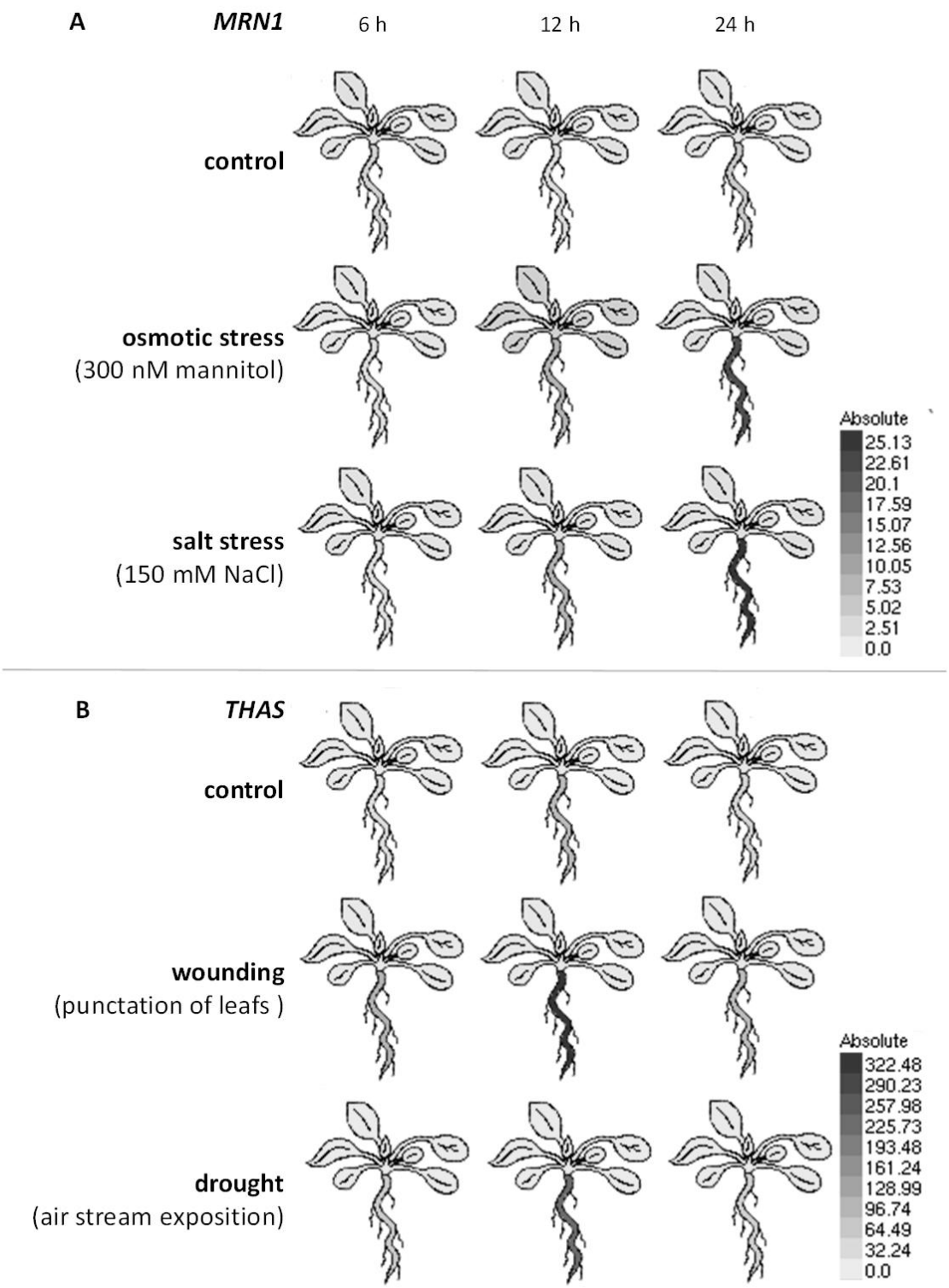

Figure 4-6: Absolute gene expression of *MRN1* and *THAS* in Arabidopsis seedlings after abiotic stress treatments

MRN1 expression is induced 12 h after osmotic (max. fold change 4.48) and salt stress osmotic (max. fold change 5.25) treatment. *THAS* expression is induced 12 h after wounding by leaf puncturing with needles (max. fold change 3.57) and slightly after drought simulation (max. fold change 2.5) (Kilian et al., 2007; Winter et al., 2007).

4.1.4 Aim

To date, the function of triterpenes in plants is largely unknown. This chapter studies the physiological function of triterpenes on plant growth through investigation of marneral and thalianol in *Arabidopsis thaliana* in a reverse genetic approach.

This chapter should validate whether marneral and thalianol share a redundant function by crossing of Arabidopsis T-DNA *mrn1* and *thas* mutants and their functional characterization. To elucidate effects of marneral and thalianol on plant growth, *mrn1*thas* will be morphologically characterized and *mrn1*thas* reaction to chemically induced abiotic and biotic stress from root-associated microbes will be studied in growth assays. Moreover, the connection between marneral and thalianol with plant hormone signaling will be investigated. This chapter focuses on PSK-α and JA hormone signaling and including hormone treatments of representative knock-out mutants.

4.2 Results

To test the hypothesis that marneral and thalianol might share a redundant function, crosses between *marneral*- and *thalianol synthase* loss-of-function mutants were generated. Next, the phenotype of *Arabidopsis thaliana mrn1*thas* and their response to abiotic stress as well as their growth rate in presence of root-associated microbes were analyzed.

4.2.1 Crossing of *marneral*- and *thalianol synthase* mutants

To obtain *mrn1*thas* double knock-out plants, the Arabidopsis homozygous T-DNA lines *mrn1* (SALK_152492; AT5G42600) and *thas* (SALK_064244; AT5G48010) were crossed (Figure 2-3). Double homozygous T-DNA insertions were confirmed by PCR. Afterwards *MRN*1 and *THAS* transcript levels in young seedlings were investigated in *mrn1*thas* by reverse transcription polymerase chain reaction (RT-PCR). The *mrn1*thas* double mutant was free of any *THAS* and *MRN1* transcripts (Figure 4-7). Two different primer pairs for *MRN1* amplification were used due to uncertainties of *mrn1* homozygosity as described in literature (Go et al., 2012).

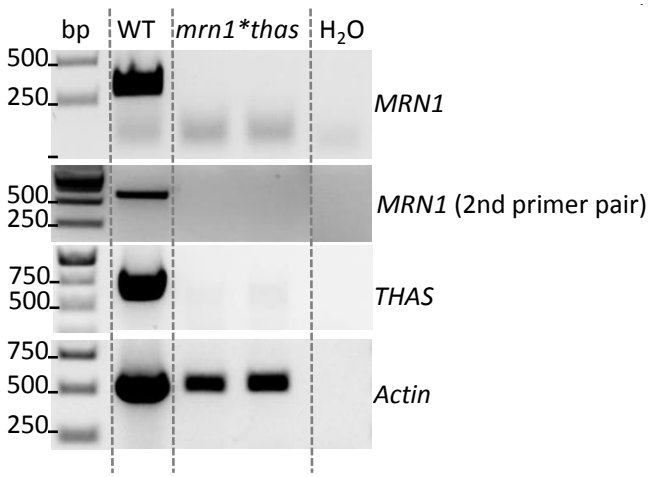

Figure 4-7: Confirmation of T-DNA knock-out in *mrn1*thas*
RT-PCR analysis of *MRN1*, *THAS* (40 cycles) and *Actin* (At3g18780) (31 cycles) transcripts in roots of 14 do seedlings. Expected product sizes: RT_MRN_LP1 + RT_MRN_RP1 → 309 bp; RT_MRN_LP2 + RT_MRN_RP2 → 663 bp; RT_THAS_LP + RT_THAS_RP → 642 bp; RT_ACTIN_LP + RT_ACTIN_RP → 522 bp.

4.2.2 Growth phenotype of *mrn1*thas* mutant

In the next step the general plant morphology of *mrn1*thas* was documented to investigate the effect of marneral and thalianol on plant growth. Col-0, *mrn1*thas*, *mrn1*, and *thas* seeds were stratified in cold for 4 days and germinated for 7 d at long-day conditions (16 h light/ 8 h darkness), 22 °C and 150 µE light. Afterwards, seedlings were transferred onto soil.

The growth of Col-0, *mrn1*thas*, *mrn1*, and *thas* was documented once a week starting from 2nd week after germination at long-day conditions. The rosette leaf area, diameter, compactness and stockiness of Col-0, *mrn1*thas*, *mrn1*, and *thas* was calculated with rosette tracker software (De Vylder et al., 2012). The compactness describes the ratio between the area of the rosette and the area enclosed by a convex hull around the rosette (Arvidsson et al., 2011). The stockiness describes the circularity of a plant. It is defined as 4xπxrosette area/(perimeter)^2 and ranging from 0 to 1 (perfect circle) (Jansen et al., 2009; De Vylder et al., 2012). Rosette size, maximal rosette dimeter, and compactness in *mrn1*thas* as well as in *mrn1* and *thas* were not altered in comparison to Col-0 during vegetative period (Figure 4-8). At the 2nd week, all mutant lines displayed slightly but significantly rosette stockiness. The reduced stockiness returned to wild-type level after 3rd week (Figure 6-7). Photographic documentations of 4 week old rosettes are in supplement (Figure 6-8). In addition, average leaf number in *mrn1* was slightly increased by one additional leaf in comparison to *mrn1*thas*, *thas*, and Col-0 (Figure 4-9). Leaflets of *mrn1* were slightly narrowed (Figure 4-10). However, leaflets from *mrn1*thas* and were similar to Col-0.

Furthermore, Col-0, *mrn1*thas*, *mrn1*, *mrn1_2*, and *thas* grew inflorescences after 21 days and started flowering after 24 days (Figure 6-9 A+D). *mrn1_2* was as *mrn1* free of *MRN1* transcripts (Figure 6-10). No alterations in *mrn1*thas* in comparison to Col-0 in flower- and silique morphology were observed (Figure 6-9 B + C). Plants had four sepals, four petals inside this, six stamens, and a central carpel. Flower- and silique morphology in respective single mutants were similar to *mrn1*thas* (not shown). Moreover, progeny of *mrn1*thas* had a ~100% seed germination rate (n=48), and no significant changes in general root growth of *mrn1*thas* were found (Figure 4-11).

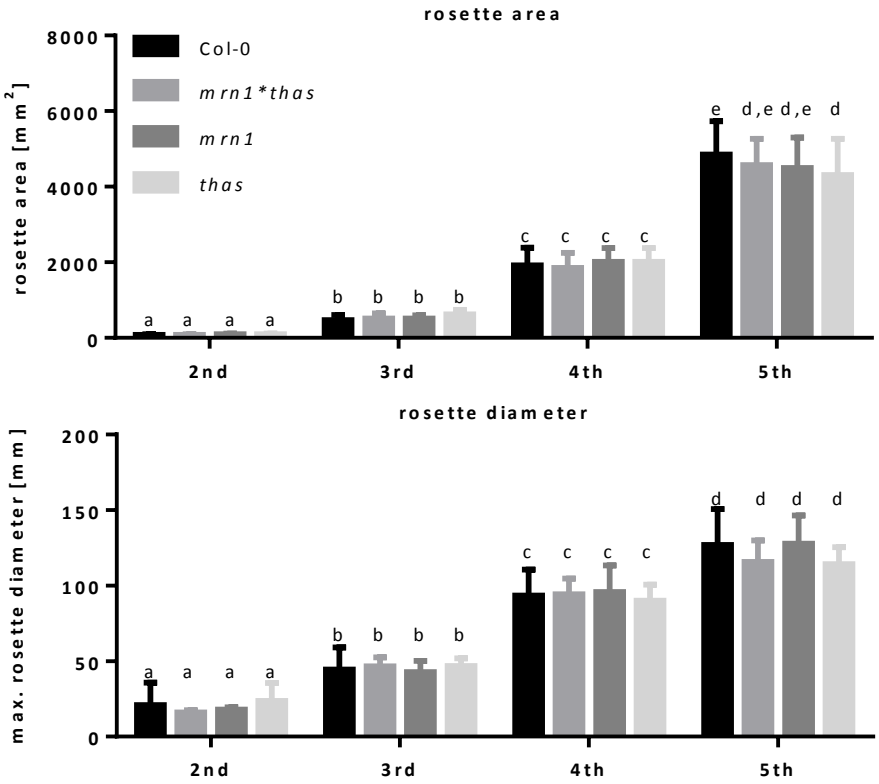

Figure 4-8: Rosette area and maximal rosette diameter of Col-0, *mrn1*thas*, *mrn1*, and *thas*
Plants were grown on soil under long-day conditions. Pictures were taken 2, 3, 4, and 5 weeks after germination (1st to 4th. week n=15; 5th week n=12). Rosette area and diameter were automatically calculated with rosette tracker software. Statistical data analysis was performed by one-way ANOVA with Tukey's test and significance levels were set at $P \leq 0.05$ and indicated by small letters. Standard deviation is shown.

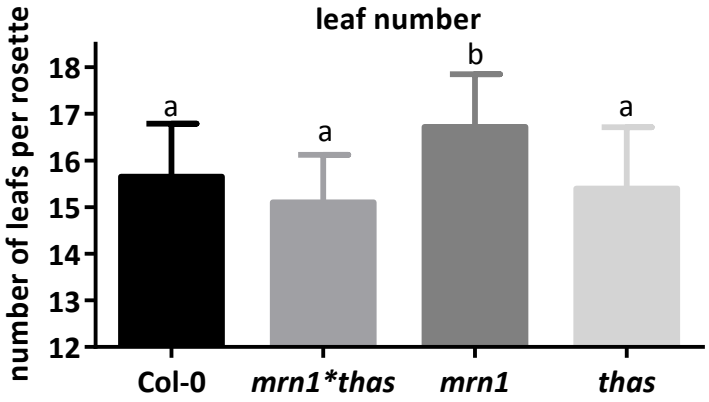

Figure 4-9: Leaf number in 4 week old Col-0, *mrn1*thas*, *mrn1*, and *tha*
Plants were grown for 4 weeks on soil under long-day conditions (n=18). Statistical data analysis was performed by one-way ANOVA with Tukey's test and significance levels were set at $P \leq 0.05$ and indicated by small letters. Standard deviation is shown.

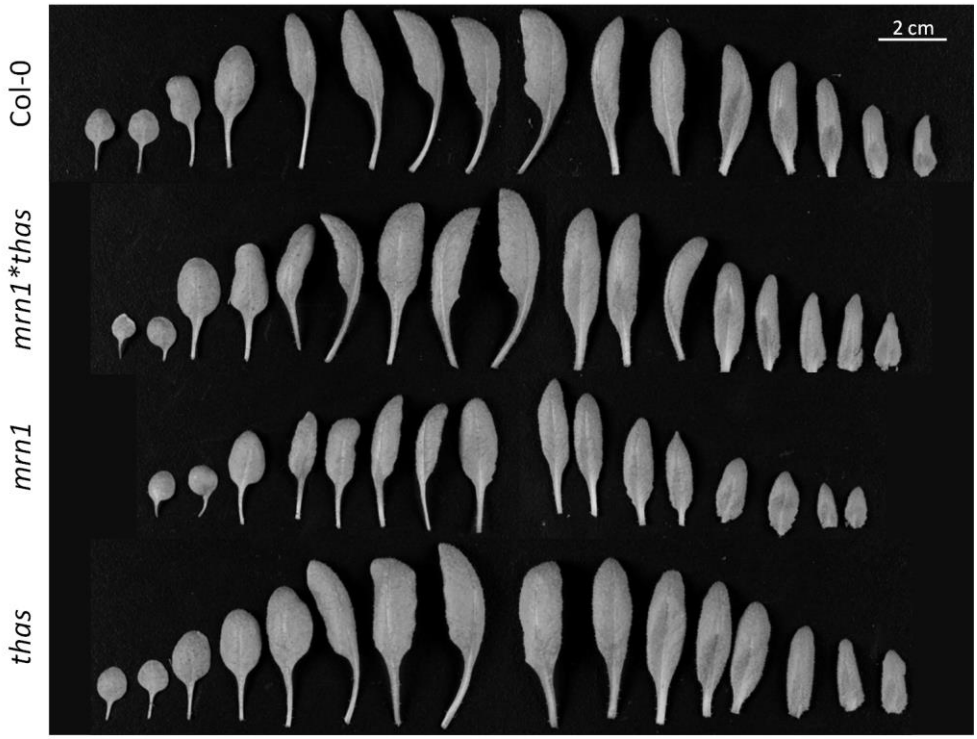

Figure 4-10: Leaflets of 4 week old Col-0, *mrn1*thas*, *mrn1*, and *thas*
Plants were grown on soil under long-day conditions.

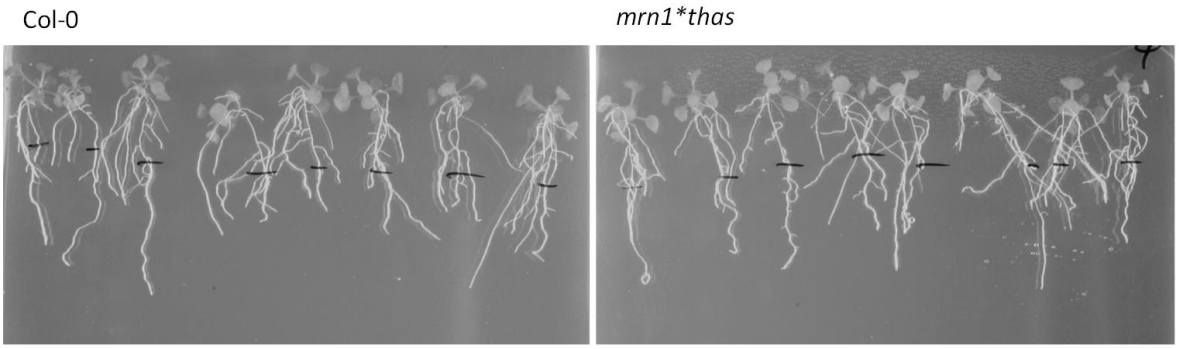

Figure 4-11: Root growth of 14 days old Col-0 and *mrn1*thas*
Plants were grown 7 days on ½ MS (+Suc) and 7 days on ½ MS under long-day conditions.

4.2.3 Functional characterization of *mrn1*thas* mutant

No drastic changes in growth of *mrn1*thas* were observed. However, how are marneral and thalianol connected to PSK-α or JA signaling, and do they obtain a function in abiotic stress responses? Are both triterpenes involved in root-associated microbe interactions? These questions were studied in plant growth assays as described below.

4.2.3.1 Connection between PSK-α signaling with marneral and thalianol

Previous results indicated a connection between PSK-α signaling with marneral and thalianol gene expression (Figure 4-5). Therefore, the capability of PSK-α to induce root growth in *mrn1*thas*, *mrn1*, *thas*, and *pskr1,2*psy1r* triple mutant was analyzed. *pskr1,2*psy1r* (AT2G02220, AT5G53890, AT1G72300) is incapable of sensing PSK, PSK-α, and PSY1 (Mosher and Kemmerling, 2013). In addition, PSK-α induced root growth was analyzed in *ninja-1* (AT4G28910) and *coi1-34* (AT2G39940) mutants (Acosta et al., 2013). In *ninja-1,* JA response is constantly active and *coi1-34* is incapable of jasmonate sensing. This approach would give insights into relation of marneral and thalianol with PSK-α and jasmonate signaling.

Plants were grown on ½ MS plates (+sucrose) for 7 days. Thereafter, seedlings were transferred onto ½ MS plates containing 0.1 µM PSK-α. Gain of root length was measured after further 7 days (Figure 4-12). PSK-α significantly induced root growth in wild-type (1.3 cm to 1.8 cm) and in *coi1-34* (1.5 cm to 2.0 cm). No growth enhancement by PSK-α was observed in *mrn1*thas*, *mrn1*, *thas*, and *pskr1,2*psy1r* and *ninja-1*. Root length in *ninja-1* was slightly enlarged, but not significantly. Marneral and thalianol gene expression were analyzed in Col-0 and *pskr1,2*psy1r* 4 h after 1 µM PSK-α treatment (Figure 4-13 A-D). In *pskr1,2*psy1r*, basal gene expression of *MRN1*, *MRO*, *THAS* and *THAH* were strongly impaired down to a 4% of wild-type value (*MRN1*). PSK-α induced *MRN1* and *MRO* expression two fold in Col-0, but not in *pskr1,2*psy1r*. On the other hand, *THAS* and *THAH* expression was neither increased in Col-0 nor in *pskr1,2*psy1r*.

Phytosulfokine-α was insufficient to induce plant root growth in *mrn1* and *thas* deficient mutants. Expression studies revealed that activation of marneral and thalianol gene cluster are linked to PSKR1/2 and/or PSY1R signaling. Next, interaction of jasmonate signaling with marneral and thalianol metabolism was investigated in more detail.

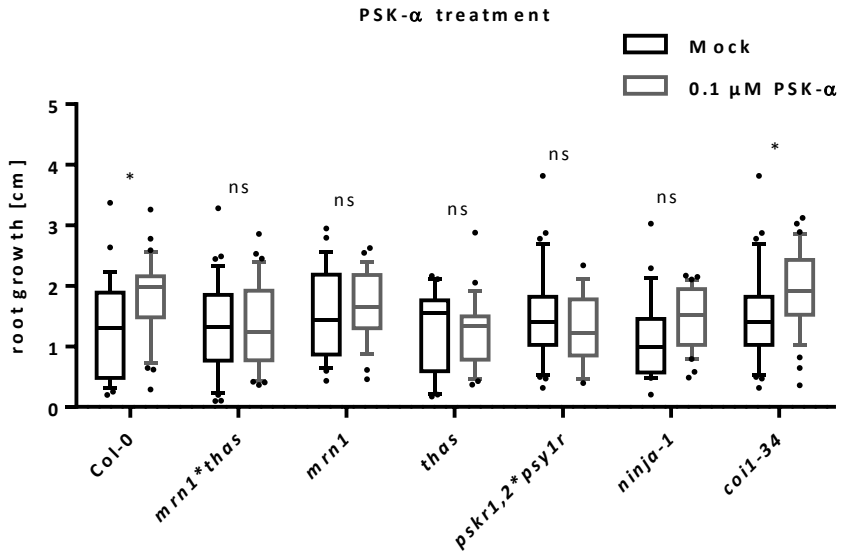

Figure 4-12: PSK-α treatment of Col-0, *mrn1*thas*, *mrn1*, *thas*, *pskr1,2*psyr*, *ninja*, and *coi1_34*
Seedlings were grown on ½ MS agar plates (+sucrose) on long-day conditions and transferred after 7 days onto ½ MS agar plates supplemented with 0.1 µM PSK-α. Gain of root length after transfer was measured after further 7 d (n=15-38). Box plot shows 10-90% percentile. Statistical data analysis was performed by one-way ANOVA with Tukey's test and significance levels were set at $P \leq 0.05$ and indicated by *; ns = non-significant change.

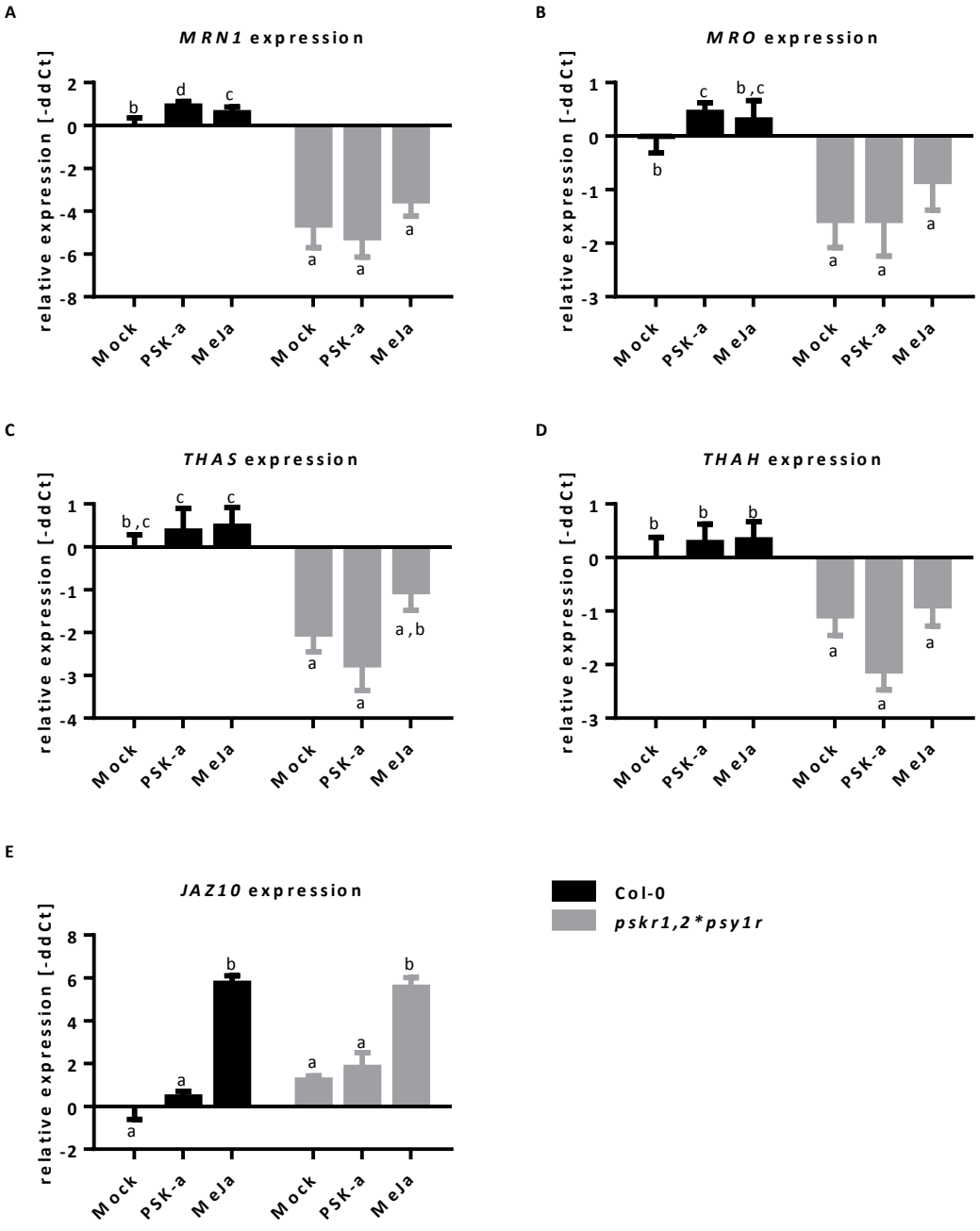

Figure 4-13: Gene expression of *MRN1, MRO, THAS, THAH* and *JAZ10* in Col-0 and *pskr1,2*psy1r* after PSK-α and MeJa treatment

Plants were grown for 14 d on ½ MS plates (+sucrose) under long-day conditions. Next, plants were sprayed with water (n=3-4), 1 µM PSK-α or 10 µM MeJA solution (n≤3). Roots were harvested 4 h after treatment and qPCR analysis was performed (2 technical replicates). $RQ=2^{-ddCT}$ was calculated. Statistical data analysis was performed by two-way ANOVA with Tukey's test and significance levels were set at $P \leq 0.05$, indicated by small letters. -ddCT was plotted. Standard deviation is shown. A: *MRN1* expression; B: *MRO* expression, C: *THAS* expression, D: *THAH* expression, E: *JAZ10* expression.

4.2.3.2 Connection between JA signaling with marneral and thalianol

Chapter 4.1.3.2 introduced evidence for marneral and thalianol synthesis being dependent on JA signaling. We addressed the question whether marneral and thalianol gene cluster are

dependent on JA signaling and whether this dependence is linked to PSK-α signaling, or not. Therefore Col-0, *mrn1*thas*, *mrn1*, *thas*, and *pskr1,2*psy1r* were treated with 10 µM MeJA, also in combination with 0.1 and 1.0 µM PSK-α. Gain in root growths as well as expression of genes from marneral and thalianol clusters were evaluated.

Root growth after MeJA treatment was strongly inhibited in Col-0, *mrn1*thas*, *mrn1*, *thas*, and *pskr1,2*psy1r* (Figure 4-14). Gene expression analysis of Col-0 and *pskr1,2*psy1r* treated with 10 µM MeJa revealed a slight induction of marneral gene cluster expression (Figure 4-13 A-D). JAZ10 expression was used as control for MeJa treatment and is induced in Col-0 and *pskr1,2*psy1r* (Figure 4-13 E).

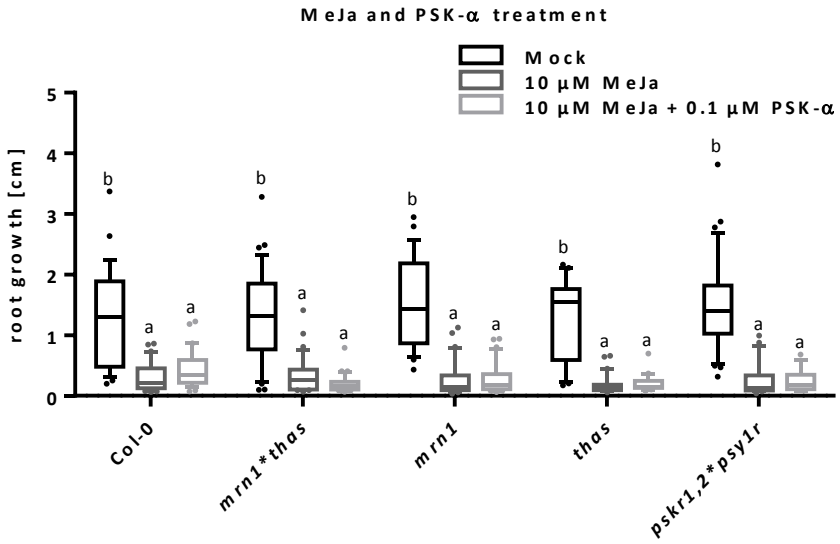

Figure 4-14: MeJA and MeJa + PSK-α treatment of Col-0, *mrn1*thas*, *mrn1*, *thas*, and *pskr1,2*psyr*
Seedlings were grown on ½ MS agar plates (+sucrose) on long-day conditions and transferred after 7 days onto ½ MS agar plates supplemented with 10 µM MeJA or 10 µM MeJA+ 0.1 µM PSK-α. Plants were grown in parallel with experiment shown in Figure 4-12. Gain of root length after transfer was measured after further 7 d (n=15-38). Box plot contain 10-90% percentiles. Statistical data analysis was performed by one-way ANOVA with Tukey's test and significance levels were set at $P \leq 0.05$ and indicated by small letters.

4.2.3.3 Connection between abiotic stress response with marneral and thalianol

In nature, plants are daily challenged with changing environmental conditions. Marneral and thalianol gene clusters are mainly expressed in roots, especially in seedlings. Therefore they might have a root specific function linked to differing soil conditions. Transcriptome data revealed induction of *MRN1* expression in roots under osmotic and salt stress while *THAS* is induced in roots after leaf wounding and drought (Figure 4-6) (Kilian et al., 2007; Winter et al., 2007). These subchapters focus on osmotic, salt and ROS stress by chemical inducers.

Sorbitol (25 mM; osmotic potential Ψ_s=-0,061 MPa) and mannitol (75 mM; Ψ_s=-0.184 MPa) treatments were used for osmotic stress/ drought simulation (Verslues et al., 2006; Claeys et al., 2014). For simulating salt stress response 50 µM NaCl were used. 1 mM hydrogen peroxide was used to expose plants to ROS. ROS production is naturally triggered in plants by many abiotic factors like high-light (UV-B radiation), drought, salinity, chilling, nutrient deficiency, but also by biotic factors like herbivores (Shin et al., 2005; Einset et al., 2007; Maffei et al., 2007; Miller et al., 2010; Hideg et al., 2013). The chemical concentrations were selected upon weak to medium growth inhibition in Arabidopsis (Claeys et al., 2014).

Col-0 and *mrn1*thas* were grown on ½ MS agar plates (+sucrose) supplemented with 25 mM mannitol, 75 mM sorbitol, 50 mM NaCl, or 1 mM H_2O_2 for 3 weeks under long-day conditions. Rosette area, diameter and stockiness were calculated with rosette tracker software (Figure 4-15). Mannitol, sorbitol, NaCl, and H_2O_2 inhibited plant growth, strongly. Overall rosette area and maximal rosette diameter were most impaired under mannitol and sorbitol treatments (Figure 4-15 A+B). However, *mrn1*thas* growth did not differ from Col-0. Only in *mrn1*thas* Mock, rosette size was slightly smaller than in Col-0. The overall rosette compactness slightly differs between genotypes in sorbitol and H_2O_2 treatments (Figure 4-15 C).

Taken together, in this experimental setup chemical induced abiotic stress responses suppressed plant growth, but no alteration in *mrn1*thas* were observed.

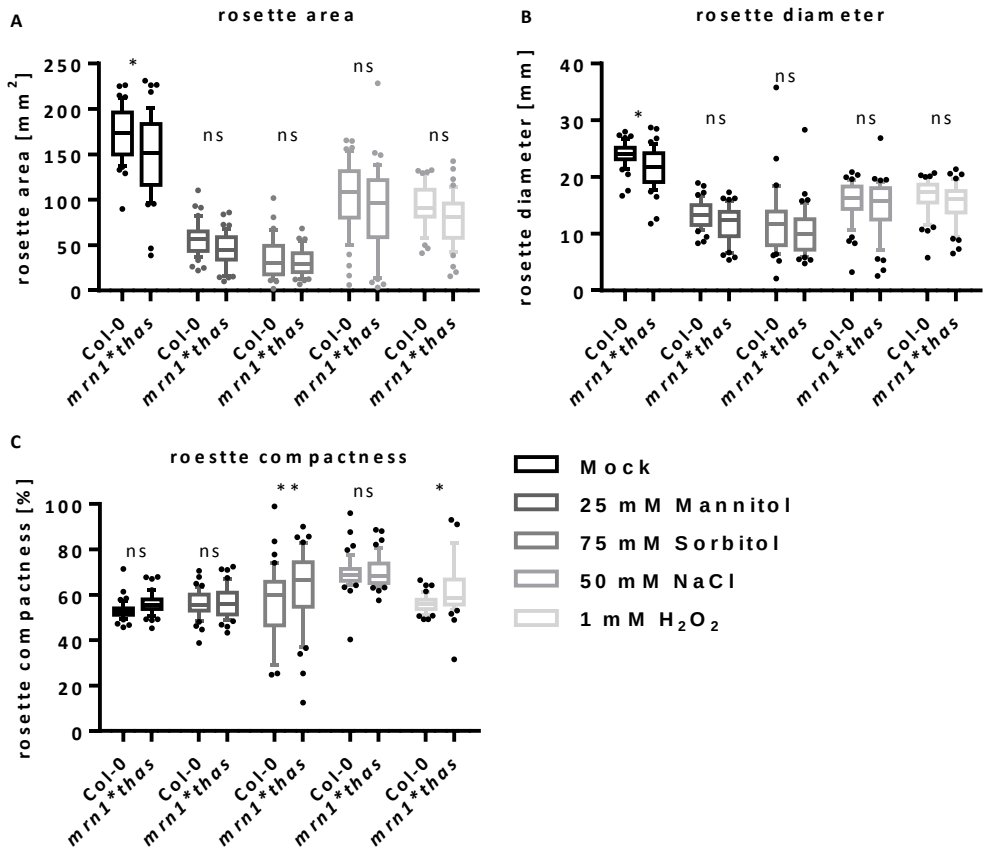

Figure 4-15: Col-0 and *mrn1*thas* growth under chemical induced abiotic stress
Plants were grown on ½ MS media (+sucrose) supplemented with 25 mM mannitol, 75 mM sorbitol, 50 mM naCl, or 1 mM H_2O_2 for 3 weeks under long-day conditions (n=48). Next, plant rosettes were photographically documented and evaluated with rosette tracker software. Box plot contain 10-90% percentiles. A: rosette area in mm^2; B: rosette diameter in mm; C: rosette compactness in percent. Statistical data analysis was performed by two-way ANOVA with Tukey's test only comparing treatments and significance levels were set at * $P \leq 0.05$ * and $P \leq 0.005$ **.

4.2.3.4 Connection between root-associated microbes with marneral and thalianol

Triterpenes, especially saponins, are involved plant pathogen defense (Papadopoulou et al., 1999; Osbourn, 2003). Marneral and thalianol are mainly synthesized in roots and could fulfill their role in plant microbe interaction, since their expression is regulated by *PSKR1* which is involved in plant microbe/pathogen interaction (Field et al., 2011; Mosher et al., 2013). To verify this hypothesis, Col-0, *mrn1*thas, mrn1*, *thas,* and *pskr1,2*psy1r* were co-cultivated with *Burkholderia glumae*, a known soil pathogen, and effect on plant growth were documented (Jeong et al., 2003; personal communication with Prof. Dr. Stanislav Kopriva, 2016, University of Cologne, Germany). Furthermore, bacterial strains containing *TPST* orthologues were co-cultivated with Col-0 and *mrn1*thas,* that could potentially trigger

PSKR1 receptor and activate gene cluster expression (Lorbiecke and Sauter, 2002; Igarashi et al., 2012; Mosher et al., 2013).

Col-0, *mrn1*thas*, *mrn1*, *thas*, and *pskr1,2*psy1r* were grown on ½ MS media (+sucrose) for 7 days. Next, they were transferred onto ½ ms media supplemented with *Burkholderia glumae* (OD_{600}=5*10^{-6}) for further 11 days. Thereafter seedlings fresh weight (FW) was calculated (Figure 4-16). In Mock control treatment seedlings FW of *mrn1*thas*, *mrn1*, and *thas* was slightly, but significant lower in comparison to Col-0. *Burkholderia glumae* strongly inhibited plant growth in all genotypes. FW of Col-0, *mrn1*thas*, *mrn1* and *thas* were statistically similar. In addition, no significant differences in fold change data could be obtained (data not shown). *pskr1,2*psy1r* FW after co-cultivation was slightly lower than in Col-0, but did not differ from *mrn1*thas*, *mrn1*, and *thas* FW. In another approach, root material from *Burkholderia glumae* (OD_{600}=5x10^{-6}; OD_{600}=5x10^{-7}) infection was collected and transcription level of defense marker genes were studied (Figure 4-17). *CYP71A12* is involved in camalexin biosynthesis and is strongly expressed after *Burkholderia glumae* treatments of Col-0 and *mrn1*thas* (Figure 4-17 A) (Müller et al., 2015). The transcription factor HIGH INDOLIC GLUCOSINOLATE 1 (MYB51) induces camalexin biosynthesis and its expression was activated in *mrn1*thas* after *Burkholderia glumae* (OD_{600}=5x10^{-5}) treatment (Figure 4-17 B) (Frerigmann and Gigolashvili, 2014). *JAZ10* expression is induced by SA signaling and was also induced upon *Burkholderia glumae* infection (Figure 4-17 C) (Moreno et al., 2013; Frerigmann and Gigolashvili, 2014). However, after *Burkholderia glumae* (OD_{600}=5x10^{-6}) treatment, *JAZ10* expression in *mrn1*thas* was lower than in Col-0. The *VEGETATIVE STORAGE PROTEIN 2 (VSP2)* is induced by wounding, MeJA, insect feeding, and phosphate deprivation (Liu, 2005). It was also induced after *Burkholderia glumae* infection in Col-0 (Figure 4-17 D). In *mrn1*thas*, *VSP2* was only expressed when using higher bacteria concentration. *MRN1* expression was 4-fold increased in Col-0 and could not be detected in *mrn1*thas* after *Burkholderia glumae* (OD_{600}=5x10^{-5}) treatment (Figure 4-17 E). Unspecific fragment was amplified in *mrn1*thas* Mock control. Moreover, *THAS* expression was increased 3-fold in Col-0 after both *Burkholderia glumae* treatments (Figure 4-17 F). Unfortunately, unspecific amplification products were detected in *mrn1*thas*.

Furthermore, Col-0 and *mrn1*thas* were co-cultivated with bacteria containing *TPST* orthologues (Table 4-1). Co-cultivation of *Pseudomonas spec. root68* (*root68*), *Massilia spec. root133* (*root133*), *Psudoxanthomonas spec. root65* (root65), *Rhodobacter spec. root480* (*root480*) had no impact on Col-0 growth in used concentration range, but low concentrated *root68* culture (OD_{600}=4x10^{-7}) in MS media slightly promoted growth in wild-type (Figure

4-18A+B+C+D). However, growth was not enhanced in *mrn1*thas* by *root68*. *Pseudomonas spec. root401* (*root401*) repressed growth in wild-type and *mrn1*thas* in a similar manner, but lower concentration (OD_{600}=4x10^{-7}) had smaller impact on *mrn1*thas* in comparison to other treatments in this genotype (Figure 4-18 E). Notably, variations in Mock treatments between experiments were observed, due to variance in growth conditions, seed sterilization process or unknown factors.

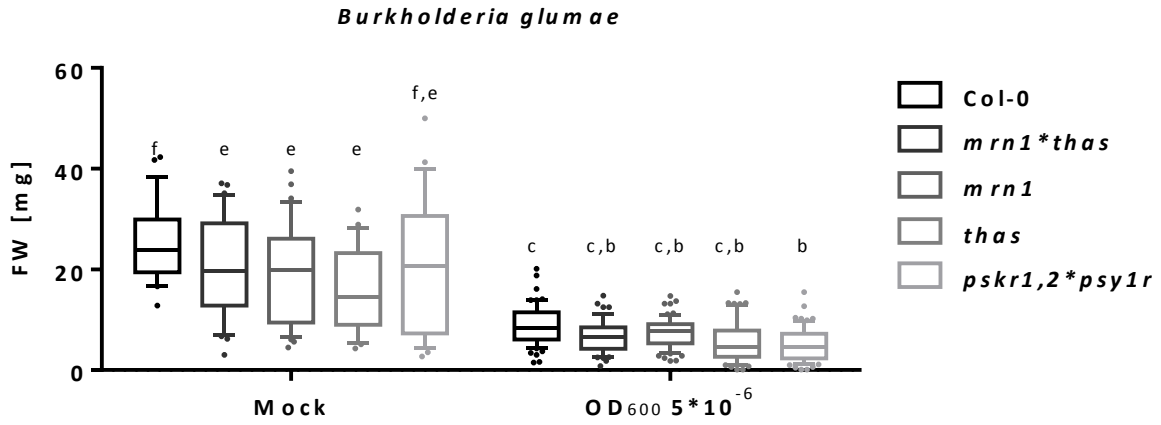

Figure 4-16: *Burkholderia gluamae* co-cultivation with Col-0, *mrn1*thas, mrn1, thas,* and *pskr1,2*psyr*
Seedlings were grown on ½ MS agar plates (+sucrose) on long-day conditions and transferred after 7 days onto ½ MS agar plates supplemented with *Burkholderia glumae* (OD_{600}=5*10^{-6}). After further 11 days, seedlings were weight and harvested (Mock n>26; treatment n>53). Box plot contain 10-90% percentiles. Statistical data analysis was performed by two-way ANOVA with Tukey's test and significance levels were indicated with small letters.

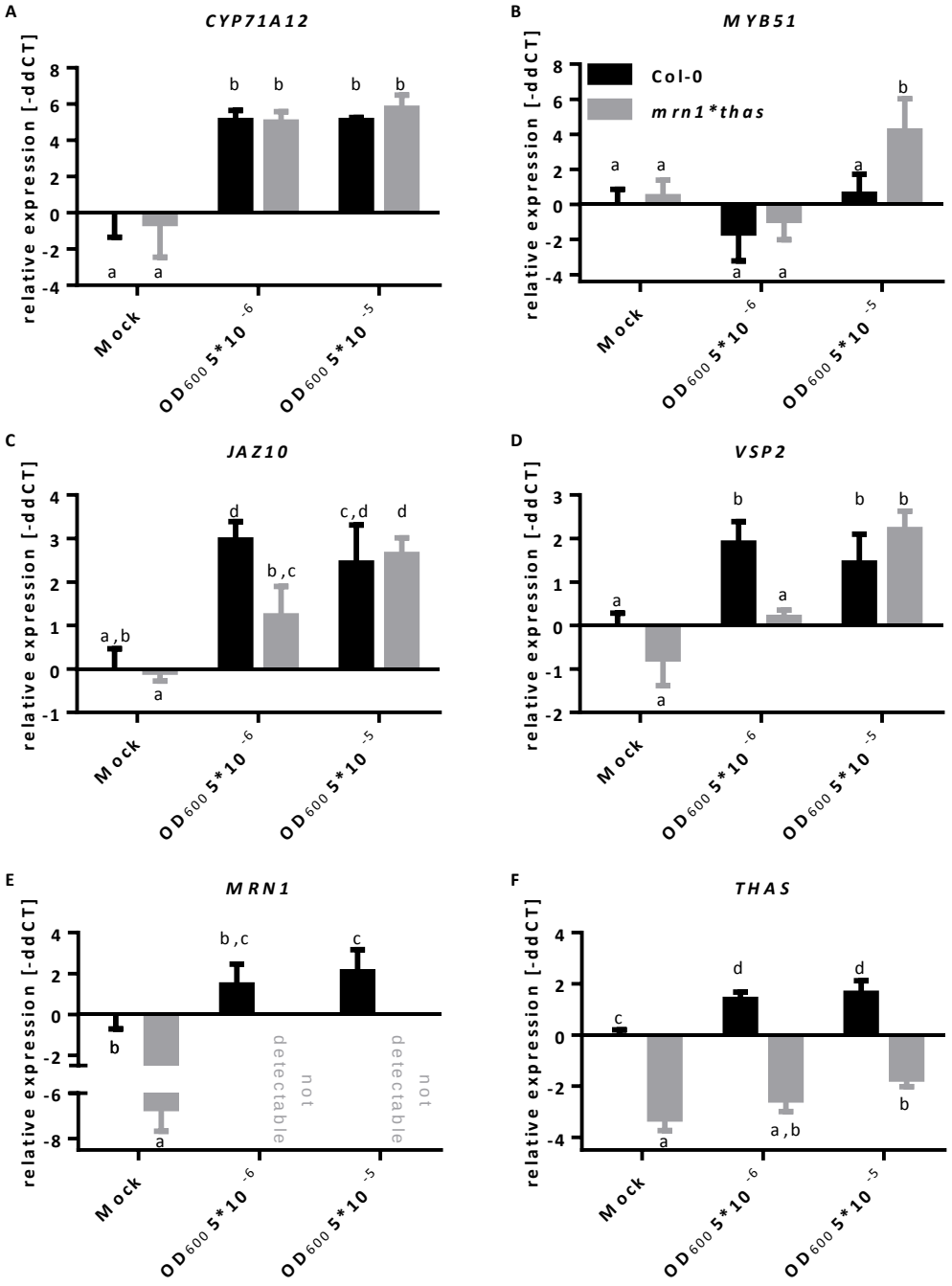

Figure 4-17: Marker gene expression after *Burkholderia gluamae* co-cultivation with Col-0 and *mrn1*thas*
Seedlings were grown on ½ MS agar plates (+sucrose) on long-day conditions and transferred after 7 days onto ½ MS agar plates supplemented with *Burkholderia glumae* ($OD_{600}=5*10^{-6}$). After further 14 days, roots were harvested. Transcription levels were analyzed using ddCT method (n=4). A: *CYP71A12*; B: *MYB51*; C: *JAZ10*; D: *VSP2*; E: *MRN1*; F: *THAS*. Statistical data analysis was performed by two-way ANOVA with Tukey's test and significance levels were indicated with small letters. Standard deviation is presented.

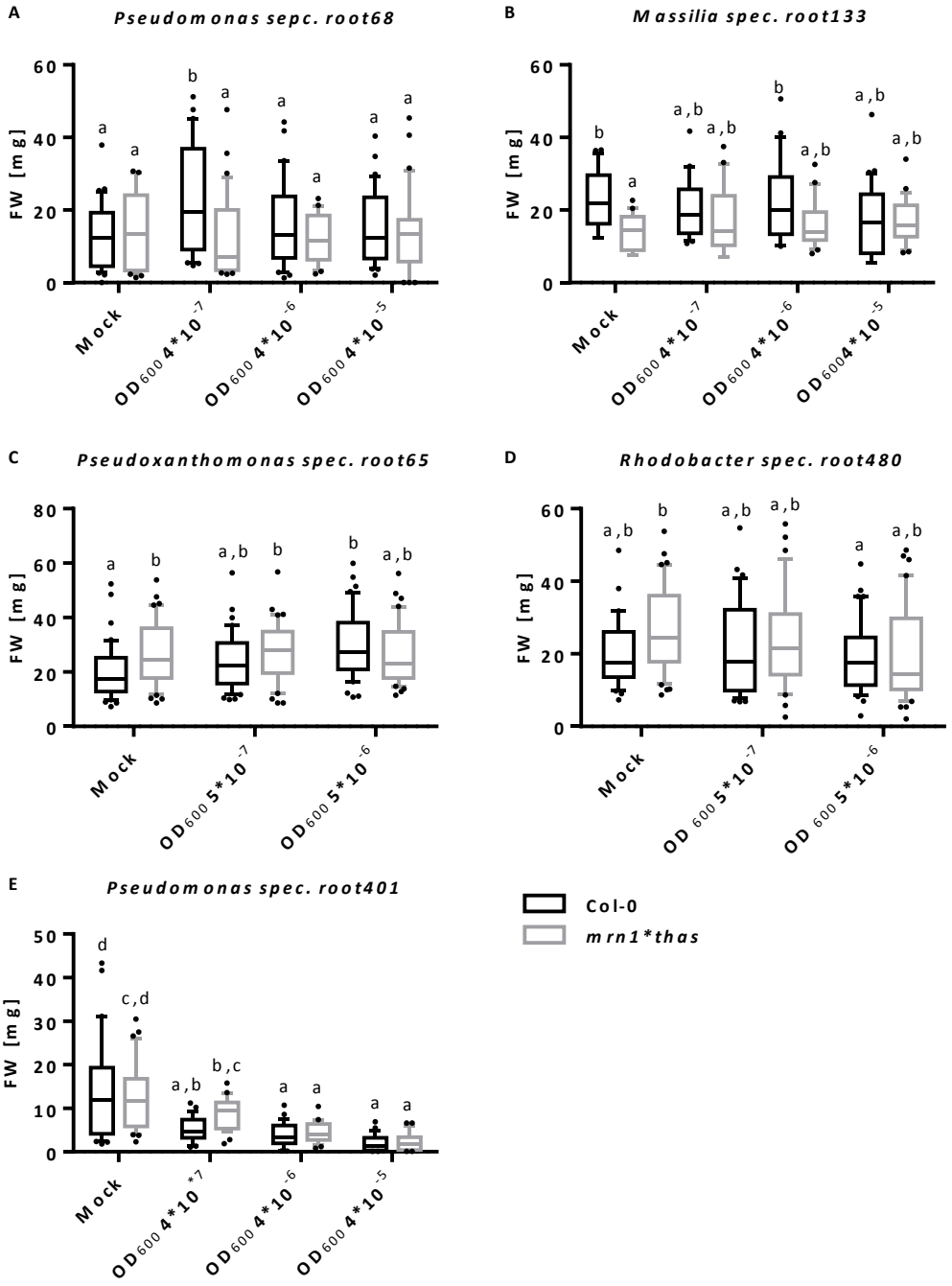

Figure 4-18: Bacteria co-cultivation with Col-0 and *mrn1*thas*

Seedlings were grown on ½ MS agar plates (+sucrose) on long-day conditions and transferred after 7 days onto ½ MS agar plates supplemented with A: *Pseudomonas spec. root68* (OD_{600}=4x10^{-7}; 4x10^{-6}; 4x10^{-5}); B: *Massilia spec. root133* (OD_{600}=4x10^{-7}; 4x10^{-6}; 4x10^{-5}); C: *Pseudoxanthomonas spec. root65* (OD_{600}=4x10^{-7}; 4x10^{-6}); D: *Rhodobacter spec. root480* (OD_{600}=4x10^{-7}; 4x10^{-6}); E: *Pseudomonas spec. root401* (OD_{600}=4x10^{-7}; 4x10^{-6}; 4x10^{-5}). After further 14 days, seedlings were weight and harvested (n=20-40). Box plot contain 10-90% percentiles. Statistical data analysis was performed by two-way ANOVA with Tukey's test and significance levels were indicated with small letters.

4.3 Discussion

4.3.1 Loss of *MRN1* and *THAS* has minor impact on plant growth and development

The huge amount of triterpene scaffolds stand in contrast to how little is actually known about them. To unravel plant triterpene function, this chapter focusses on their physiological role in plants instead of their bioactivity in animal systems. Effects of marneral and thalianol on *Arabidopsis thaliana* were studied in a reverse genetic approach. Because marneral and thalianol might share are redundant function, *mrn1* and *thas* knock-out mutants were crossed.

The overall plant growth of *mrn1*thas* was quite similar to Col-0 (Figure 4-8). In detail, no alteration in general rosette morphology and leaf shape of this mutant were observed. The average leaf number was also similar to Col-0 (Figure 4-9). However, only *mrn1*, but not *mrn1*thas*, had slightly smaller leaflets and one additional leaf in rosettes. Furthermore, flowering time was not altered in *mrn1*thas* and single mutants (Figure 4-9; Figure 4-10). Also seed germination rate in *mrn1*thas* was 100%. Loss of marneral and thalianol synthase did not alter root growth.

When comparing these observations with literature, Field et. al. did not reported any changes in growth in the *thas* mutant line that was used for *mrn1*thas* crossing. Only *thah* and *thad* which accumulate thalianol derivates had slightly longer roots in their studies (Field and Osbourn, 2008). For *mrn1*, there is only one other study characterizing a *mrn1* knock-out mutant (Go et al., 2012). In this study, a late flowering phenotype with short leaves, greater rosette leaf number, short flower anther filaments, and small siliques was documented for *mrn1* (Go et al., 2012). However, this phenotype was not observed in this study in *mrn1*thas*, *mrn1*, and *mrn1_2*. Only slightly shorter leaflets and more rosettes leaves were observed in *mrn1*. Furthermore, in *mro1* T-DNA lines (SALK_073803 and SALK_045988) and *mro1*thas* mutant, no striking alterations in plant growth and development were reported (Field et al., 2011; Weckopp, 2014; Klunder, 2016). Two scenarios are plausible to explain discrepancy for observed phenotypes in *mrn1* mutants between this thesis and literature: First possibility regards growth conditions. The study presented by Go et. al. were conducted at slightly higher temeperatures (23 °C, instead of 22 °C) and they used a different light source (Go et al., 2012). In agreement with this, Arabidopsis genotypes grown in 10 different laboratories have shown strong changes in leaf growth variables as well as variations in metabolite profiles (Massonnet et al., 2010). However, it is more likely that differences in phenotype observations could lead from genetic background of *mrn1* mutants. Here, SALK T-

DNA knock out lines for *mrn1* were used (Alonso et al., 2003). T-DNA fragments used for SALK lines are >12 kb in length and their integration impair target gene transcription (Alonso et al., 2003). In the study of Go et. al., a T-DNA activation tagged *mrn1* Arabidopsis line was characterized (Weigel et al., 2000; Go et al., 2012). Activation tagged lines contain a constitutive CaMV 35S promoter element and are mainly used for generation of gain-of-function mutations (Weigel et al., 2000). These promoter elements should enhance expression of genes near T-DNA insertion site. No altered gene expression levels were detected 20 kb down- or upstream of T-DNA insertion site. It was concluded that observed phenotype derived from T-DNA insertion and not from gene trans-activation (Go et al., 2012). However, a different study demonstrated gene trans-activation 78 kb distant from promoter insertion site. In the same study they proposed distal activation is more prevalent than previously recognized because the relatively simple cases of proximal activation were easier to discern and report (Ren et al., 2004). Another study reported long-distance 84 kb trans-repression effect by T-DNA insertion in Arabidopsis (ten Hove et al., 2011). Moreover, there are other examples for long-distance trans-activation by inserted promoter elements in other species from Drosophila to humans (Merli et al., 1996; Calhoun and Levine, 2003; Nobrega et al., 2003). Trans-activation could be caused by DNA-looping (Rippe et al., 1995). An additional argument is the presence of repressing chromatin signatures in the marneral gene cluster (Yu et al., 2016). In other eukaryotes, like yeast, differences in chromatin structures were shown to affect the potential for long-distance gene expression positively (Dobi and Winston, 2007). Even earlier, Blackwood and Kadonaga reviewed in 1998 that genomic chromatin modifications could promote long-distance interactions among DNA-bound factors as a consequence of the DNA compaction. Additionally, integration of 35S promoters into Arabidopsis were shown to deplete repressing H3K27me3 histone modifications (Chen et al., 2013). These evidences could explain phenotype differences between *mrn1*thas* and the previously described *mrn1* (Go et al., 2012). Therefore, transcription status in both lines should be investigated and compared.

4.3.2 Marneral and thalianol biosynthesis is mediated by PSK-α signaling

Previous studies have shown positive correlation between phytosulfokine-α signaling with marneral and thalianol metabolism (personal communication with Prof. Dr. Margret Sauter, 2013, Institute for Plant Developmental Biology and Physiology, University Kiel, Germany). PSK-α is sulfated peptide hormone and induce root growth elongation (Stührwohldt et al.,

2011). To verify interconnection between PSK-α and marneral and thalianol, PSK- α promoted growth were studied in marneral and thalianol deficient mutants (Chapter 4.2.3.1). Exogenous applied PSK-α did not induce root growth promotion in *mrn1*thas*, *mrn1*, and *thas*, but induced expression in WT (Figure 4-12). Furthermore, in *pskr1/2* and *psy1r* triple mutant *MRN1*, *MRO*, *THAS*, and *THAH* gene expression was strongly reduced, e.g., *MRN1* down to 0.03-fold compared to WT (Figure 4-13). These findings support the hypothesis that marneral and thalianol share a function in PSK-α promoted growth and act downstream of PSK-α receptor signaling. However, *MRN1* expression is only slightly increased (2-fold) in roots in roots upon PSK-α treatment for 4h (Figure 4-13 A). *THAS* expression was not induced 4 h after PSK-α.

This thesis provides evidence that marneral and thalianol share a common function in PSK-α mediated root growth (Figure 4-19). Both gene clusters are strongly downregulated in *pskr1/2, psy1r* knock-out mutants and exogenous PSK-α application is unable to induce root growth promotion in marneral and thalianol knock-out mutants (Figure 4-12; Figure 4-13). The function of marneral and thalianol downstream in this pathway remains unknown, but they might be involved in growth processes (Field and Osbourn, 2008; Field et al., 2011; Go et al., 2012). For explanation: turgor pressure and mechanical properties of cell walls are the driving force for cell expansion (Dolan and Davies, 2004; Guerriero et al., 2014). Turgor pressure is modulated by ion transport during vacuolar growth and results in cell wall expansion (Pritchard, 1994). Triterpenes are often located in surface wax layers (Buschhaus et al., 2007; Buschhaus and Jetter, 2012; Szakiel et al., 2012). Since roots lack cuticles, marneral and thalianol might be present in other unpolar membrane layers. In the tonoplast or cell membrane might be present and affecting PSK-α mediated cell elongation. Otherwise, final metabolism of marneral and thalianol is unknown, but hydroxylation by *MRO*, *THAH*, or unknown enzymes might lead to an increased solubility and transportation of these compounds into vacuoles similar to saponins (Kesselmeier and Urban, 1983; Field and Osbourn, 2008; Mylona et al., 2008; Field et al., 2011).

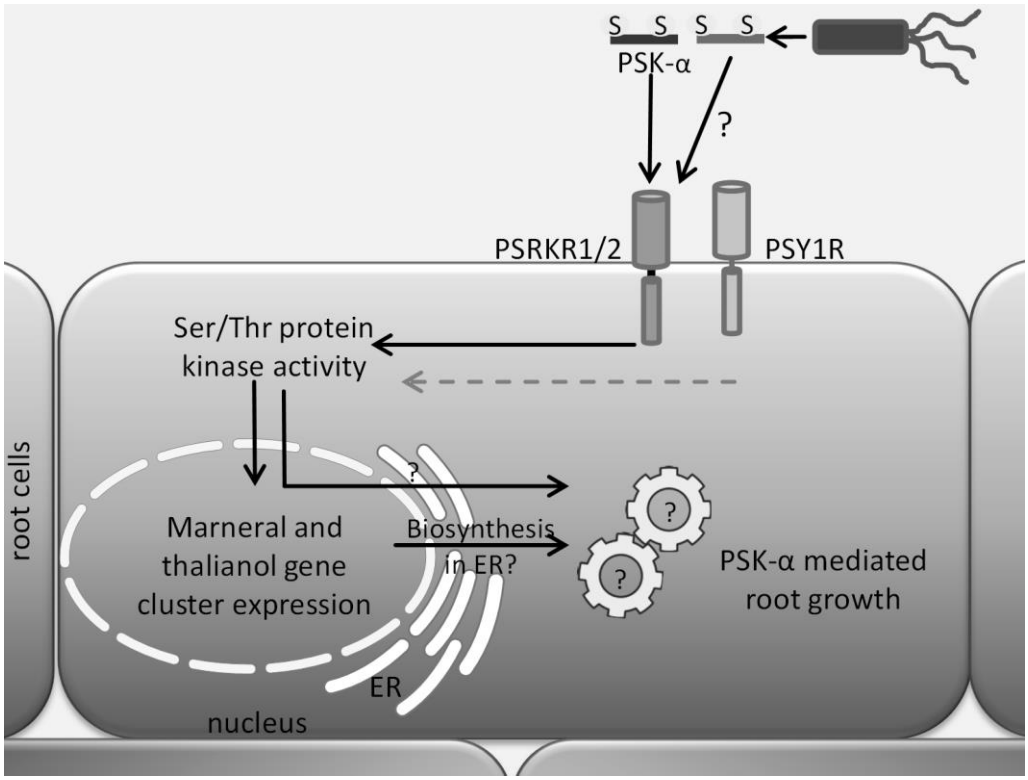

Figure 4-19: Hypothetical pathway for marneral and thalianol in PSK-α mediated rot growth
PSKR1/2 and PSY1R is activated upon PSK-α or PSK-α analog (Stührwohldt et al., 2011; Mosher and Kemmerling, 2013). PSK-α receptors initiate kinase cascade that probably induce marneral and thalianol gene cluster expression (Hartmann et al., 2014). Marneral and thalinol are probably synthesized in the ER and then induce PSK-α mediated growth by cell expansion (Go et al., 2012).

4.3.3 Marneral and thalianol share no significant function in JA signaling

Transcriptome data of JA signaling knock-out mutants indicated JA dependent marneral and thalianol gene cluster expression (Winter et al., 2007; Sundaravelpandian et al., 2013; Gasperini et al., 2015; Campos et al., 2016). To study how JA signaling is linked to marneral and thalianol metabolism, growth experiments of marneral and thalianol loss-of-function mutants under MeJA treatment were conducted.

Growth of *Col-0*, *mrn1*thas*, *mrn1*, *thas* grown on 10 µM MeJA were strongly inhibited (Figure 4-14). No differences between genotypes in MeJA treatments were observed. Combined treatments of 10 µM MeJA and 0.1 µM PSK-α did not complement reduced growth in Col-0 and mutants. Moreover, gene expression of *MRN1* in roots was increased upon 4 h MeJA treatment (Figure 4-13 A). Significant induction in *MRO*, *THAS* and *THAH* was not observed at this time point, but *JAZ10* expression increased dramatically Figure 4-13 B - E). The growth assays indicate that marneral and thalianol are not essential for JA mediated growth repression, but small induction of *MRN1* expression could hint to highly specific function that was not discovered, yet.

There might be a connection between JA- and PSK-α signaling because PSK-α did not complement MeJA growth inhibition. To provide evidence for interconnection between JA- and PSK-α signaling, *pskr1,2*psy1r was* treated with 10 µM MeJA (Figure 4-14). However, *pskr1,2*psy1r* growth response did not differ from Col-0 and *JAZ10* expression was also not altered (Figure 4-13). Additionally, PSK-α treatment of *coi1-34* did increase root growth, but no growth induction in in *ninja-1* was observed (Figure 4-14). These findings led to the conclusion that JA signaling does not affect the PSK-α mediated cell elongation, but PSK-α might influence JA signaling upstream. Literature supports a function for PSK-α in balancing the JA response (Igarashi et al., 2012; Mosher and Kemmerling, 2013).

No distinct link between marneral and thalianol signaling with JA response were identified. Loss of *MRN1* and *THAS* did also not lead to an alternated observation in JA signaling. Therefore, these compounds might share a function in JA signaling and to plant defense response against necrotrophic pathogens and herbivores.

4.3.4 Marneral and thalianol are not crucial for abiotic stress response

Transcriptome data provide evidence that in seedlings *MRN1* gene expression is linked to osmotic and salt stress, while *THAS* is induced upon drought and leaf damage (Kilian et al., 2007; Winter et al., 2007). To investigate connection between abiotic stress with marneral and thalianol metabolism, abiotic stress was chemically induced in *mrn1*thas* (Chapter 4.2.3.3) (Claeys et al., 2014). Sorbitol and mannitol were used to imitate osmotic stress/ drought (Verslues et al., 2006; Claeys et al., 2014). Plants were treated with NaCl to induce salt stress response or H_2O_2 to trigger ROS production for broad simulation of high-light (UV-B radiation), drought, salinity, chilling, nutrient deficiency, and wounding (Shin et al., 2005; Einset et al., 2007; Maffei et al., 2007; Miller et al., 2010; Hideg et al., 2013). Rosette size was used as output for defense response since this parameter is very sensitive to environmental changes (Claeys et al., 2014).

Col-0 and *mrn1*thas* rosette leaf area and diameter were strongly affected by sorbitol, mannitol, NaCl and H_2O_2 (Figure 4-15 A+B). However, no significant differences in rosette size were observed between Col-0 and *mrn1*thas* in single treatments. Only rosette compactness was slightly increased in *mrn1*thas* after sorbitol and H_2O_2 treatment. (Figure 4-15 C).

Data provide evidence for marneral and thalianol are not crucial for abiotic stress response. There might be small changes in rosette compactness, but no greater changes were observed.

However, growth in *mrn1*thas* altered by non-chemical induced abiotic stress e.g. in the field might look different.

4.3.5 Marneral and thalianol are not essential for plant growth in presence of root-associated microbiota

Microbial interactions in thalianol and marneral deficient plants were never analyzed in depth. Field et. al. (2008) challenged *thas*, *thah*, and *thad* roots with *Pseudomonas syringae* pv. tomato DC3000 and *Botrytis cinerea*. *Botrytis cinerea* did not colonized any roots and *Pseudomonas syringae* colonized mutants and wild-type equally (Field and Osbourn, 2008). In this thesis *mrn1* and *thas* knock-out mutants were challenged with root pathogen *Burkolderia glumae*. Furthermore, mutants were co-cultivated with root associated bacteria expressing *TPST* orthologues.

Co-cultivation with *Burkholderia glumae* strongly inhibited plant growth in Col-0 as well as in *mrn1*thas, mrn1, thas* and *pskr1/2*psy1r* (Figure 4-16). Biomass of Col-0, *mrn1*thas, mrn1*, and *thas* were equal to each other, except for *psrk1/2*psy1r*. p*skr1/2*psy1r* growth was more inhibited by *Burkholderia glumae* than Col-0. Also worth mentioning, initial plant FW was lower in *mrn1*thas*, *mrn1* and *thas* than Col-0, indicating a slight increased resistance which was observed in multiple experiments. Furthermore, *MRN1* and *THAS* transcription level was ~4-fold increased upon *Burkholderia glumae* treatment (Figure 4-17 E+F). Defense related transcripts *JAZ10*, *VSP2*, and *CYP71A2* were similarly regulated in *Col-0* and in *mrn1*thas*, but after lower *Burkholderia glumae* concentrations, *JAZ10* and *VSP2* were lower expressed in *mrn1*thas* than in Col-0 (Figure 4-17 A, C+D). In addition, *MYB51* transcription level was more increased in *mrn1*thas* after co-cultivation with high concentrated *Burkholderia glumae* culture, but not at the concentration used presented in growth assays (Figure 4-17 B). The results indicate that slight increased resistance might be independent of JA signaling, because *VSP2* and *JAZ10* expression was not significantly altered. Both are marker genes for JA signaling (Liu, 2005; Moreno et al., 2013). However, absence of marneral and thalianol might increase camalexin and indolic glucosinolate biosynthesis during strong *Burkholderia glumae* infection by increasing *MYB51* transcription (Frerigmann and Gigolashvili, 2014). *MYB34* and *MYB122* expression was not tested, but their analysis could provide stronger evidence for this hypothesis.

Besides co-cultivation with plant pathogen *Burkholderia glumae*, *mrn1*thas* was also co-cultivated with root associated bacteria expressing *TPST* orthologues, since marneral and thalianol metabolism is dependent on PSK-α receptor activity and might be modulated by

other sulfated peptides than PSK-α (Table 4-1). However, co-cultivation *mrn1*thas* with *root68*, *root133*, *root65*, *root401*, or *root480* did not result in a different growth in comparison to Col-0 (Figure 4-18). In detail, Co-cultivation with *root68*, *root133*, *root65*, or *root480* did not cause remarkable changes in biomass at all, but *root401* strongly inhibited growth in Col-0 and *mrn1*thas.* Remarkably, at lower *root401* concentration (OD_{600}=4x10^{-7}), *mrn1*thas* was slightly less affected by growth inhibition (Figure 4-18 E). This observation is in consents with previous observation in *Burkholderia glumae* co-cultivation.

Taken together, these results provide evidence for marneral and thalianol play a minor role for plant growth in presence of root-associated microbiota and in root resistance. Presence of marneral and thalianol synthesis pathway could lead to slightly decreased plant fitness against *Burkholderia glumae* and *Pseudomonas spec*. *root401*. Whether slightly increased resistance in *mrn1*thas* has to be tested in further studies. Moreover, plant biomass slightly differed between experiments due to slight changes in setup like switching plant incubators or unknown factors, like different bacteria vitality. Therefore, for simulating a more natural plant microbe interaction and growth, plant co-cultivation assay could be optimized. Seedling transfer onto inoculated media is a critical step and might induce stress responses in plants that interfere with the assay. Therefore a system without seedling transfer might offer a solution in future. Through microbial seed coating, plants could already establish microbe interaction during germination as *in field* and are not exposed to abrupt transfer from sterile to inoculated media. Seed coating is a used method in agricultural industry (O'Callaghan, 2016). Another way for improvement could be the use of hydroponic cultures. In this setup, seeds are grown on mesh in inoculated liquid media. This method has the advantage of easy accessibility to various plant tissues, root exudates and bacteria in media, as well as tight nutrient regulation and disease control (Nathoo et al., 2017).

Chapter 5

Concluding discussion

5.1 Relevance of plant triterpenes in animal health and plant physiology

In animal cells, plant triterpenes are known for their anti-cancerous, anti-microbial and anti-inflammatory properties. Especially oleanolic acid, betulinic acid, and synthetic variation of them are promising drug candidates (Liby et al., 2007; Ci et al., 2017). However, variations in triterpene scaffolds are immense and not fully studied in this context, but they could contain yet undiscovered bioactive molecules (Thimmappa et al., 2014; Hill and Connolly, 2015). On the other side, extensive studies on the avenacin gene cluster were conducted in plants (Chapter 1.4) (Papadopoulou et al., 1999; Qi et al., 2006; Mylona et al., 2008; Kemen et al., 2014). Besides research in this cluster, many other studies focus on evolutionary background and composition of triterpene gene clusters than on research of their physiological function (Field et al., 2011; Kliebenstein and Osbourn, 2012; Castillo et al., 2013; Boutanaev et al., 2015; Nützmann and Osbourn, 2015; Yu et al., 2016). Therefore, the aim of this thesis was to shed a light on the physiological function of triterpenes in plants and elucidate their potential in triggering anti-inflammatory Nrf2-EpRE pathway in animal cells.

To study anti-inflammatory activity of plant triterpenes in animal cells, an efficient assay system had to be established. It should be capable of detecting bioactive triterpenes contained in bacterial extracts to enable a quick screenings process without prior substance purification. In this thesis, an EpRE-LUX based reporter-gene-assay in murine hepatoma cells served for anti-inflammatory triterpene identification contained in extracts of *Rhodobacter capsulatu*s which functioned as heterologous expression hosts. This cell line was originally established to screen for purified plant flavonoids that activate the Nrf2-EpRE pathway (Boerboom et al., 2006). The Nrf2-EpRE pathway is relevant in several diseases including cancer, diabetes, atherosclerosis, hypertension, cystic fibrosis, Parkinson′s and Alzheimer′s diseases, and it is used as point of application for modern drug discovery (Gao et al., 2014; Abed et al., 2015; Kim et al., 2015; Yoshizaki et al., 2017). In this gene-reporter-assay, betulin bioactivity on EpRE induction confirmed prior observations (Ci et al., 2017). However, new anti-inflammatory triterpenes from *Rhodobacter capsulatus* extracts could not be reported in this thesis. Differentiation between an insufficient triterpene concentration in extracts and non-bioactive triterpenes was not possible. It is likely that triterpene production yields were too low for assay sensitivity. Nevertheless, using heterologous synthesized pigment prodigiosin in *Pseudomonas putida* extracts, a proof of concept could be demonstrated. Heterologous biosynthesis of plant triterpenes and new-to-nature triterpenes in heterologous expression

hosts cold become a relevant industrial branch (Arendt et al., 2016; Yasumoto et al., 2016; Arendt et al., 2017; Loeschcke et al., 2017). This thesis provides a new methodological approach in animal cells for screenings of anti-inflammatory compounds within bacterial extracts, without prior compound isolation, for future studies.

To gain a better understanding of triterpene function in plants, marneral and thalianol were studied in *Arabidopsis thaliana* using a reverse genetic approach. Previously, it was demonstrated that over accumulation of marneral or thalianol lead to a dwarfed phenotype and both molecules are probably involved in plant growth and development (Field and Osbourn, 2008; Field et al., 2011). In contrast, no altered growth phenotypes in *thas* loss-of-function mutants were reported, while a *mrn1* loss-of-function mutant displayed a late flowering phenotype with impaired cell expansion or elongation in root and shoot apical meristems (Field and Osbourn, 2008; Go et al., 2012). Since marneral and thalianol are both mainly expressed in roots of seedlings and are regulated by H3K27me3 chromatin signatures, and are induced by PSK-α and MeJa hormone treatment in transcriptome studies, we hypothesized that marneral and thalianol could share redundant function (Winter et al., 2007; Field et al., 2011; Go et al., 2012; Weckopp, 2014; Yu et al., 2016). To test this hypothesis and characterize physiological function of marneral and thalianol, an Arabidopsis *mrn1*thas* line was generated. Loss of *MRN1* and *THAS* together did not result in an impaired growth phenotype in comparison to wild-type. Moreover, in a functional characterization approach, positive correlation between a functional PSK-α hormone receptors with *MRN1* and *THAS* transcription could be demonstrated. Furthermore, in *mrn1*thas* as well as in *mrn1* and *thas*, root growth induction upon PSK-α treatment was not observed and provides evidence for a functional role in phytosulfokine signaling. On the other hand, relation of marneral and thalianol to JA signaling were not discovered by MeJA growth experiments. However, small induction of *MRN1* expression by MeJA point to existence of highly specific and fine tuning function of JA, which was not discovered in this study. Furthermore, both triterpenes did also not alter plant growth under abiotic stress treatments, but loss of marneral or thalianol led to a small increase in resistance in non-beneficial plant microbiome interaction. Taken together, loss of *MRN1* and *THAS* did not cause significant changes in plant growth. Both metabolites could be involved in fine tuning processes of PSK-α dependent plant pathogen interaction assays. Previously it was demonstrated that *PSKR1* and *PSY1R* mediate regulation of plant defense response to biotrophic and necrotophic pathogens in an antagonistic manner (Igarashi et al., 2012; Mosher et al., 2013; Mosher and Kemmerling, 2013). *pskr1* mutants were shown to be more susceptible to necrotrophic pathogens (Mosher et al., 2013). This thesis gave first

evidence for a function of marneral and thalianol in plant defense and phytosulfokine-α signaling and provide a *mrn1*thas* double mutant for future targeted studies.

5.2 Future perspectives

In this thesis, new evidence for marneral and thalianol role in plant PSK-α signaling and root-associated pathogen interaction were depicted. A connection between marneral and thalianol to abiotic stress responses and jasmonate signaling could not be confirmed. This thesis also provided a *mrn1*thas* double mutant line for targeted triterpene studies in plants. Moreover, a new approach for screenings of anti-inflammatory compounds within bacterial extracts was demonstrated and could be used in future screenings. In this chapter, some potential future approaches are presented.

The anti-inflammatory, anti-cancerous, and anti-bacterial properties of a vast variety of plant triterpenes is not discovered, yet. Heterologous triterpene synthesis in microbes have the advantage of tight controlled growth conditions which could push synthesis towards higher production yields and enable production of naturally low concentrated triterpenes, such as marneral or thalianol. Combinatorial expression of OSCs with P450s and UDP dependent glycosyltransferases in expression platforms could result in new-to-nature triterpenoids with increased bioactivity. There are already semi-synthetic bioactive CDDO derivatives and approaches for synthesis of plant derived but new-to-nature triterpenes (Liby et al., 2005; Loboda et al., 2012; Arendt et al., 2016). To screen future triterpene expression strain libraries this thesis provides an EpRe-LUX gene reporter assay for anti-inflammatory screenings in an easy and efficient way.

To further investigate physiological function of marneral and thalianol in plant growth and defense should be conducted. Marneral and thalianol gene cluster expression is mediated by PSK-α receptors which is involved in cell expansion/ elongation and pathogen interaction. Therefore, further co-cultivation experiments with more root pathogens like *Phytophthora parasitica*, *Fusarium oxysporum*, or *Pythium spec.* should be conducted to validate this observations (Geraats et al., 2002; Larroque et al., 2013; Chen et al., 2014). Plant microbe co-cultivation with marneral and thalianol overexpression lines or addition of purified marneral and thalianol could also bring another view on the plant defense topic. However, only marneral and not thalianol could be synthesized in adequate amounts, to date (Loeschcke et al., 2017; Kranz-Finger et al., 2018). Gained observations could be verified in GFP reporter lines driven under endogenous *MRN1* or *THAS* promoters. Furthermore, combinatorial treatments with PSK-α and MeJa in *mrn1*thas* could unravel the linkage between both

hormone pathways to marneral and thalianol metabolism and provide evidence for possible interconnection. To answer the actual question what marneral and thalianol compounds do in plant cells after their biosynthesis, it is important to know where they are localized. Due to marneral and thalianol low polarity, they might be present in plasma membrane of root cells, or in the tonoplast of vacuoles. In these cell compartments they might act as interaction partners for unknown membrane bound proteins. Therefore, plasma membranes and vacuoles could be isolated and triterpene content should be analyzed by LC-MS or gas chromatography-MS. Protocols for tonoplast and root cell membrane isolation are already reported (Shimaoka et al., 2004; Jozefowicz et al., 2018). *Arabidopsis thaliana* root cell culture could come in handy for isolation in comparison to whole plants, because of better accessibility to plant root material. This thesis provides a *marneral synthase 1* and *thalianol synthase* double knock-out mutant which should be used as resource for future targeted approaches.

Chapter 6

Supplementary data

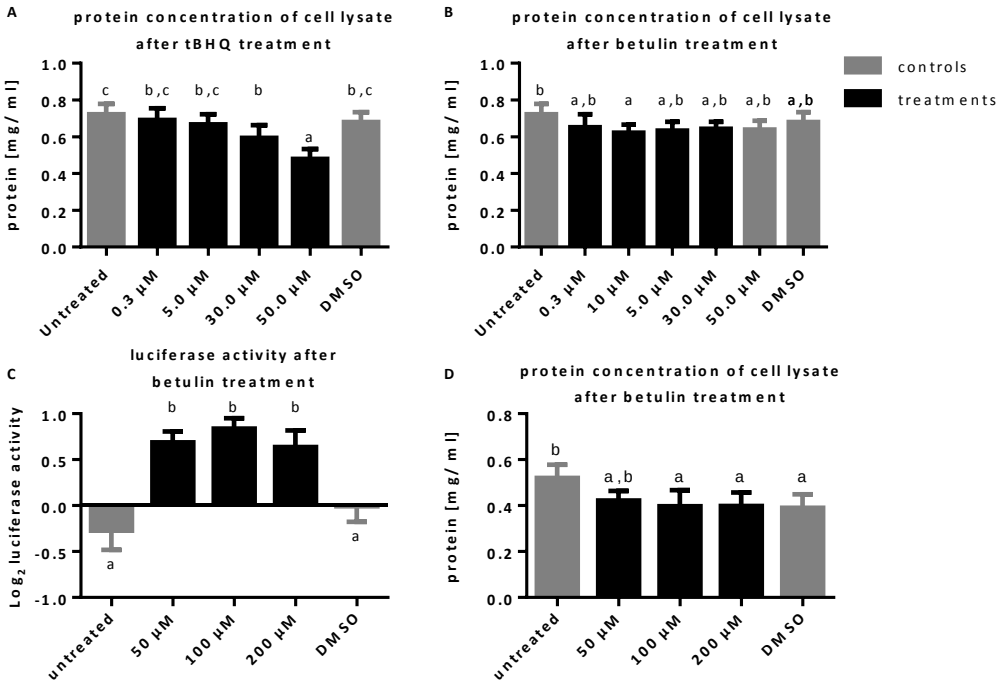

Figure 6-1: Protein concentrations of EpRE-LUX cells treated with tBHQ or betulin; and luciferase activity after ≥50 µM betulin treatment

A: Protein concentration in cell lysate of tBHQ treated EpRE-LUX cells, corresponding to Figure 2 1A (n=6). B: Protein concentration in cell lysate of betulin treated EpRE-LUX cells, corresponding to Figure 2 1B (n=6). C: EpRE-LUX cells treated with 50.0 to 200 µM betulin (n=6). RLUs were normalized to protein level and set in ratio to 1.4% DMSO control. The y-axes represent luciferase activity on a Log2 scale. D: Protein concentration in cell lysate of betulin treated EpRE-LUX cells, corresponding to C. Statistical analysis were performed by one-way ANOVA with Tukey's test and significance levels were set at $P \leq 0.05$ and indicated by small letters. Controls are visualized in gray. Samples are presented in black. Standard deviation is presented as error bar.

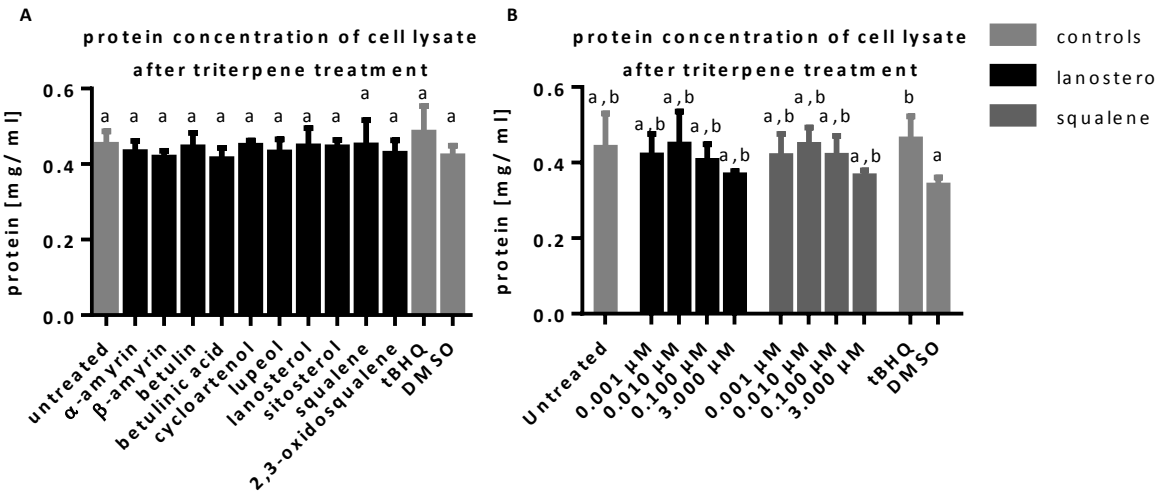

Figure 6-2: Cell lysate protein concentration of EpRE-LUX cell treated with triterpenes at different concentrations

A: Protein concentration in cell lysate of triterpene treated EpRE-LUX cells, corresponding to (Figure 3-4 A) (n=6). B: Cells were treated with 2 µM α-amyrin, β-amyrin, betulin. betulinic acid, cycloartenol, lupeol, lanosterol, sitosterol, squalene or 2,3-oxidosqualene. B: Protein concentration in cell lysate of lanosteraol and squalene treated EpRE-LUX cells, corresponding to (Figure 3-4 B) (n=6). Statistical analysis was performed by one-way ANOVA with Tukey's test and significance levels were set at $P \leq 0.05$ and indicated by small letters. Controls are visualized in gray. Samples are presented in black. Standard deviation is presented as error bar.

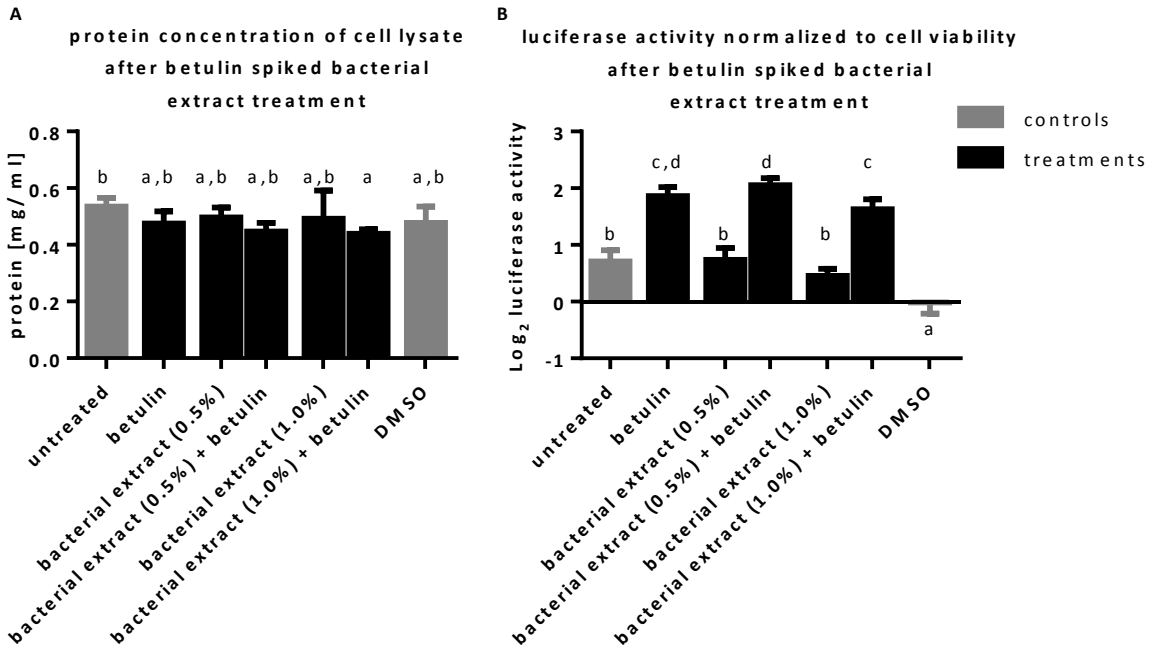

Figure 6-3: Protein concentrations of EpRE-LUX cells treated with betulin spiked bacterial extract; luciferase activity normalized to cell viability

A: protein concentration in cell lysate of triterpene treated betulin spiked *Rhodobacter capsulatus* extract, corresponding to Figure 3-5A (n=6). B: luciferase activity normalized to cell viability of EpRE-LUX cells treated with *Rhodobacter capsulatus* spiked bacterial extracts, corresponding to Figure 3-5B (n=6). Statistical analysis was performed by one-way ANOVA with Tukey's test and significance levels were set at $P \leq 0.05$ and indicated by small letters. Controls are visualized in gray. Samples are presented in black, including 50 µM betulin treatments. Standard deviation is presented as error bar.

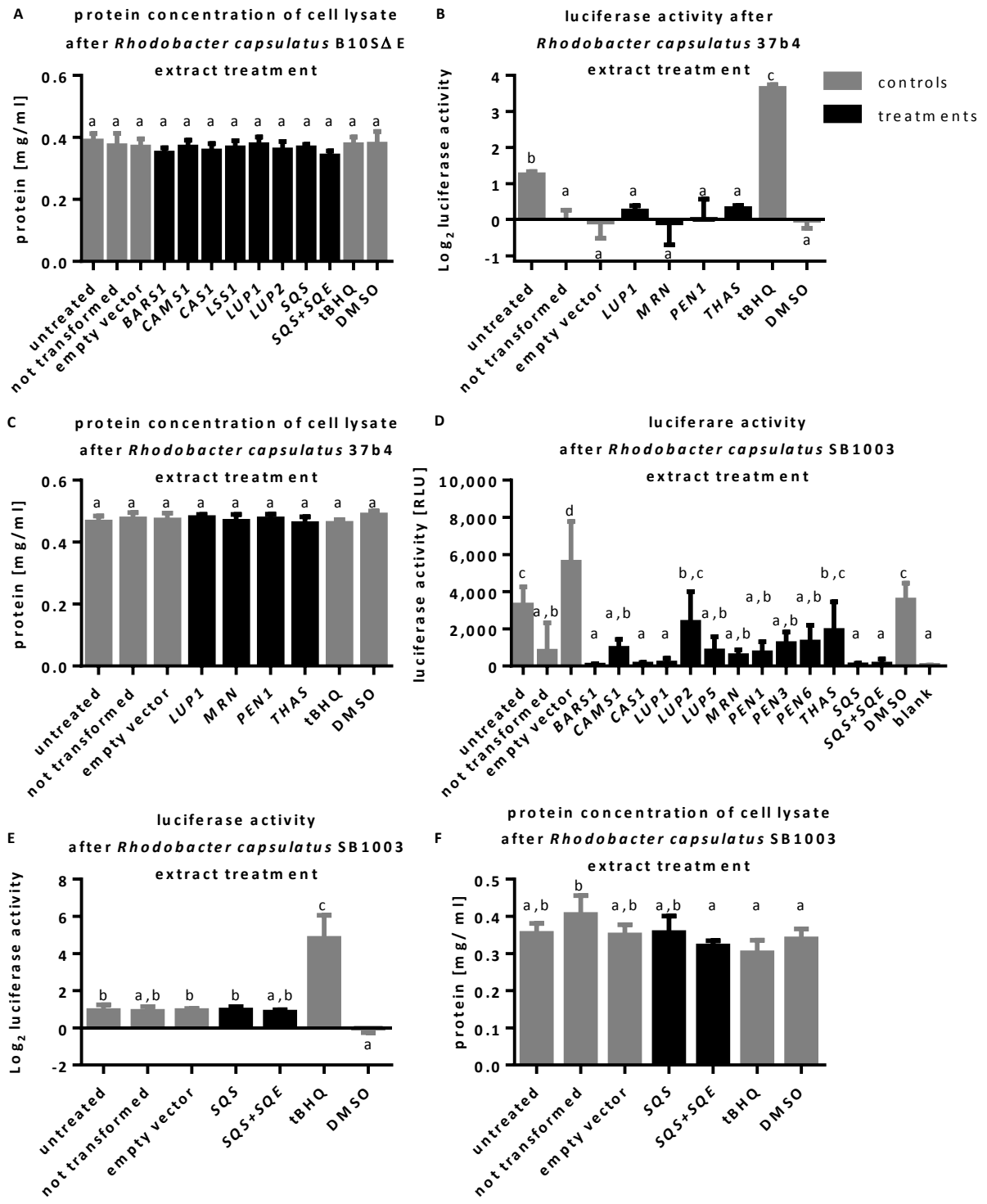

Figure 6-4: Protein concentration and luciferase activity of EpRE-LUX cell lysate treated with *Rhodobacter capsulatus* extracts

A: Protein concentration of cell lysate of *Rhodobacter capsulatus* B10SΔE extract treated EpRE-LUX cells, corresponding to Figure 3-6 (n=6). B: EpRE-LUX cells were treated with 0.5% *Rhodobacter capsulatus* 37b4 extracts containing *SQS*, *SQS+SQE* or *SQS+SQE+OSC* (*LUP1*, *MRN*, *PEN1*, *THAS*) (n=6). RLUs at λ=550 nm were measured in cell lysate, normalized to protein level and set in ratio to 0.5% DMSO control. The y-axis represents luciferase activity on a Log_2 scale. C: Protein concentration in cell lysate of tBHQ treated EpRE-LUX cells, corresponding to B. D: EpRE-LUX cells were treated with 1.0% *Rhodobacter capsulatus* SB1003 extracts containing *SQS*, *SQS+SQE* or *SQS+SQE+OSC* (*BARS1*, *CAMS1*, *CAS1*, *LUP1*, *LUP2*, *LUP5*, *MRN*, *PEN1*, *PEN2*, *THAS*) (n=8). The y-axis represents luciferase activity in RLUs on a Log_2 scale. E: EpRE-LUX cells were treated with 1.0% *Rhodobacter capsulatus* SB1003 extracts containing *SQS*, *SQS+SQE* (n=6). RLUs at λ=550

nm were measured in cell lysate, normalized to protein level and set in ratio to 1.0% DMSO control. The y-axis represents luciferase activity on a Log_2 scale. F: Protein concentration of cell lysate of *Rhodobacter capsulatus* B10SΔE extract treated EpRE-LUX cells, corresponding to E (n=6). Statistical analysis was performed by one-way ANOVA with Tukey's test and significance levels were set at $P \leq 0.05$ and indicated by small letters. Controls are visualized in gray: untreated, not transformed bacteria, bacteria containing empty vector, 30 µM tBHQ, DMSO and or blank. Samples are presented in black. Standard deviation is presented as error bar.

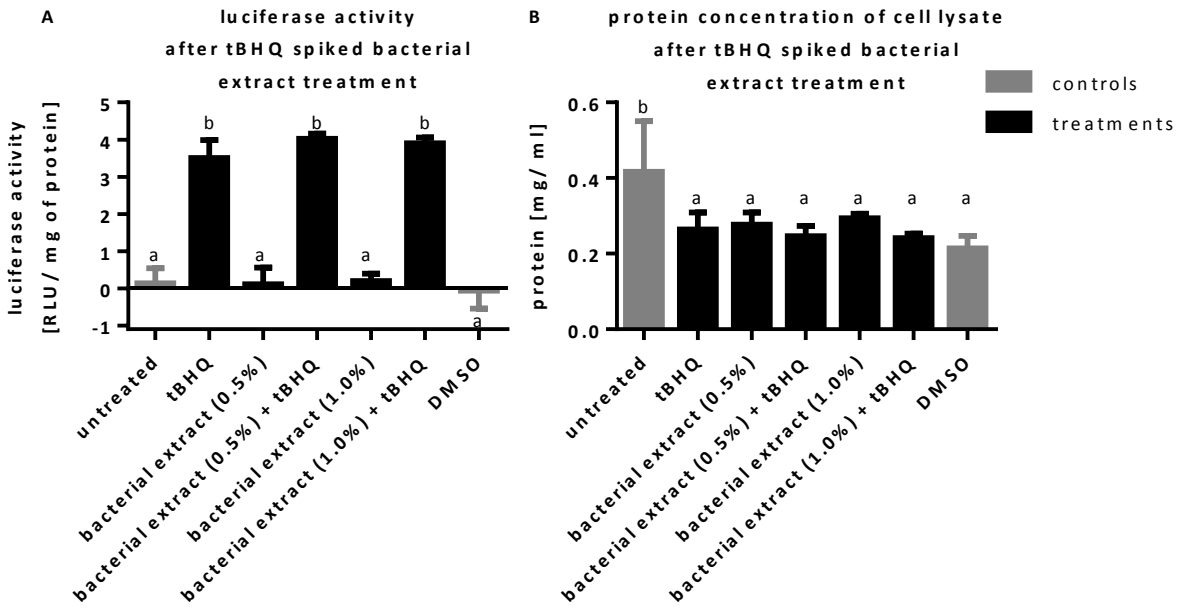

Figure 6-5: Luciferase activity of EpRE-LUX cells treated with *Pseudomonas putida* extract spiked with 30 µM tBHQ

EpRE-LUX cells were seeded onto a 96-well plate with 20.000 cells/ well and incubated for 1 day. Dried ethanol extracts from *Pseudomonas putida* wild-type were diluted in 306 µl DMSO/ 1 ml bacteria. Next, cells were treated with 0.5% or 1.0% bacterial extract in presence or absence of 30 µM tBHQ (n=6). After 1 day incubation protein content and RLUs at RLUs at λ=550 nm were measured in cell lysate. A: The y-axis represents luciferase activity on a Log_2 scale by normalizing RLUs to protein level and set them in ratio to 1.2% DMSO control. B: Protein concentration of cell lysate of *Pseudomonas putida* extract treated EpRE-LUX cells, corresponding to A (n=6). Statistical data analysis was performed by one-way ANOVA with Tukey's test and significance levels were set at $P \leq 0.05$ and indicated by small letters. Controls are visualized in gray: untreated and 1.4% DMSO. Samples are presented in black. Standard deviation is presented as error bar.

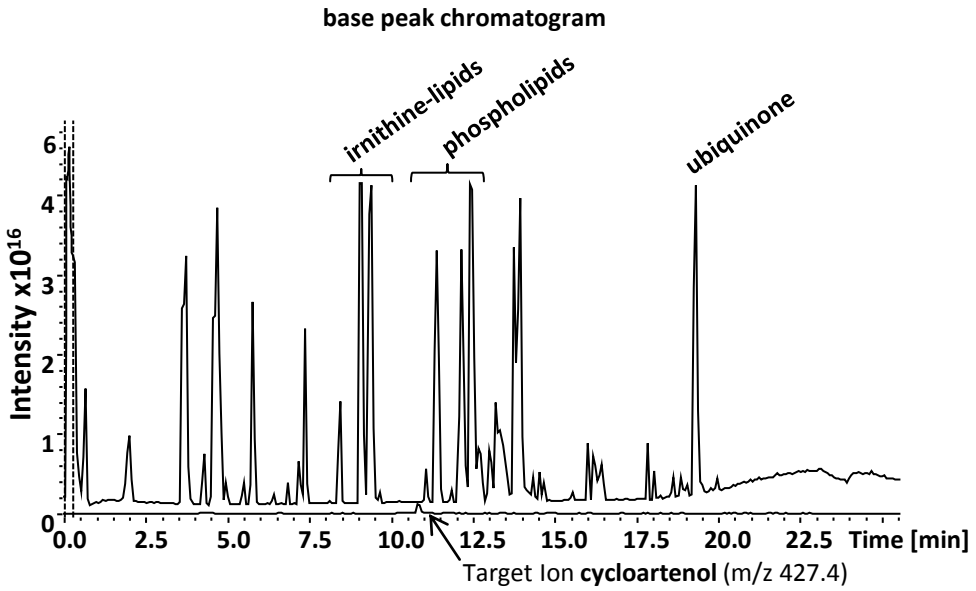

Figure 6-6: Base peak chromatogram of *Rhodobacter capsulatus* extract
Personal communication with Dr. Vera Wewer, 2016, MS Platform, University of Cologne, Germany.

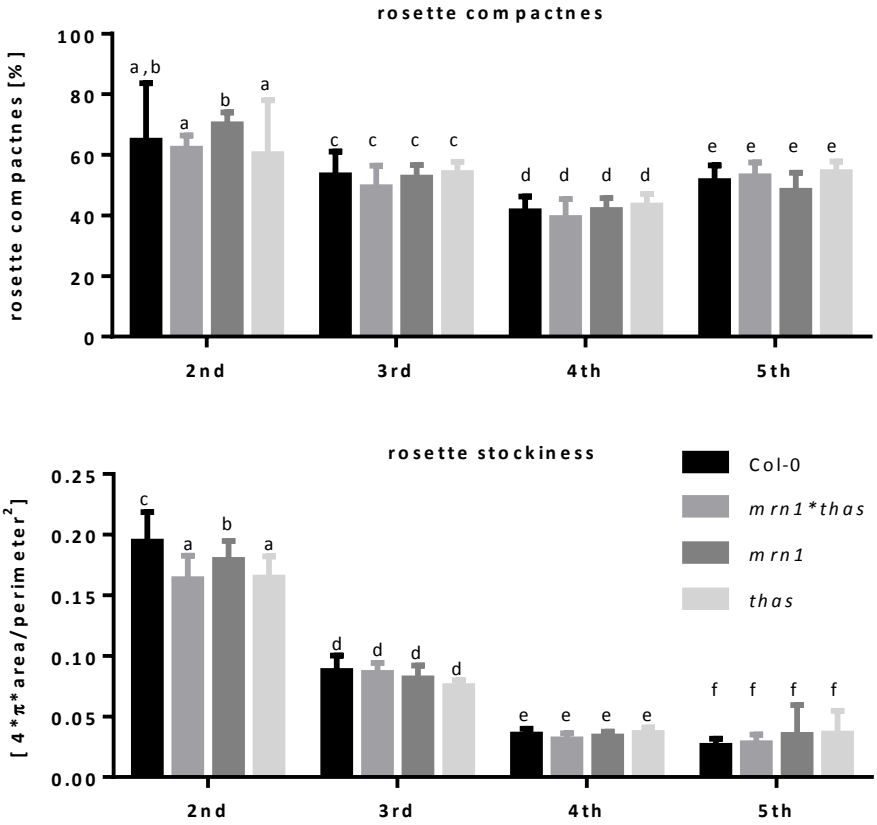

Figure 6-7: Rosette compactness and stockiness of Col-0, *mrn1*thas*, *mrn1*, and *thas*
Plants were grown on soil under long-day conditions. Pictures were taken 2, 3, 4, and 5 weeks after germination (n=15). Rosette area and diameter were automatically calculated with rosette tracker software. Statistical data analysis was performed by two-way ANOVA with Tukey's test comparing plants from the same week and significance levels were set at $P \leq 0.05$ and indicated by small letters.

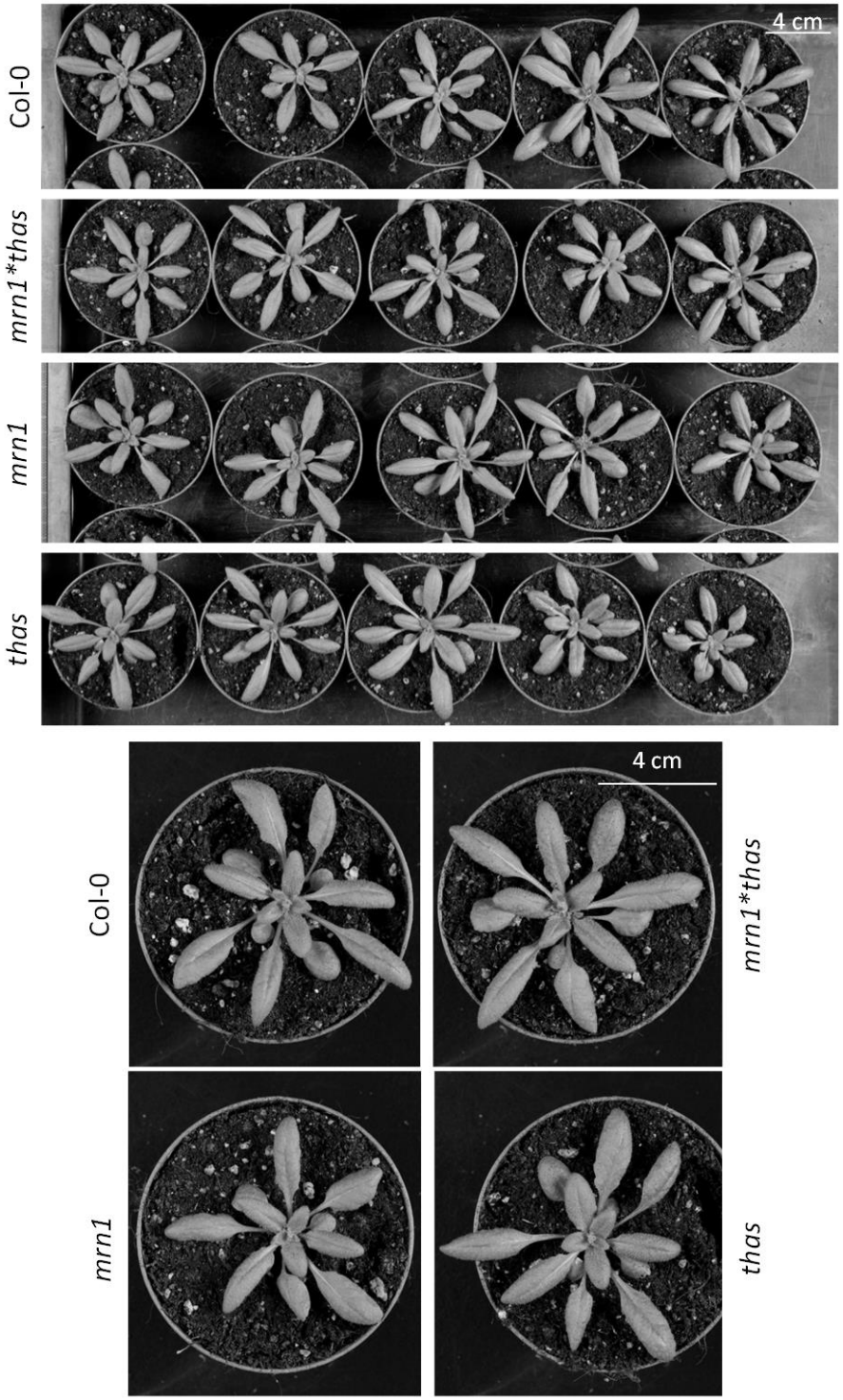

Figure 6-8: Rosettes of 4 weeks old *Arabidopsis thaliana* Col-0, *mrn1*thas*, *mrn1*, *thas*

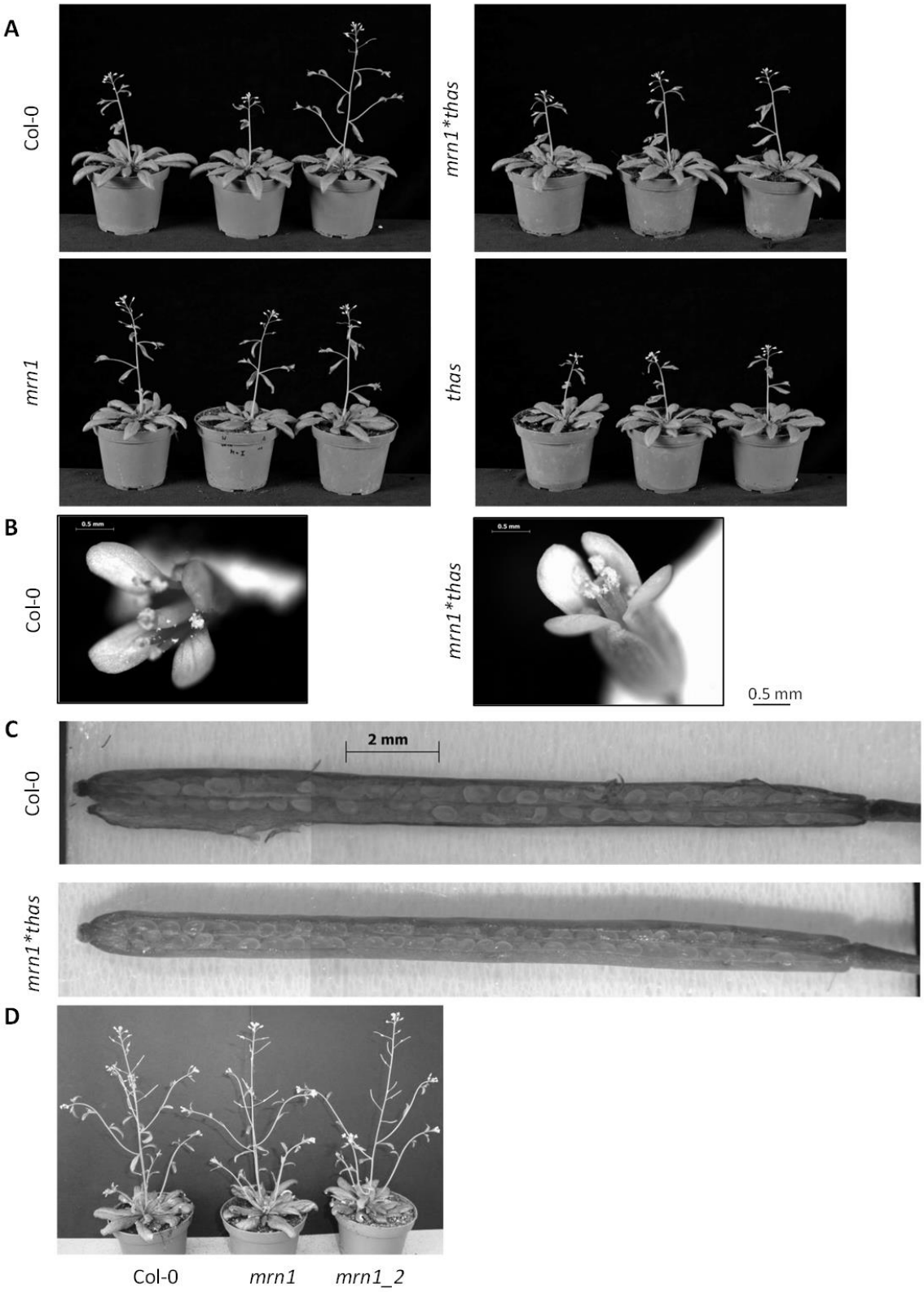

Figure 6-9: Flowering und siliques of *mrn1*thas*
A: Shoots of 5 week old Col-0, *mrn1*thas*, *mrn1*, and *thas*. B: Flowers of *mrn1*thas* and Col-0. C: 8th silique on main shoot of *mrn1*thas* and Col-0. D: Flowering of 6 weeks old Col-0, *mrn1*, and *mrn1_2*.

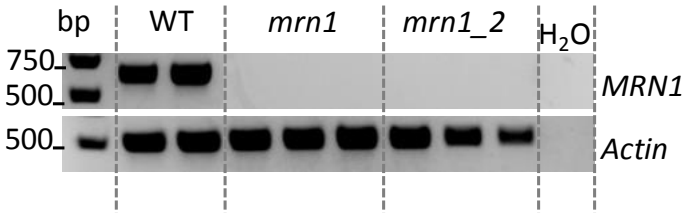

Figure 6-10: *mrn1_2* is free of *MRN1* transcripts
RT-PCR analysis of *MRN1* (45 cycles) and *Actin* (At3g18780) (31 cycles) transcripts in 14 do Col-0 *mrn1* and *mrn1_2* seedlings. Expected product sizes: RT_MRN_LP2 + RT_MRN_RP2 → 663 bp; RT_ACTIN_LP + RT_ACTIN_RP → 522 bp.

Chapter 7

Literature

Abed DA, Goldstein M, Albanyan H, Jin H, Hu L (2015) Discovery of direct inhibitors of Keap1-Nrf2 protein-protein interaction as potential therapeutic and preventive agents. Acta Pharm Sin B **5**: 285–299

Acosta IF, Gasperini D, Chetelat A, Stolz S, Santuari L, Farmer EE (2013) Role of NINJA in root jasmonate signaling. Proc Natl Acad Sci **110**: 15473–15478

Ahuja I, Kissen R, Bones AM (2012) Phytoalexins in defense against pathogens. Trends Plant Sci **17**: 73–90

Aichinger E, Villar CBR, Farrona S, Reyes JC, Hennig L, Köhler C (2009) CHD3 proteins and polycomb group proteins antagonistically determine cell identity in Arabidopsis. PLoS Genet. doi: 10.1371/journal.pgen.1000605

Aichinger E, Villar CBR, Di Mambro R, Sabatini S, Köhler C (2011) The CHD3 chromatin remodeler PICKLE and polycomb group proteins antagonistically regulate meristem activity in the Arabidopsis root. Plant Cell **23**: 1047–1060

Alakurtti S (2013) Synthesis of betulin derivatives against intracellular pathogens. University Helsinki

Alonso JM, Stepanova AN, Leisse TJ, Kim CJ, Chen H, Shinn P, Stevenson DK, Zimmerman J, Barajas P, Cheuk R, et al (2003) Genome-wide insertional mutagenesis of Arabidopsis thaliana. Science **301**: 653–7

Arendt P, Miettinen K, Pollier J, De Rycke R, Callewaert N, Goossens A (2017) An endoplasmic reticulum-engineered yeast platform for overproduction of triterpenoids. Metab Eng **40**: 165–175

Arendt P, Pollier J, Callewaert N, Goossens A (2016) Synthetic biology for production of natural and new-to-nature terpenoids in photosynthetic organisms. Plant J **87**: 16–37

Arvidsson S, Pérez-Rodríguez P, Mueller-Roeber B (2011) A growth phenotyping pipeline for Arabidopsis thaliana integrating image analysis and rosette area modeling for robust quantification of genotype effects. New Phytol **191**: 895–907

Bai Y, Müller DB, Srinivas G, Garrido-Oter R, Potthoff E, Rott M, Dombrowski N, Münch PC, Spaepen S, Remus-Emsermann M, et al (2015) Functional overlap of the Arabidopsis leaf and root microbiota. Nature **528**: 364–369

Balogun E, Hoque M, Gong P, Killeen E, Green CJ, Foresti R, Alam J, Motterlini R (2003) Curcumin activates the haem oxygenase-1 gene via regulation of Nrf2 and the antioxidant-responsive element. Biochem J **371**: 887–895

Barker MS, Vogel H, Schranz ME (2010) Paleopolyploidy in the Brassicales: Analyses of the Cleome Transcriptome Elucidate the History of Genome Duplications in Arabidopsis

and Other Brassicales. Genome Biol Evol **1**: 391–399

Barnes B, Kraywinkel K, Nowossadeck E, Schönfeld I, Starker A, Wienecke A, Wolf U (2016) Krebs - Bericht zum Krebsgeschehen in Deutschland. doi: 10.17886/rkipubl-2016-014

Berardini TZ, Reiser L, Li D, Mezheritsky Y, Muller R, Strait E, Huala E (2015) The arabidopsis information resource: Making and mining the "gold standard" annotated reference plant genome. Genesis. doi: 10.1002/dvg.22877

Berendzen K, Searle I, Ravenscroft D, Koncz C, Batschauer A, Coupland G, Somssich IE, Ülker B (2005) A rapid and versatile combined DNA/RNA extraction protocol and its application to the analysis of a novel DNA marker set polymorphic between Arabidopsis thaliana ecotypes Col-0 and Landsberg erecta. Plant Methods **1**: 4

Blackwood EM, Kadonaga JT (1998) Going the distance: A current view of enhancer action. Science (80-) **281**: 60–63

Blumenthal T (1998) Gene clusters and polycistronic transcription in eukaryotes. BioEssays **20**: 480–487

Boerboom AMJF, Vermeulen M, van der Woude H, Bremer BI, Lee-Hilz YY, Kampman E, van Bladeren PJ, Rietjens IMCM, Aarts JMMJG (2006) Newly constructed stable reporter cell lines for mechanistic studies on electrophile-responsive element-mediated gene expression reveal a role for flavonoid planarity. Biochem Pharmacol **72**: 217–226

Boutanaev AM, Moses T, Zi J, Nelson DR, Mugford ST, Peters RJ, Osbourn A (2015) Investigation of terpene diversification across multiple sequenced plant genomes. Proc Natl Acad Sci **112**: E81–E88

Boycheva S, Daviet L, Wolfender JL, Fitzpatrick TB (2014) The rise of operon-like gene clusters in plants. Trends Plant Sci **19**: 447–459

Buschhaus C, Herz H, Jetter R (2007) Chemical composition of the epicuticular and intracuticular wax layers on adaxial sides of Rosa canina leaves. Ann Bot **100**: 1557–1564

Buschhaus C, Jetter R (2012) Composition and Physiological Function of the Wax Layers Coating Arabidopsis Leaves: -Amyrin Negatively Affects the Intracuticular Water Barrier. PLANT Physiol **160**: 1120–1129

Busquets A, Keim V, Closa M, del Arco A, Boronat A, Arró M, Ferrer A (2008) Arabidopsis thaliana contains a single gene encoding squalene synthase. Plant Mol Biol **67**: 25–36

Calhoun VC, Levine M (2003) Long-range enhancer-promoter interactions in the Scr-Antp interval of the Drosophila Antennapedia complex. Proc Natl Acad Sci **100**: 9878–9883

Campos ML, Yoshida Y, Major IT, De Oliveira Ferreira D, Weraduwage SM, Froehlich JE, Johnson BF, Kramer DM, Jander G, Sharkey TD, et al (2016) Rewiring of jasmonate and phytochrome B signalling uncouples plant growth-defense tradeoffs. Nat Commun. doi: 10.1038/ncomms12570

Castillo D a., Kolesnikova MD, Matsuda SPT (2013) An effective strategy for exploring unknown metabolic pathways by genome mining. J Am Chem Soc **135**: 5885–5894

Chandramu C, Manohar RD, Krupadanam DGL, Dashavantha R V (2003) Isolation, characterization and biological activity of betulinic acid and ursolic acid from Vitex negundo L. Phytother Res **17**: 129–34

Chappell J (2002) The genetics and molecular genetics of terpene and sterol origami. Curr Opin Plant Biol **5**: 151–157

Chen X, Huang H, Xu L (2013) The CaMV 35S enhancer has a function to change the histone modification state at insertion loci in Arabidopsis thaliana. J Plant Res **126**: 841–846

Chen YC, Wong CL, Muzzi F, Vlaardingerbroek I, Kidd BN, Schenk PM (2014) Root defense analysis against fusarium oxysporum reveals new regulators to confer resistance. Sci Rep. doi: 10.1038/srep05584

Chu HY, Wegel E, Osbourn A (2011) From hormones to secondary metabolism: The emergence of metabolic gene clusters in plants. Plant J **66**: 66–79

Ci X, Zhou J, Lv H, Yu Q, Peng L, Hua S (2017) Betulin exhibits anti-inflammatory activity in LPS-stimulated macrophages and endotoxin-shocked mice through an AMPK/AKT/Nrf2-dependent mechanism. Cell Death Dis **8**: e2798

Claeys H, Van Landeghem S, Dubois M, Maleux K, Inze D (2014) What Is Stress? Dose-Response Effects in Commonly Used in Vitro Stress Assays. PLANT Physiol **165**: 519–527

Colotta F, Allavena P, Sica A, Garlanda C, Mantovani A (2009) Cancer-related inflammation, the seventh hallmark of cancer: links to genetic instability. Carcinogenesis **30**: 1073–1081

Corey EJ, Matsuda SP, Bartel B (1993) Isolation of an Arabidopsis thaliana gene encoding cycloartenol synthase by functional expression in a yeast mutant lacking lanosterol synthase by the use of a chromatographic screen. Proc Natl Acad Sci U S A **90**: 11628–32

D'Abrosca B, Fiorentino A, Monaco P, Pacifico S (2005) Radical-scavenging activities of new hydroxylated ursane triterpenes from cv. Annurca apples. Chem Biodivers **2**: 953–958

Dávila López M, Marťne Guerra JJ, Samuelsson T (2010) Analysis of gene order conservation in eukaryotes identifies transcriptionally and functionally linked genes. PLoS One. doi: 10.1371/journal.pone.0010654

Dinkova-Kostova AT, Talalay P (2008) Direct and indirect antioxidant properties of inducers of cytoprotective proteins. Mol Nutr Food Res. doi: 10.1002/mnfr.200700195

Dobi KC, Winston F (2007) Analysis of transcriptional activation at a distance in Saccharomyces cerevisiae. Mol Cell Biol **27**: 5575–5586

Dolan L, Davies J (2004) Cell expansion in roots. Curr Opin Plant Biol **7**: 33–39

Domröse A, Klein AS, Hage-Hülsmann J, Thies S, Svensson V, Classen T, Pietruszka J, Jaeger KE, Drepper T, Loeschcke A (2015) Efficient recombinant production of prodigiosin in Pseudomonas putida. Front Microbiol. doi: 10.3389/fmicb.2015.00972

Doyle MR, Amasino RM (2009) A Single Amino Acid Change in the Enhancer of Zeste Ortholog CURLY LEAF Results in Vernalization-Independent, Rapid Flowering in Arabidopsis. PLANT Physiol **151**: 1688–1697

Drag-Zalesińska M, Drag M, Poreba M, Borska S, Kulbacka J, Saczko J (2017) Anticancer properties of ester derivatives of betulin in human metastatic melanoma cells (Me-45). Cancer Cell Int. doi: 10.1186/s12935-016-0369-3

Ebizuka Y, Katsube Y, Tsutsumi T, Kushiro T, Shibuya M (2003) Functional genomics approach to the study of triterpene biosynthesis. Pure Appl Chem **75**: 369–374

Eggler AL, Gay KA, Mesecar AD (2008) Molecular mechanisms of natural products in chemoprevention: Induction of cytoprotective enzymes by Nrf2. Mol Nutr Food Res. doi: 10.1002/mnfr.200700249

Einset J, Winge P, Bones A (2007) ROS signaling pathways in chilling stress. Plant Signal Behav **2**: 365–367

El-Sayed WM, Aboul-Fadl T, Roberts JC, Lamb JG, Franklin MR (2007) Murine hepatoma (Hepa1c1c7) cells: A responsive in vitro system for chemoprotective enzyme induction by organoselenium compounds. Toxicol Vitr **21**: 157–164

Elinav E, Nowarski R, Thaiss CA, Hu B, Jin C, Flavell RA (2013) Inflammation-induced cancer: crosstalk between tumours, immune cells and microorganisms. Nat Rev Cancer **13**: 759–771

Fazio GC, Xu R, Matsuda SPT (2004) Genome Mining to Identify New Plant Triterpenoids.

J Am Chem Soc **126**: 5678–5679

Field B, Fiston-Lavier A-S, Kemen A, Geisler K, Quesneville H, Osbourn AE (2011) Formation of plant metabolic gene clusters within dynamic chromosomal regions. Proc Natl Acad Sci U S A **108**: 16116–21

Field B, Osbourn A (2012) Order in the playground: Formation of plant gene clusters in dynamic chromosomal regions. Mob Genet Elem **2**: 46–50

Field B, Osbourn AE (2008) Metabolic diversification--independent assembly of operon-like gene clusters in different plants. Science **320**: 543–547

Frerigmann H, Gigolashvili T (2014) MYB34, MYB51, and MYB122 distinctly regulate indolic glucosinolate biosynthesis in arabidopsis Thaliana. Mol Plant **7**: 814–828

Frey M, Chomet P, Glawischnig E, Stettner C, Gru S, Winklmair a, Eisenreich W, Bacher a, Meeley RB, Briggs SP, et al (1997) Analysis of a chemical plant defense mechanism in grasses. Science (80-) **277**: 696–699

Fujiwara Y, Komohara Y, Kudo R, Tsurushima K, Ohnishi K, Ikeda T, Takeya M (2011) Oleanolic acid inhibits macrophage differentiation into the M2 phenotype and glioblastoma cell proliferation by suppressing the activation of STAT3. Oncol Rep **26**: 1533–1537

Fukushima EO, Seki H, Sawai S, Suzuki M, Ohyama K, Saito K, Muranaka T (2013) Combinatorial biosynthesis of legume natural and rare triterpenoids in engineered yeast. Plant Cell Physiol **54**: 740–749

Gao B, Doan A, Hybertson BM (2014) The clinical potential of influencing Nrf2 signaling in degenerative and immunological disorders. Clin Pharmacol Adv Appl **6**: 19–34

Gasperini D, Chételat A, Acosta IF, Goossens J, Pauwels L, Goossens A, Dreos R, Alfonso E, Farmer EE (2015) Multilayered Organization of Jasmonate Signalling in the Regulation of Root Growth. PLoS Genet. doi: 10.1371/journal.pgen.1005300

Geraats BPJ, Bakker PAHM, van Loon LC (2002) Ethylene Insensitivity Impairs Resistance to Soilborne Pathogens in Tobacco and *Arabidopsis thaliana*. Mol Plant-Microbe Interact **15**: 1078–1085

Go YS, Lee SB, Kim HJ, Kim J, Park HY, Kim JK, Shibata K, Yokota T, Ohyama K, Muranaka T, et al (2012) Identification of marneral synthase, which is critical for growth and development in Arabidopsis. Plant J **72**: 791–804

Gong Y, Raj KM, Luscombe CA, Gadawski I, Tam T, Chu J, Gibson D, Carlson R, Sacks SL (2004) The synergistic effects of betulin with acyclovir against herpes simplex viruses. Antiviral Res **64**: 127–130

Goodrich J, Puangsomlee P, Martin M, Long D, Meyerowitz EM, Coupland G (1997) A Polycomb-group gene regulates homeotic gene expression in Arabidopsis. Nature **386**: 44–51

Guerriero G, Hausman JF, Cai G (2014) No stress! relax! mechanisms governing growth and shape in plant cells. Int J Mol Sci **15**: 5094–5114

Gupta MB, Bhalla TN, Gupta GP, Mitra CR, Bhargava KP (1969) Anti-inflammatory activity of natural products (I) triterpenoids. Eur J Pharmacol **6**: 67–70

Halliday GM (2005) Inflammation, gene mutation and photoimmunosuppression in response to UVR-induced oxidative damage contributes to photocarcinogenesis. Mutat Res - Fundam Mol Mech Mutagen **571**: 107–120

Han SB, Kim HM, Kim YH, Lee CW, Jang ES, Son KH, Kim SU, Kim YK (1998) T-cell specific immunosuppression by prodigiosin isolated from Serratia marcescens. Int J Immunopharmacol **20**: 1–13

Han SW, Lee SW, Bahar O, Schwessinger B, Robinson MR, Shaw JB, Madsen JA, Brodbelt JS, Ronald PC (2012) Tyrosine sulfation in a Gram-negative bacterium. Nat Commun. doi: 10.1038/ncomms2157

Harris AKP, Williamson NR, Slater H, Cox A, Abbasi S, Foulds I, Simonsen HT, Leeper FJ, Salmond GPC (2004) The Serratia gene cluster encoding biosynthesis of the red antibiotic, prodigiosin, shows species- and strain-dependent genome context variation. Microbiology **150**: 3547–3560

Hartmann J, Fischer C, Dietrich P, Sauter M (2014) Kinase activity and calmodulin binding are essential for growth signaling by the phytosulfokine receptor PSKR1. Plant J **78**: 192–202

Hartmann J, Stührwohldt N, Dahlke RI, Sauter M (2013) Phytosulfokine control of growth occurs in the epidermis, is likely to be non-cell autonomous and is dependent on brassinosteroids. Plant J **73**: 579–590

Hassankhani R, Sam MR, Esmaeilou M, Ahangar P (2015) Prodigiosin isolated from cell wall of Serratia marcescens alters expression of apoptosis-related genes and increases apoptosis in colorectal cancer cells. Med Oncol **32**: 1–8

Hattori Y, Nishigori C, Tanaka T, Uchida K, Nikaido O, Osawa T, Hiai H, Imamura S, Toyokuni S (1996) 8-Hydroxy-2'-deoxyguanosine is increased in epidermal cells of hairless mice after chronic ultraviolet B exposure. J Invest Dermatol **107**: 733–737

Herrera JBR, Bartel B, Wilson WK, Matsuda SP. (1998) Cloning and characterization of the Arabidopsis thaliana lupeol synthase gene. Phytochemistry **49**: 1905–1911

Hideg É, Jansen MAK, Strid Å (2013) UV-B exposure, ROS, and stress: Inseparable companions or loosely linked associates? Trends Plant Sci **18**: 107–115

Hill RA, Connolly JD (2015) Triterpenoids. Nat Prod Rep **32**: 273–327

Hong DS, Kurzrock R, Supko JG, He X, Naing A, Wheler J, Lawrence D, Eder JP, Meyer CJ, Ferguson DA, et al (2012) A phase I first-in-human trial of bardoxolone methyl in patients with advanced solid tumors and lymphomas. Clin Cancer Res **18**: 3396–406

Hotta H, Yano I, Yabuuchi E, Kosako Y, Oyaizu H, Ezaki T, Hashimoto Y, Arakawa M (1992) Proposal of Burkholderia gen. Anov. And Transfer of Seven Species of the Genus Pseudomonas Homology Group II to the New Genus, with the Type Species Burkholderia cepacia (Palleroni and Holmes 1981) comb: Nov. Microbiol Immunol **36**: 1251–1275

ten Hove CA, de Jong M, Lapin D, Andel A, Sanchez-Perez GF, Tarutani Y, Suzuki Y, Heidstra R, van den Ackerveken G (2011) Trans-repression of gene activity upstream of T-DNA tagged rlk902 links Arabidopsis root growth inhibition and downy mildew resistance. PLoS One. doi: 10.1371/journal.pone.0019028

Howe GA, Jander G (2008) Plant Immunity to Insect Herbivores. Annu Rev Plant Biol **59**: 41–66

Hruz T, Laule O, Szabo G, Wessendorp F, Bleuler S, Oertle L, Widmayer P, Gruissem W, Zimmermann P (2008) Genevestigator v3: a reference expression database for the meta-analysis of transcriptomes. Adv Bioinformatics **2008**: 420747

Hurst LD, Pál C, Lercher MJ (2004) The evolutionary dynamics of eukaryotic gene order. Nat Rev Genet **5**: 299–310

Igarashi D, Tsuda K, Katagiri F (2012) The peptide growth factor, phytosulfokine, attenuates pattern-triggered immunity. Plant J **71**: 194–204

Itoh K, Chiba T, Takahashi S, Ishii T, Igarashi K, Katoh Y, Oyake T, Hayashi N, Satoh K, Hatayama I, et al (1997) An Nrf2/Small Maf Heterodimer Mediates the Induction of Phase II Detoxifying Enzyme Genes through Antioxidant Response Elements. Biochem Biophys Res Commun **236**: 313–322

Jacoby R, Peukert M, Succurro A, Koprivova A, Kopriva S (2017) The Role of Soil Microorganisms in Plant Mineral Nutrition—Current Knowledge and Future Directions. Front Plant Sci. doi: 10.3389/fpls.2017.01617

Jagadeesh SG, Krupadanam GLD, Srimannarayana G, Murthy SS, Kaur A, Raja SS (1998) Tobacco caterpillar antifeedent from the Gotti stem wood triterpene betulinic

acid. J Agric Food Chem **46**: 2797–2799

Jäger S, Trojan H, Kopp T, Laszczyk MN, Scheffler A (2009) Pentacyclic triterpene distribution in various plants - rich sources for a new group of multi-potent plant extracts. Molecules **14**: 2016–2031

Jansen M, Gilmer F, Biskup B, Nagel KA, Rascher U, Fischbach A, Briem S, Dreissen G, Tittmann S, Braun S, et al (2009) Simultaneous phenotyping of leaf growth and chlorophyll fluorescence via Growscreen Fluoro allows detection of stress tolerance in Arabidopsis thaliana and other rosette plants. Funct Plant Biol **36**: 902–914

Jeong Y, Kim J, Kim S, Kang Y, Nagamatsu T, Hwang I (2003) Toxoflavin Produced by *Burkholderia glumae* Causing Rice Grain Rot Is Responsible for Inducing Bacterial Wilt in Many Field Crops. Plant Dis **87**: 890–895

Jeyapaul J, Jaiswal AK (2000) Nrf2 and c-Jun regulation of antioxidant response element (ARE)-mediated expression and induction of gamma-glutamylcysteine synthetase heavy subunit gene. Biochem Pharmacol **59**: 1433–9

Johnson EE (2012) Dissertation: Profile of the expression of a metabolic gene cluster in Arabidopsis. The University of British Columbia, Vancouver

Jozefowicz AM, Matros A, Witzel K, Mock H-P (2018) Mini-Scale Isolation and Preparation of Plasma Membrane Proteins from Potato Roots for LC/MS Analysis. Humana Press, New York, NY, pp 195–204

Kadereit JW, Körner C, Sonnewald U (2014) Strasburger - Lehrbuch der Pflanzenwissenschaften, 37. Springer Verlag, Berlin

Katzke N, Arvani S, Bergmann R, Circolone F, Markert A, Svensson V, Jaeger KE, Heck A, Drepper T (2010) A novel T7 RNA polymerase dependent expression system for high-level protein production in the phototrophic bacterium Rhodobacter capsulatus. Protein Expr Purif **69**: 137–146

Kemen AC, Honkanen S, Melton RE, Findlay KC, Mugford ST, Hayashi K, Haralampidis K, Rosser SJ, Osbourn A (2014) Investigation of triterpene synthesis and regulation in oats reveals a role for β-amyrin in determining root epidermal cell patterning. Proc Natl Acad Sci U S A **111**: 8679–84

Kesselmeier J, Urban B (1983) Subcellular localization of saponins in green and etiolated leaves and green protoplasts of oat (Avena sativa L.). Protoplasma **114**: 133–140

Khan NE, Nybo SE, Chappell J, Curtis WR (2015) Triterpene hydrocarbon production engineered into a metabolically versatile host-Rhodobacter capsulatus. Biotechnol Bioeng **112**: 1523–1532

Kidd BN, Edgar CI, Kumar KK, Aitken EA, Schenk PM, Manners JM, Kazan K (2009) The Mediator Complex Subunit PFT1 Is a Key Regulator of Jasmonate-Dependent Defense in Arabidopsis. PLANT CELL ONLINE **21**: 2237–2252

Kilian J, Whitehead D, Horak J, Wanke D, Weinl S, Batistic O, D'Angelo C, Bornberg-Bauer E, Kudla J, Harter K (2007) The AtGenExpress global stress expression data set: Protocols, evaluation and model data analysis of UV-B light, drought and cold stress responses. Plant J **50**: 347–363

Kim GH, Kim JE, Rhie SJ, Yoon S (2015) The Role of Oxidative Stress in Neurodegenerative Diseases. Exp Neurobiol **24**: 325

Kim YR, Oh JE, Kim MS, Kang MR, Park SW, Han JY, Eom HS, Yoo NJ, Lee SH (2010) Oncogenic NRF2 mutations in squamous cell carcinomas of oesophagus and skin. J Pathol **220**: 446–451

Kirby J, Romanini DW, Paradise EM, Keasling JD (2008) Engineering triterpene production in Saccharomyces cerevisiae-β-amyrin synthase from Artemisia annua. FEBS J **275**: 1852–1859

Klein AS, Domröse A, Bongen P, Brass HUC, Classen T, Loeschcke A, Drepper T, Laraia L, Sievers S, Jaeger KE, et al (2017) New Prodigiosin Derivatives Obtained by Mutasynthesis in Pseudomonas putida. ACS Synth Biol **6**: 1757–1765

Kliebenstein DJ, Osbourn A (2012) Making new molecules - evolution of pathways for novel metabolites in plants. Curr Opin Plant Biol **15**: 415–423

Klipp W, Masepohl B, Pühler A (1988) Identification and mapping of nitrogen fixation genes of Rhodobacter capsulatus: duplication of a nifA-nifB region. J Bacteriol **170**: 693–699

Klunder V (2016) Bachelor Thesis: Redundancy and specificity of marneral and thalianol in PSK-induced plant growth. University of Cologne, Cologne

Kolesnikova MD, Obermeyer AC, Wilson WK, Lynch DA, Xiong Q, Matsuda SPT (2007a) Stereochemistry of water addition in triterpene synthesis: The structure of arabidiol. Org Lett **9**: 2183–2186

Kolesnikova MD, Wilson WK, Lynch DA, Obermeyer AC, Matsuda SPT (2007b) Arabidopsis camelliol C synthase evolved from enzymes that make pentacycles. Org Lett **9**: 5223–5226

Kolesnikova MD, Xiong Q, Lodeiro S, Hua L, Matsuda SPT (2006) Lanosterol biosynthesis in plants. Arch Biochem Biophys **447**: 87–95

Komori R, Amano Y, Ogawa-Ohnishi M, Matsubayashi Y (2009) Identification of

tyrosylprotein sulfotransferase in Arabidopsis. Proc Natl Acad Sci U S A **106**: 15067–72

Kranz-Finger S, Mahmoud O, Ricklefs E, Ditz N, Bakkes PJ, Urlacher VB (2018) Insights into the functional properties of the marneral oxidase CYP71A16 from Arabidopsis thaliana. Biochim Biophys Acta - Proteins Proteomics **1866**: 2–10

Król SK, Kiełbus M, Rivero-Müller A, Stepulak A (2015) Comprehensive review on betulin as a potent anticancer agent. Biomed Res Int **2015**: 11

Kushiro T, Shibuya M, Masuda K, Ebizuka Y (2000) A novel multifunctional triterpene synthase from Arabidopsis thaliana. Tetrahedron Lett **41**: 7705–7710

Kutschmar A, Rzewuski G, Stührwohldt N, Beemster GTS, Inzé D, Sauter M (2009) PSK-α promotes root growth in Arabidopsis. New Phytol **181**: 820–831

Kwak MK, Wakabayashi N, Itoh K, Motohashi H, Yamamoto M, Kensler TW (2003) Modulation of gene expression by cancer chemopreventive dithiolethiones through the Keap1-Nrf2 pathway. Identification of novel gene clusters for cell survival. J Biol Chem **278**: 8135–8145

Kwezi L, Ruzvidzo O, Wheeler JI, Govender K, Iacuone S, Thompson PE, Gehring C, Irving HR (2011) The phytosulfokine (PSK) receptor is capable of guanylate cyclase activity and enabling cyclic GMP-dependent signaling in plants. J Biol Chem **286**: 22580–22588

Lapenda JC, Silva PA, Vicalvi MC, Sena KXFR, Nascimento SC (2014) Antimicrobial activity of prodigiosin isolated from Serratia marcescens UFPEDA 398. World J Microbiol Biotechnol **31**: 399–406

Larroque M, Belmas E, Martinez T, Vergnes S, Ladouce N, Lafitte C, Gaulin E, Dumas B (2013) Pathogen-associated molecular pattern-triggered immunity and resistance to the root pathogen Phytophthora parasitica in Arabidopsis. J Exp Bot **64**: 3615–3625

Laszczyk M, Jäger S, Simon-Haarhaus B, Scheffler A, Schempp CM (2006) Physical, chemical and pharmacological characterization of a new oleogel-forming triterpene extract from the outer bark of birch (Betulae cortex). Planta Med **72**: 1389–1395

Lawrence JG, Roth JR (1996) Selfish operons: Horizontal transfer may drive the evolution of gene clusters. Genetics **143**: 1843–1860

Lee JM, Sonnhammer ELL (2003) Genomic gene clustering analysis of pathways in eukaryotes. Genome Res **13**: 875–882

Lewis DH (1973) CONCEPTS IN FUNGAL NUTRITION AND THE ORIGIN OF BIOTROPHY. Biol Rev **48**: 261–277

Liby K, Hock T, Yore MM, Suh N, Place AE, Risingsong R, Williams CR, Royce DB,

Honda T, Honda Y, et al (2005) The Synthetic Triterpenoids, CDDO and CDDO-Imidazolide, Are Potent Inducers of Heme Oxygenase-1 and Nrf2/ARE Signaling. Cancer Res **65**: 4789–4798

Liby KT, Sporn MB (2012) Synthetic Oleanane Triterpenoids: Multifunctional Drugs with a Broad Range of Applications for Prevention and Treatment of Chronic Disease. Pharmacol Rev **64**: 972–1003

Liby KT, Yore MM, Sporn MB (2007) Triterpenoids and rexinoids as multifunctional agents for the prevention and treatment of cancer. Nat Rev Cancer **7**: 357–369

Lichten M, De Massy B (2011) The impressionistic landscape of meiotic recombination. Cell **147**: 267–270

Lichtenthaler HK (1999) THE 1-DEOXY-D-XYLULOSE-5-PHOSPHATE PATHWAY OF ISOPRENOID BIOSYNTHESIS IN PLANTS. Annu Rev Plant Physiol Plant Mol Biol **50**: 47–65

Linnewiel-Hermoni K, Khanin M, Danilenko M, Zango G, Amosi Y, Levy J, Sharoni Y (2015) The anti-cancer effects of carotenoids and other phytonutrients resides in their combined activity. Arch Biochem Biophys **572**: 28–35

Linnewiel K, Ernst H, Caris-Veyrat C, Ben-Dor A, Kampf A, Salman H, Danilenko M, Levy J, Sharoni Y (2009) Structure activity relationship of carotenoid derivatives in activation of the electrophile/antioxidant response element transcription system. Free Radic Biol Med **47**: 659–667

Liu Y (2005) Arabidopsis Vegetative Storage Protein Is an Anti-Insect Acid Phosphatase. PLANT Physiol **139**: 1545–1556

Livak KJ, Schmittgen TD (2001) Analysis of relative gene expression data using real-time quantitative PCR and the 2-ΔΔCT method. Methods **25**: 402–408

Loboda A, Rojczyk-Golebiewska E, Bednarczyk-Cwynar B, Lucjusz Z, Jozkowicz A, Dulak J (2012) Targeting nrf2-mediated gene transcription by triterpenoids and their derivatives. Biomol Ther (Seoul) **20**: 499–505

Lodeiro S, Xiong Q, Wilson WK, Kolesnikova MD, Onak CS, Matsuda SPT (2007) An oxidosqualene cyclase makes numerous products by diverse mechanisms: A challenge to prevailing concepts of triterpene biosynthesis. J Am Chem Soc **129**: 11213–11222

Loeschcke A, Dienst D, Wewer V, Hage-Hülsmann J, Dietsch M, Kranz-Finger S, Hüren V, Metzger S, Urlacher VB, Gigolashvili T, et al (2017) The photosynthetic bacteria Rhodobacter capsulatus and Synechocystis sp. PCC 6803 as new hosts for cyclic plant triterpene biosynthesis. PLoS One **12**: e0189816

Lorbiecke R, Sauter M (2002) Comparative analysis of PSK peptide growth factor precursor homologs. Plant Sci **163**: 321–332

Lützow M, Beyer P (1988) The isopentenyl-diphosphate Δ-isomerase and its relation to the phytoene synthase complex in daffodil chromoplasts. Biochim Biophys Acta (BBA)/Lipids Lipid Metab **959**: 118–126

Machado KE, Cechinel Filho V, Cruz RCB, Meyre-Silva C, Cruz AB (2009) Antifungal activity of Eugenia umbelliflora against dermatophytes. Nat Prod Commun **4**: 1181–4

Maffei ME, Mithöfer A, Boland W (2007) Insects feeding on plants: Rapid signals and responses preceding the induction of phytochemical release. Phytochemistry **68**: 2946–2959

Marner F -J, Longerich I (1992) Isolation and Structure Determination of new Iridals from Iris sibirica and Iris versicolor. Liebigs Ann der Chemie **1992**: 269–272

Marrs B (1974) Genetic Recombination in Rhodopseudomonas capsulata. Proc Natl Acad Sci **71**: 971–973

Massonnet C, Vile D, Fabre J, Hannah MA, Caldana C, Lisec J, Beemster GTS, Meyer RC, Messerli G, Gronlund JT, et al (2010) Probing the Reproducibility of Leaf Growth and Molecular Phenotypes: A Comparison of Three Arabidopsis Accessions Cultivated in Ten Laboratories. PLANT Physiol **152**: 2142–2157

Matsubayashi Y (2006) Disruption and Overexpression of Arabidopsis Phytosulfokine Receptor Gene Affects Cellular Longevity and Potential for Growth. PLANT Physiol **142**: 45–53

Matsubayashi Y, Ogawa M, Morita A, Sakagami Y (2002) An LRR receptor kinase involved in perception of a peptide plant hormone, phytosulfokine. Science (80-) **296**: 1470–1472

Matsubayashi Y, Sakagami Y (1996) Phytosulfokine, sulfated peptides that induce the proliferation of single mesophyll cells of Asparagus officinalis L. Proc Natl Acad Sci U S A **93**: 7623–7627

Matsubayashi Y, Sakagami Y (2006) Peptide hormones in plants. Annu Rev Plant Biol **57**: 649–674

Matsuzaki Y, Ogawa-Ohnishi M, Mori A, Matsubayashi Y (2010) Secreted peptide signals required for maintenance of root stem cell niche in Arabidopsis. Science **329**: 1065–1067

McGarvey DJ, Croteau R (1995) Terpenoid metabolism. Plant Cell **7**: 1015–26

McMahon M, Itoh K, Yamamoto M, Chanas SA, Henderson CJ, McLellan LI, Wolf CR,

Cavin C, Hayes JD (2001) The cap "n" collar basic leucine zipper transcription factor Nrf2 (NF-E2 p45-related factor 2) controls both constitutive and inducible expression of intestinal detoxification and glutathione biosynthetic enzymes. Cancer Res **61**: 3299–3307

Merli C, Bergstrom DE, Cygan JA, Blackman RK (1996) Promoter specificity mediates the independent regulation of neighboring genes. Genes Dev **10**: 1260–1270

Michael B. Jarstfer ‡, Dong-Lu Zhang and, Poulter* CD (2002) Recombinant Squalene Synthase. Synthesis of Non-Head-to-Tail Isoprenoids in the Absence of NADPH. doi: 10.1021/JA020410I

Miettinen K, Iñigo S, Kreft L, Pollier J, De Bo C, Botzki A, Coppens F, Bak S, Goossens A (2017a) The TriForC database: a comprehensive up-to-date resource of plant triterpene biosynthesis. Nucleic Acids Res. doi: 10.1093/nar/gkx925

Miettinen K, Pollier J, Buyst D, Arendt P, Csuk R, Sommerwerk S, Moses T, Mertens J, Sonawane PD, Pauwels L, et al (2017b) The ancient CYP716 family is a major contributor to the diversification of eudicot triterpenoid biosynthesis. Nat Commun **8**: 14153

Mikhed Y, Görlach A, Knaus UG, Daiber A (2015) Redox regulation of genome stability by effects on gene expression, epigenetic pathways and DNA damage/repair. Redox Biol **5**: 275–289

Miller G, Suzuki N, Ciftci-Yilmaz S, Mittler R (2010) Reactive oxygen species homeostasis and signalling during drought and salinity stresses. Plant, Cell Environ **33**: 453–467

Moolgavkar SH (1978) The multistage theory of carcinogenesis and the age distribution of cancer in man. J Natl Cancer Inst **61**: 49–52

Moreno JE, Shyu C, Campos ML, Patel LC, Chung HS, Yao J, He SY, Howe GA (2013) Negative feedback control of jasmonate signaling by an alternative splice variant of JAZ10. Plant Physiol **162**: 1006–17

Morlacchi P, Wilson WK, Xiong Q, Bhaduri A, Sttivend D, Kolesnikova MD, Matsuda SPT (2009) Product profile of PEN3: The last unexamined oxidosqualene cyclase in arabidopsis thaliana. Org Lett **11**: 2627–2630

Morris S-AL, Huang S (2016) Crosstalk of the Wnt/β-catenin pathway with other pathways in cancer cells. Genes Dis **3**: 41–47

Mosher S, Kemmerling B (2013) PSKR1 and PSY1R-mediated regulation of plant defense responses. Plant Signal Behav **8**: e24119

Mosher S, Seybold H, Rodriguez P, Stahl M, Davies K a., Dayaratne S, Morillo S a., Wierzba M, Favery B, Keller H, et al (2013) The tyrosine-sulfated peptide receptors PSKR1 and PSY1R modify the immunity of Arabidopsis to biotrophic and necrotrophic pathogens in an antagonistic manner. Plant J **73**: 469–482

Mosmann T (1983) Rapid colorimetric assay for cellular growth and survival: application to proliferation and cytotoxicity assays. J Immunol Methods **65**: 55–63

Müller TM, Böttcher C, Morbitzer R, Götz CC, Lehmann J, Lahaye T, Glawischnig E (2015) TRANSCRIPTION ACTIVATOR-LIKE EFFECTOR NUCLEASE-Mediated Generation and Metabolic Analysis of Camalexin-Deficient *cyp71a12 cyp71a13* Double Knockout Lines. Plant Physiol **168**: 849–858

Mylona P, Owatworakit A, Papadopoulou K, Jenner H, Qin B, Findlay K, Hill L, Qi X, Bakht S, Melton R, et al (2008) Sad3 and Sad4 Are Required for Saponin Biosynthesis and Root Development in Oat. PLANT CELL ONLINE **20**: 201–212

Nathoo N, Bernards MA, MacDonald J, Yuan Z-C (2017) A Hydroponic Co-cultivation System for Simultaneous and Systematic Analysis of Plant/Microbe Molecular Interactions and Signaling. J Vis Exp e55955–e55955

Nobrega MA, Ovcharenko I, Afzal V, Rubin EM (2003) Scanning Human Gene Deserts for Long-Range Enhancers. Science (80-) **302**: 413

Nützmann H-W, Osbourn A (2015) Regulation of metabolic gene clusters in Arabidopsis thaliana. New Phytol **205**: 503–10

Nützmann HW, Osbourn A (2014) Gene clustering in plant specialized metabolism. Curr Opin Biotechnol **26**: 91–99

O'Callaghan M (2016) Microbial inoculation of seed for improved crop performance: issues and opportunities. Appl Microbiol Biotechnol **100**: 5729–5746

Ogas J, Kaufmann S, Henderson J, Somerville C (1999) PICKLE is a CHD3 chromatin-remodeling factor that regulates the transition from embryonic to vegetative development in Arabidopsis. Proc Natl Acad Sci U S A **96**: 13839–13844

Okada A, Okada K, Miyamoto K, Koga J, Shibuya N, Nojiri H, Yamane H (2009) OsTGAP1, a bZIP Transcription Factor, Coordinately Regulates the Inductive Production of Diterpenoid Phytoalexins in Rice. J Biol Chem **284**: 26510–26518

Omar AS, Flammann HT, Golecki JR, Weckesser J (1983) Detection of capsule and slime polysaccharide layers in two strains of Rhodopseudomonas capsulata. Arch Microbiol **134**: 114–117

Osbourn AE (2003) Saponins in cereals. Phytochemistry **62**: 1–4

Özaydin B, Burd H, Lee TS, Keasling JD (2013) Carotenoid-based phenotypic screen of the yeast deletion collection reveals new genes with roles in isoprenoid production. Metab Eng **15**: 174–183

Paddon CJ, Westfall PJ, Pitera DJ, Benjamin K, Fisher K, McPhee D, Leavell MD, Tai A, Main A, Eng D, et al (2013) High-level semi-synthetic production of the potent antimalarial artemisinin. Nature **496**: 528–532

Papadopoulou K, Melton RE, Leggett M, Daniels MJ, Osbourn a E (1999) Compromised disease resistance in saponin-deficient plants. Proc Natl Acad Sci U S A **96**: 12923–12928

Park EJ, Pezzuto JM (2002) Botanicals in cancer chemoprevention. Cancer Metastasis Rev **21**: 231–255

Park HJ, Park CJ, Bae N, Han SW (2016) Deciphering the role of tyrosine sulfation in Xanthomonas oryzae pv. Oryzae using shotgun proteomic analysis. Plant Pathol J **32**: 266–272

Peplow M (2013) Malaria drug made in yeast causes market ferment. Nature **494**: 160–161

Perfect SE, Green JR (2001) Infection structures of biotrophic and hemibiotrophic fungal plant pathogens. Mol Plant Pathol **2**: 101–8

Pergola PE, Raskin P, Toto RD, Meyer CJ, Huff JW, Grossman EB, Krauth M, Ruiz S, Audhya P, Christ-Schmidt H, et al (2011) Bardoxolone Methyl and Kidney Function in CKD with Type 2 Diabetes. N Engl J Med **365**: 327–336

Pfarr K, Danciu C, Arlt O, Neske C, Dehelean C, Pfeilschifter JM, Radeke HH (2015) Simultaneous and dose dependent melanoma cytotoxic and immune stimulatory activity of betulin. PLoS One. doi: 10.1371/journal.pone.0118802

Phillips MA, D'Auria JC, Gershenzon J, Pichersky E (2008) The Arabidopsis thaliana Type I Isopentenyl Diphosphate Isomerases Are Targeted to Multiple Subcellular Compartments and Have Overlapping Functions in Isoprenoid Biosynthesis. PLANT CELL ONLINE **20**: 677–696

Pritchard J (1994) The control of cell expansion in roots. New Phytol **127**: 3–26

Pruitt RN, Schwessinger B, Joe A, Thomas N, Liu F, Albert M, Robinson MR, Chan LJG, Luu DD, Chen H, et al (2015) The rice immune receptor XA21 recognizes a tyrosine-sulfated protein from a Gram-negative bacterium. Sci Adv **1**: e1500245–e1500245

Qi X, Bakht S, Qin B, Leggett M, Hemmings A, Mellon F, Eagles J, Werck-Reichhart D, Schaller H, Lesot A, et al (2006) A different function for a member of an ancient and

highly conserved cytochrome P450 family: from essential sterols to plant defense. Proc Natl Acad Sci U S A **103**: 18848–53

Rada P, Rojo AI, Offergeld A, Feng GJ, Velasco-Martín JP, González-Sancho JM, Valverde ÁM, Dale T, Regadera J, Cuadrado A (2015) WNT-3A Regulates an Axin1/NRF2 Complex That Regulates Antioxidant Metabolism in Hepatocytes. Antioxid Redox Signal **22**: 555–571

Rasbery JM, Shan H, LeClair RJ, Norman M, Matsuda SPT, Bartel B (2007) Arabidopsis thaliana squalene epoxidase 1 is essential for root and seed development. J Biol Chem **282**: 17002–17013

Rautengarten C, Steinhauser D, Büssis D, Stintzi A, Schaller A, Kopka J, Altmann T (2005) Inferring hypotheses on functional relationships of genes: Analysis of the Arabidopsis thaliana subtilase gene family. PLoS Comput Biol **1**: 0297–0312

Ren S, Johnston JS, Shippen DE, McKnight TD (2004) TELOMERASE ACTIVATOR1 induces telomerase activity and potentiates responses to auxin in Arabidopsis. Plant Cell **16**: 2910–2922

Rippe K, von Hippel PH, Langowski J (1995) Action at a distance: DNA-looping and initiation of transcription. Trends Biochem Sci **20**: 500–506

Ro D-K, Paradise EM, Ouellet M, Fisher KJ, Newman KL, Ndungu JM, Ho KA, Eachus RA, Ham TS, Kirby J, et al (2006) Production of the antimalarial drug precursor artemisinic acid in engineered yeast. Nature **440**: 940–943

Saiki RK, Gelfand DH, Stoffel S, Scharf SJ, Higuchi R, Horn GT, Mullis KB, Erlich HA (1988) Primer-directed enzymatic amplification of DNA with a thermostable DNA polymerase. Science (80-) **239**: 487–491

Sauter M (2015) Phytosulfokine peptide signalling. J Exp Bot. doi: 10.1093/jxb/erv071

Schimmer AD, Raza A, Carter TH, Claxton D, Erba H, DeAngelo DJ, Tallman MS, Goard C, Borthakur G (2014) A multicenter phase l/ll study of obatoclax mesylate administered as a 3- Or 24-hour infusion in older patients with previously untreated acute myeloid leukemia. PLoS One **9**: e108694

Seki H, Tamura K, Muranaka T (2015) P450s and UGTs: Key Players in the Structural Diversity of Triterpenoid Saponins. Plant Cell Physiol **56**: 1463–1471

Serhan CN (2014) Pro-resolving lipid mediators are leads for resolution physiology. Nature **510**: 92–101

Shai LJ, McGaw LJ, Aderogba MA, Mdee LK, Eloff JN (2008) Four pentacyclic triterpenoids with antifungal and antibacterial activity from Curtisia dentata (Burm.f)

C.A. Sm. leaves. J Ethnopharmacol **119**: 238–244

Shang Y, Ma Y, Zhou Y, Zhang H, Duan L, Chen H, Zeng J, Zhou Q, Wang S, Gu W, et al (2014) Biosynthesis, regulation, and domestication of bitterness in cucumber. Science (80-) **346**: 1084–1088

Shiba Y, Paradise EM, Kirby J, Ro DK, Keasling JD (2007) Engineering of the pyruvate dehydrogenase bypass in Saccharomyces cerevisiae for high-level production of isoprenoids. Metab Eng **9**: 160–168

Shibuya M, Katsube Y, Otsuka M, Zhang H, Tansakul P, Xiang T, Ebizuka Y (2009) Identification of a product specific β-amyrin synthase from Arabidopsis thaliana. Plant Physiol Biochem **47**: 26–30

Shimaoka T, Ohnishi M, Sazuka T, Mitsuhashi N, Hara-Nishimura I, Shimazaki KI, Maeshima M, Yokota A, Tomizawa KI, Mimura T (2004) Isolation of intact vacuoles and proteomic analysis of tonoplast from suspension-cultured cells of Arabidopsis thaliana. Plant Cell Physiol **45**: 672–683

Shin R, Berg RH, Schachtman DP (2005) Reactive oxygen species and root hairs in arabidopsis root response to nitrogen, phosphorus and potassium deficiency. Plant Cell Physiol **46**: 1350–1357

Šiman P, Filipová A, Tichá A, Niang M, Bezrouk A, Havelek R (2016) Effective method of purification of betulin from birch bark: The importance of its purity for scientific and medicinal use. PLoS One. doi: 10.1371/journal.pone.0154933

de Souza LF, Barreto F, da Silva EG, Andrades ME, Guimarães ELM, Behr GA, Moreira JCF, Bernard EA (2007) Regulation of LPS stimulated ROS production in peritoneal macrophages from alloxan-induced diabetic rats: Involvement of high glucose and PPARγ. Life Sci **81**: 153–159

Srivastava R, Liu JX, Howell SH (2008) Proteolytic processing of a precursor protein for a growth-promoting peptide by a subtilisin serine protease in Arabidopsis. Plant J **56**: 219–227

Stahl FW, Murray NE (1966) The evolution of gene clusters and genetic circularity in microorganisms. Genetics **53**: 569–576

Strnad H, Lapidus A, Paces J, Ulbrich P, Vlcek C, Paces V, Haselkorn R (2010) Complete genome sequence of the photosynthetic purple nonsulfur bacterium Rhodobacter capsulatus SB 1003. J Bacteriol **192**: 3545–3546

Stührwohldt N, Dahlke RI, Steffens B, Johnson A, Sauter M (2011) Phytosulfokine-α controls hypocotyl length and cell expansion in Arabidopsis thaliana through

phytosulfokine receptor 1. PLoS One. doi: 10.1371/journal.pone.0021054

Su'udi M, Park JM, Park SR, Hwang DJ, Bae SC, Kim S, Ahn IP (2013) Quantification of Alternaria brassicicola infection in the Arabidopsis thaliana and Brassica rapa subsp. pekinensis. Microbiol (United Kingdom) **159**: 1946–1955

Sundaravelpandian K, Chandrika NNP, Schmidt W (2013) PFT1, a transcriptional Mediator complex subunit, controls root hair differentiation through reactive oxygen species (ROS) distribution in Arabidopsis. New Phytol **197**: 151–161

Surh YJ, Kundu JK, Na HK (2008) Nrf2 as a master redox switch in turning on the cellular signaling involved in the induction of cytoprotective genes by some chemopreventive phytochemicals. Planta Med **74**: 1526–1539

Szakiel A, Pączkowski C, Pensec F, Bertsch C (2012) Fruit cuticular waxes as a source of biologically active triterpenoids. Phytochem Rev **11**: 263–284

Thimmappa R, Geisler K, Louveau T, O'Maille P, Osbourn A (2014) Triterpene biosynthesis in plants. Annu Rev Plant Biol **65**: 225–57

Tokuda H, Ohigashi H, Koshimizu K, Ito Y (1986) Inhibitory effects of ursolic and oleanolic ancid on skin tumor promotion by 12-O-tetradecanoylphorbol-13-acetate. Cancer Lett **33**: 279–285

Tong KI, Kobayashi A, Katsuoka F, Yamamoto M (2006) Two-site substrate recognition model for the Keap1-Nrf2 system: A hinge and latch mechanism. Biol. Chem. pp 1311–1320

Troost K (2017) Dissertation: Rhodobacter capsulatus an alternativ host for the production of plant sesquiterpenoids. Heinrich-Heine-Universität Düsseldorf, Düsseldorf

Verslues PE, Agarwal M, Katiyar-Agarwal S, Zhu J, Zhu JK (2006) Methods and concepts in quantifying resistance to drought, salt and freezing, abiotic stresses that affect plant water status. Plant J **45**: 523–539

Vincken J-P, Heng L, de Groot A, Gruppen H (2007) Saponins, classification and occurrence in the plant kingdom. Phytochemistry **68**: 275–297

De Vylder J, Vandenbussche F, Hu Y, Philips W, Van Der Straeten D (2012) Rosette Tracker: An Open Source Image Analysis Tool for Automatic Quantification of Genotype Effects. PLANT Physiol **160**: 1149–1159

Walker TS (2003) Root Exudation and Rhizosphere Biology. PLANT Physiol **132**: 44–51

Wang Z, Li B, Zhou L, Yu S, Su Z, Song J, Sun Q, Sha O, Wang X, Jiang W, et al (2016) Prodigiosin inhibits Wnt/β-catenin signaling and exerts anticancer activity in breast cancer cells. Proc Natl Acad Sci U S A **113**: 201616336

Weckopp SC (2014) Bachelor Thesis: PSK-related regulation of triterpene biosynthesis in Arabiodpsis thaliana and its role in plant microbe interactions. University of Cologne, Cologne

Weigel D, Ahn JH, Blázquez MA, Borevitz JO, Christensen SK, Fankhauser C, Ferrándiz C, Kardailsky I, Malancharuvil EJ, Neff MM, et al (2000) Activation Tagging in Arabidopsis. Plant Physiol **122**: 1003–1014

Windram O, Madhou P, McHattie S, Hill C, Hickman R, Cooke E, Jenkins DJ, Penfold CA, Baxter L, Breeze E, et al (2012) Arabidopsis Defense against Botrytis cinerea: Chronology and Regulation Deciphered by High-Resolution Temporal Transcriptomic Analysis. Plant Cell **24**: 3530–3557

Wink M (2010) Annual Plant Reviews, Biochemistry of Plant Secondary Metabolism. Annu Plant Rev **40**: 483

Winter D, Vinegar B, Nahal H, Ammar R, Wilson G V., Provart NJ (2007) An "electronic fluorescent pictograph" Browser for exploring and analyzing large-scale biological data sets. PLoS One. doi: 10.1371/journal.pone.0000718

Woody ST, Austin-Phillips S, Amasino RM, Krysan PJ (2007) The WiscDsLox T-DNA collection: an arabidopsis community resource generated by using an improved high-throughput T-DNA sequencing pipeline. J Plant Res **120**: 157–165

Wu KC, McDonald PR, Liu J, Klaassen CD (2014) Screening of natural compounds as activators of the keap1-nrf2 pathway. Planta Med **80**: 97–104

Xiang T, Shibuya M, Katsube Y, Tsutsumi T, Otsuka M, Zhang H, Masuda K, Ebizuka Y (2006) A new triterpene synthase from Arabidopsis thaliana produces a tricyclic triterpene with two hydroxyl groups. Org Lett **8**: 2835–2838

Xin X-F, He SY (2013) Pseudomonas syringae pv. tomato DC3000: a model pathogen for probing disease susceptibility and hormone signaling in plants. Annu Rev Phytopathol **51**: 473–98

Xiong Q, Wilson WK, Matsuda SPT (2006) An Arabidopsis oxidosqualene cyclase catalyzes iridal skeleton formation by grob fragmentation. Angew Chemie - Int Ed **45**: 1285–1288

Xiu JW, Hayes JD, Wolf CR (2006) Generation of a stable antioxidant response element-driven reporter gene cell line and its use to show redox-dependent activation of Nrf2 by cancer chemotherapeutic agents. Cancer Res **66**: 10983–10994

Yadav VR, Prasad S, Sung B, Kannappan R, Aggarwal BB (2010) Targeting inflammatory pathways by triterpenoids for prevention and treatment of cancer. Toxins

(Basel) **2**: 2428–2466

Yang H, Matsubayashi Y, Nakamura K, Sakagami Y (2001) Diversity of Arabidopsis Genes Encoding Precursors for Phytosulfokine, a Peptide Growth Factor. PLANT Physiol **127**: 842–851

Yasumoto S, Fukushima EO, Seki H, Muranaka T (2016) Novel triterpene oxidizing activity of Arabidopsis thaliana CYP716A subfamily enzymes. FEBS Lett **590**: 533–540

Yoshimi N, Wang A, Morishita Y, Tanaka T, Sugie S, Kawai K, Yamahara J, Mori H (1992) Modifying Effects of Fungal and Herb Metabolites on Azoxymethane-induced Intestinal Carcinogenesis in Rats. Japanese J Cancer Res **83**: 1273–1278

Yoshioka K, Deng T, Cavigelli M, Karin M (1995) Antitumor promotion by phenolic antioxidants: inhibition of AP-1 activity through induction of Fra expression. Proc Natl Acad Sci U S A **92**: 4972–6

Yoshizaki Y, Mori T, Ishigami-Yuasa M, Kikuchi E, Takahashi D, Zeniya M, Nomura N, Mori Y, Araki Y, Ando F, et al (2017) Drug-Repositioning Screening for Keap1-Nrf2 Binding Inhibitors using Fluorescence Correlation Spectroscopy. Sci Rep. doi: 10.1038/s41598-017-04233-3

Yu N, Nützmann HW, Macdonald JT, Moore B, Field B, Berriri S, Trick M, Rosser SJ, Kumar SV, Freemont PS, et al (2016) Delineation of metabolic gene clusters in plant genomes by chromatin signatures. Nucleic Acids Res **44**: 2255–2265

de Zeeuw D, Akizawa T, Audhya P, Bakris GL, Chin M, Christ-Schmidt H, Goldsberry A, Houser M, Krauth M, Lambers Heerspink HJ, et al (2013) Bardoxolone Methyl in Type 2 Diabetes and Stage 4 Chronic Kidney Disease. N Engl J Med **369**: 2492–2503

Zhang DD (2013) Bardoxolone Brings Nrf2-Based Therapies to Light. Antioxid Redox Signal **19**: 517–518

Zhang DD, Lo S-C, Cross J V, Templeton DJ, Hannink M (2004) Keap1 is a redox-regulated substrate adaptor protein for a Cul3-dependent ubiquitin ligase complex. Mol Cell Biol **24**: 10941–53

Zhang DD, Lo SC, Sun Z, Habib GM, Lieberman MW, Hannink M (2005) Ubiquitination of Keap1, a BTB-Kelch substrate adaptor protein for Cul3, targets Keap1 for degradation by a proteasome-independent pathway. J Biol Chem **280**: 30091–30099

Zhang Q, Zhu B, Li Y (2017) Resolution of cancer-promoting inflammation: A new approach for anticancer therapy. Front Immunol. doi: 10.3389/fimmu.2017.00071

Zhang X, Clarenz O, Cokus S, Bernatavichute Y V., Pellegrini M, Goodrich J, Jacobsen SE (2007) Whole-genome analysis of histone H3 lysine 27 trimethylation in

Arabidopsis. PLoS Biol **5**: 1026–1035

Chapter 8

Appendix

Abbreviations

α-Mem	alpha minimum essential medium
ARE	antioxidant response elements
ATP	adenosine triphosphate
BARS1	BARUOL SYNTHASE 1
BCA	bicinchoninic acid
bp	base pairs
CAMS1	CAMELLIOL C SYNTHASE
CaMV 35S	cauliflower mosaic virus 35S
CAS1	CYCLOARTENOL SYNTHASE 1
CBC	chair-boat-chair conformation
CCC	chair-chair-chair conformation
CDDO	cyano-3,12-dioxooleana-1,9(11)-dien-28-oic acid
cDNA	complementary DNA
CLF	CURLY LEAF
COI-1	CORONATINE-INSENSITIVE 1
Col-0	Columbia-0 ecotype
crtE	geranylgeranyl diphosphate synthase
Cul3	Cullin 3-dependent e3 ubiquitin ligase
DMAPP	dimethylallyl pyrophosphate
DMSO	dimethyl sulfoxide
DNA	deoxyribonucleic acid
EDTA	ethylenediaminetetra-acetic acid
EpRE	electrophile response element
ER	endoplasmic reticulum
EtBR	ethidium bromide
EtOH	ethanol
FPP	carbon farnesyl diphosphate
FPPS	farnesyl diphosphate synthase
FW	fresh weight
g	relative centrifugal force
gDNA	genomic DNA
GSK-3	glycogen synthase kinase-3
H_2O	double distilled water
H_2O_2	hydrogen peroxide
H3K27me3	histone 3 lysine trimethylation
HO-1	heme oxygenase-1
HO	homozygous T-DNA insertion
HZ	heterozygous T-DNA insertion
Im	imidazolide
IPP	isoprenoid units
JA	jasmonic acid
JAZ	JASMONATE ZIM-DOMAIN
JAZQ	quintet of JAZ repressors
kb	kilo base pairs
Keap1	kelch-like ECH-associated

	protein 1
LB	lysogeny broth
LBP	left border primer
LC-MS	liquid chromatography-mass spectrometry
LiCl	lithium chloride
LP	left primer
LPS	lipopolysaccharide
LRP5/6	lipoprotein receptor related protein 5/6
LSS1	LANOSTEROL SYNTHASE 1
LUP1	LUPEOL SYNTHASE 1
LUP2	LUPEOL SYNTHASE 2
LUP3	LUPEOL SYNTHASE 3
LUP4	LUPEOL SYNTHASE 4
LUP5	LUPEOL SYNTHASE 5
LUX	firefly luciferase
Me	methyl ester
MeJa	methyl jasmonate
MEP	peroxisomic 2-c-methyl-d-erythritiol 4-phosphate pathway
mGST-Ya	mouse glutathione-s-transferase ya
MRN1	MARNERAL SYNTHASE 1
mRNA	messenger RNA
MRO	MARNERAL OXIDASE
MS	murashige skoog
MTT	3-(4,5-dimethylthiazol-2-yl)-2,5-diphenyltetrazolium bromide
MVA	mevalonate pathway
MYC2	BASIC-HELIX-LOOP-HELIX-PROTEIN
NINJA	NOVEL INTERACTOR OF JAZ
Nrf2	nuclear factor erythroid-2-related factor-2
OA	oleanolic acid
OD	optical density
OSC	oxidosqualene cyclase
PBS	phosphate-buffered saline
PCR	polymerase chain reaction
PEN1	PENTACYCLIC TRITERPENE SYNTHASE 1
PEN3	PENTACYCLIC TRITERPENE SYNTHASE 3
PEN6	PENTACYCLIC TRITERPENE SYNTHASE 6
PFT1	PHYTOCHROME AND FLOWERING TIME 1
PHYB	phytochrome B
PKL	PICKLE
PKL2	PICKLE RELATED 2
PLB	passive lysis buffer
PP2A	SERINE/ THREONINE PROTEIN PHOSPHATASE 2A
PSKR1	PSK RECEPTOR 1
PSKR2	PSK RECEPTOR 2
PSK-α	PHYTOSULFOKINE-A
PSY1R	PSY1 RECEPTOR

qPCR	real-time polymerase chain reaction
rcf	relative centrifugal force
RLU	relative light units
RNA	ribonucleic acid
root133	*Massilia spec. root133*
root401	*Pseudomonas spec. root401*
root480	*Rhodobacter spec. root480*
root65	*Psudoxanthomonas spec. root65*
root68	*Pseudomonas spec.*
ROS	reactive oxygen species
RP	right primer
rpm	revolution per minute
RT	room temperature
RT-PCR	reverse transcription polymerase chain reaction
SA	salicylic acid
SAD	SAPONIN DEFICIENT
SO	synthetic oleanolic acid
SQE	SQUALENE EPOXIDASE
SQS	SQUALENE SYNTHASE
tBHQ	tert-butylhydroquinone
T-DNA	transfer DNA
TE	transposable element
TF	transcription factor
THAD	THALIAN-DIOL DESATURASE
THAH	THALIANOL HYDROXYLASE
THAS	THALIANOL SYNTHASE
TPST	TYROSYLPROTEIN SULFOTRANSFERASE
UDP	uridine diphosphate
UV	ultra violet
VSP2	VEGETATIVE STORAGE PROTEIN 2
Wnt	wingless
WT	wild-type

List of Figures

List of Tables

Danksagung

An dieser Stelle möchte ich mich herzlichst bei Herrn Prof. Dr. Stanislav Kopriva für die Betreuung meiner Promotion und die Diskussion meiner Arbeit bedanken. Zudem bedanke ich mich bei Frau PD Dr. Tamara Gigolashvili für die 2. Betreuung, die Anleitung im Labor und die gemeinsame Zeit im Biozentrum. Außerdem möchte ich mich bei Frau Prof. Dr. Karin Schnetz für die Prüfung meiner Disputation bedanken. Ebenfalls bedanke ich mich bei meinem Thesis Komitee und der Max Plank Gesellschaft für die Bewilligung meines Stipendiums und die Aufnahme in die IMPRS.

Neben der offiziellen Prüfungskommission danke ich Herrn Prof. Dr. Flügge für meine Anstellung an der Universität zu Köln. Außerdem bedanke ich mich bei Dr. Thomas Drepper, Dr. Anita Loeschcke, Jennifer Hage-Hülsmann, Dr. Vera Wewer und Dr. Sabine Metzger für die gute Kollaboration im Rahmen von CEPLAS.

Zudem möchte ich mich für die tatkräftige Unterstützung durch die Angestellten und Doktoranden der AG Kopriva, AG Gigolashvili, AG Krüger, der ehemaligen AG Flügge, der Gärtnerei, dem Fotolabor und der Werkstatt bedanken. Insbesondere bedanke ich mich bei Anna Koprivova, Anna Martyn, Ann-Kathrin Bahlmann, Bastian Welter, Christof Dietzen, Claudia Nothelle, Elke Hilgers, Henning Frerigmann, Irene Klinkhammer, Jana Flügge, Laura Strubl, Richard Jacoby, Ruben Benstein, Sabine Wulfert, Samira Blau, Sandra Pietraszek, Siegfried Werth, Silke Gerlich, Simon Mitreiter, Stefan Schuck, Stephan Krüger und Timothy Jobe. Zudem danke ich den Studenten Athanasios Kouklas, Janek Hankel, Oliver Trunschke, Victoria Klunder und Yvonne Peters, die ich während meiner Promotion betreut habe, für ihr Engagement.

Einen besonderen Dank möchte ich meinen engen Freunden aussprechen, die mir in allen Lebenslagen zur Seite standen. Der größte Dank gilt meiner Familie für ihre bedingungslose Unterstützung während meines gesamten Studiums und darüber hinaus.

Eidesstattliche Erklärung

Ich versichere, dass ich die von mir vorgelegte Dissertation selbständig angefertigt, die benutzten Quellen und Hilfsmittel vollständig angegeben und die Stellen der Arbeit − einschließlich Tabellen, Karten und Abbildungen −, die anderen Werken im Wortlaut oder dem Sinn nach entnommen sind, in jedem Einzelfall als Entlehnung kenntlich gemacht habe; dass diese Dissertation noch keiner anderen Fakultät oder Universität zur Prüfung vorgelegen hat; dass sie − abgesehen von unten angegebenen Teilpublikationen − noch nicht veröffentlicht worden ist, sowie, dass ich eine solche Veröffentlichung vor Abschluss des Promotionsverfahrens nicht vornehmen werde. Die Bestimmungen der Promotionsordnung sind mir bekannt. Die von mir vorgelegte Dissertation ist von Herrn Prof. Dr. Stanislav Kopriva betreut worden.

Gemäß §4 Abs. (1) Nr. 9 der Promotionsordnung.

Köln, den 17.03.2018

Dorian Alexander Baumann